COLD ATMOSPHERIC PLASMA DIFFERENTIALLY AFFECTS CELL RENEWAL AND DIFFERENTIATION OF STEM CELLS AND APC-DEFICIENT-DERIVED TUMOR CELLS IN INTESTINAL ORGANOIDS

Alia Hadefi[1,2*], Morgane Leprovots[1*], Max Thulliez[3#], Orianne Bastin[3#], Anne Lefort[1], Frédérick Libert[1], Antoine Nonclercq[3], Alain Delchambre[3], François Reniers[4], Jacques Devière[2] and Marie-Isabelle Garcia[1$]

[1]Institut de Recherche Interdisciplinaire en Biologie Humaine et Moléculaire (IRIBHM), Faculty of Medicine, Université Libre de Bruxelles ULB, Route de Lennik 808, 1070, Brussels, Belgium.

[2]Department of Gastroenterology, Hepatopancreatology and Digestive Oncology, C.U.B. Hôpital Erasme, Laboratory of Experimental Gastroenterology, Route de Lennik 808, 1070, Brussels, Belgium.

[3]Bio-, Electro- and Mechanical- system (BEAMS), Biomed Group, Ecole polytechnique de Bruxelles, av. F.D. Roosevelt 50 CP165/56 - 1050 Brussels, Belgium.

[4]Chemistry of Surfaces, Interfaces, and Nanomaterials, ChemSIN cp 255, Université libre de Bruxelles, Faculty of Sciences, Brussels, Belgium.

* First co-authors # Second co-authors

[$] **Corresponding author:** Marie-Isabelle Garcia: Marie.Garcia@ulb.be

Phone: + 32 2 555 4195

Keywords: Cold Atmospheric plasma, stem cells, tumor cells, organoids, regeneration, intestine, cell death, apoptosis, Reactive Oxygen Species

Running title: CAP effects on intestinal organoid growth and differentiation

Word count: 4, 335 words (references and Materials and methods excluded)

ABSTRACT

Cold atmospheric plasma (CAP) treatment has been proposed as a potentially innovative therapeutic tool in the biomedical field, notably for cancer due to its proposed toxic selectivity on cancer cells versus healthy cells. In the present study, we addressed the relevance of three-dimensional organoid technology to investigate the biological effects of CAP on normal epithelial stem cells and tumor cells isolated from mouse small intestine. CAP treatment exerted dose-dependent cytotoxicity on normal organoids and induced major transcriptomic changes associated with global response to oxidative stress, fetal-like regeneration reprogramming and apoptosis-mediated cell death. Moreover, we explored the potential selectivity of CAP on tumor-like Apc-deficient versus normal organoids in the same genetic background. Unexpectedly, tumor organoids exhibited higher resistance to CAP treatment, correlating with higher antioxidant activity at baseline as compared to normal organoids. This pilot study suggests that the *ex vivo* culture system could be a relevant alternative model to further investigate translational medical applications of CAP technology.

INTRODUCTION

Cold atmospheric plasma (CAP) is a partially or totally ionized gas including photons, electromagnetic fields, electrons, ions and neutral radicals such as reactive oxygen and nitrogen species (RONS)(1). In the past decade, this innovative technology has generated growing interest for various applications in the biomedical field such as blood coagulation, sterilization, wound healing and anti-cancer therapy(2). Number of studies have reported that CAP exerts cytotoxic effects when applied directly to cultured cells or indirectly through a plasma activated medium (PAM), as well as anti-tumoral activity(3)(4). The cytotoxic effects are mainly attributed to the production of short and long-lived RONS that generate a redox imbalance, leading to increased intracellular oxidative stress along with damage of cellular components, such as proteins, lipids and DNA(5)(6). Metabolically active cancer cells are reported to exhibit higher basal level of oxidative stress as compared to healthy cells, which could explain the reported selectivity of the anti-tumoral effects of CAP (7)(8). However, the underlying molecular

mechanisms of CAP tumor selectivity remain to be clarified. Additionally, most *in vivo* studies have focused on immortalized cells, which do not recapitulate the physiological complexity of epithelia, constituted of various cell types devoted to specific functions *in vivo*(7). Lastly, the impact of CAP treatment on healthy tissues that naturally have a high renewal rate has not been fully investigated.

The adult intestinal epithelium is one of the most rapidly self-renewing tissues in adult mammals, supported by a pool of Lgr5 intestinal stem cells (ISCs), also called crypt base columnar cells, that reconstitute the whole epithelium in less than 5 days(9). ISCs have the capacity to both self-renew and give rise to transit-amplifying cells which differentiate along the villus architecture into all the cell lineages of the epithelium, (i.e., absorptive enterocytes, mucus-producing goblet cells, hormone-secreting enteroendocrine cells, Paneth cells generating antimicrobial products, and chemosensory type 2 immune response-induced tuft cells)(10). The *ex vivo* culture technology has recently been developed to indefinitely grow ISCs in a Petri dish. Upon seeding into a 3D matrix, ISCs self-renew, proliferate and differentiate into the various epithelial lineages present in the normal epithelium; *ex vivo* grown organoids maintain the *in vivo* relative proportion of each cell subtype and its temporal differentiation (11). Recently, this versatile technology has been used in the context of human colorectal(12)(13) and rectal cancer (14) allowing for the accurate prediction of drug responses(15)(16) in a personalized treatment setting.

In the present study, using the *ex vivo* culture system, we investigated the impact of an endoscopic helium plasma jet application on mouse ISCs at the morphological, cellular and transcriptomic levels. Moreover, we explored the potential selectivity of CAP application on tumor versus normal organoids originating from the same genetic background. Our data suggest that the *ex vivo* culture system could be a relevant alternative model to further investigate translational medical applications of CAP.

RESULTS

CAP treatment affects normal growth of intestinal stem cell-derived organoid cultures

To assess the potential benefits and adverse consequences of CAP treatment on normal surrounding tissues in the digestive epithelium, we set out to investigate the biological effects of plasma on mouse ISCs using the plasma jet device as described in Fig. 1a. For this purpose, we first generated mouse intestinal organoid lines from individual mice (Fig. 1b). For the experiments, fully grown organoids were mechanically dissociated and replated in a tridimensional matrix (Matrigel) supplemented with complete culture medium (Fig. 1b). Twenty-four hours after organoid replating (at day 1), CAP was directly applied to the culture plate wells. Different settings were applied, with varying durations (30 s or 60 s) and powers (30 W, 60 W or 80 W). Fresh culture medium was added 24 hours after CAP treatment (at day 2) and at day 4. At the endpoint (day 5), organoid survival and morphology of the grown elements were compared (Fig. 1c, d). Control cultures, and those treated with either helium gas alone (designated “60 s/0 W”) or mild CAP dose (60 s/30 W) followed similar organoid morphological evolution and survival rates. The spheroid-like structures (primarily constituted of proliferating ISCs during the first days of culture), started protruding as crypt-like domains and then differentiated into the various epithelial lineages present in the normal epithelium by day 5. Then, differentiated cells accumulated in the lumen of fully grown organoids (Fig. 1c, d). Conversely, exposure to moderate and higher doses of CAP (60 and 80 W, respectively) significantly reduced organoid budding capacity. Meanwhile, spheroid-like elements were overrepresented as compared to controls at day 5 (Fig. 1c, d). Moreover, under the 80 W-dose condition, dark declining structures were observed, accompanied by overall reduced survival rate tendency as compared to controls [34.2 ± 1.6% in CAP 60 s/80 W versus (vs) 44.5 ± 4.3% in untreated samples, respectively, unpaired t-test p=0.0698]. Together, these experiments indicate that direct CAP treatment alters the growth capacity of healthy ISCs in a dose-dependent manner.

Next, we investigated the influence of the culture medium on ISC growth at a fixed moderate dose (60 s/ 50 W) (see experimental design in Fig. 2a). Direct CAP treatment was applied at day 1 and the treated culture medium was replaced with fresh medium at 30 min, 3 h or 1 day (1 d) later (Fig. 2a). The

morphology of grown elements was studied at day 3, an endpoint at which 61.8% of grown elements in untreated cultures showed at least one crypt-like domain (Fig. 2b, c). Removal of CAP-treated medium early after the procedure (30 min and 3 h) did not significantly alter protrusion formation. In contrast, prolonged incubation with CAP-treated culture medium (24 hours = 1 d) was associated with higher proportion of elements grown as spheroids (67%), only 9% of total elements were protruded organoids (Fig. 2b, c). Together, these data indicate that the time of exposure to reactive species generated by CAP treatment affects the capacity of ISCs to normally grow and differentiate. Interestingly, a similar negative impact on organoid budding was observed when "naïve" organoids were indirectly submitted to reactive species present in conditioned media generated either by CAP treatment applied onto another organoid culture (designated as "indirect CAP") or the Plasma-Activated Medium alone (designated as "PAM") (Fig. 2a-c). Exposure to Indirect CAP- or PAM-conditioned media 24 hours after the treatment (from day 2 to day 3) also altered organoid protrusion, albeit to a milder degree, thereby indicating that toxic long-lived reactive species were still present in culture supernatants after 24 hours (Supplementary Fig. 1S a-c). Taken together, these data demonstrated that normal ISCs are sensitive to direct as well as indirect CAP/PAM treatment *ex vivo*.

CAP treatment decreases the intestinal stem cell pool and is associated with Apoptosis

To further investigate the molecular and cellular mechanisms of CAP-induced morphological effect on intestinal organoid growth, we analyzed at day 3 the whole transcriptome of organoids treated directly or indirectly with CAP at a moderate dose (50W/60 s) during a period of 24 hours (Fig. 2a). We identified 2462 differentially expressed genes in CAP-treated vs untreated cultures (False Discovery rate 0.01 and Log2-fold change of 1 or above) (Fig 2d). Of these, CAP-treatment induced downregulation of 1195 genes involved in the following biological processes: cell cycle progression, cell division and DNA replication (Fig. 2e). ISC markers like *Lgr5*, *Olfm4*, *Smoc2* and *Axin2* genes were amongst the most downregulated genes (Fig. 2d). In particular, 35% of the genes identifying the intestinal crypt base columnar stem cell signature (i. e. 135 out of 379 genes) reported by Munoz et al, (17) were downregulated in CAP-organoids (Fig. 3a, b). Loss of ISCs in CAP-treated cultures was confirmed by *in situ* hybridization experiments and immunofluorescence staining for *Olfm4*-expressing

cells; this correlated with significant drop in canonical Wnt signaling activity (*Axin2* used as reporter gene) (Fig. 3b-d). Consistent with suggested upregulation of the apoptotic process (p value e-49, Fig. 2e), the Pycard gene, involved in regulation of apoptosis and adaptation to the inflammatory response, and genes associated with DNA repair (*Pclaf, Usp49, Hmga2*) were found to be downregulated meanwhile apoptosis-mediator/effector genes (Calpains *Capn2/5/12/13*, *Trp53inp2*, *Ctsl*, *Unc5b*, *Cidec*, *Atf3*, *Ddit3*, *Cfap157*) were upregulated in CAP-treated organoids (Fig. 3c, 4a). TUNEL assay performed on organoid sections confirmed the presence of DNA double strand breaks in CAP-treated cultures (Fig. 4b).

CAP treatment induces a global response to reactive species in intestinal stem cell-derived organoids

In addition, CAP induced upregulation of genes involved in modulation of intracellular signal transduction, negative regulation of response to stimulus, and response to oxygen containing compounds as well as in positive regulation of developmental processes (Fig. 2e). In line with response to CAP mediated-injury, pro-survival (*Dsg3*, *Phlda3*) and regeneration-associated genes (*Trop2*/*Tacstd2*, *Ptgs2*, *Hbegf*, *Ly6a*/*Sca1*, *Clu*, *Areg*, *Epn3*) were induced as early as 30 min post-direct CAP treatment (Fig. 5a). Indeed, 34% of the genes identifying the fetal-like Trop2 regeneration signature (50 out of the 148 gene list, (18)) were upregulated in CAP-treated organoids (Fig. 5b). Accordingly, both the number of Trop2-expressing cells and Areg expression were significantly increased in CAP-treated organoids (Fig. 5c, d). Furthermore, a global stress response gene expression pattern was detected with early upregulation of oxidative stress-associated transcription factors like *Fos*, *Fosb*, *Egr1*, *Nfe2l1*/*Nrf1*, *Nupr1*, *Nr4a1* and *Jdp2* (Fig. 5a, Supplementary Fig. 2Sa). In line with reported regulation of oxidative stress by long noncoding RNAs, expression of *Fer1l4*, *Gm20417*, *Neat1*, *Malat1*, *Gm37376* or *Kcnq1ot1* was induced 30 min after CAP-treatment (Supplementary Fig. 2Sa) (19). Effectors of global response to CAP-mediated oxidative stress in organoids were found upregulated. Among these, genes encoding solute/metabolite transporters such as *Slc7a11*, a cysteine/glutamate antiporter xCT, and detoxifying enzymes (*Hmox1*, *Ethe1*, *Gch1*, *Gstk1*) were identified (Fig. 5a,d). Components of the cysteamine/cystamine metabolism (*Gpr5a*, *Vnn1*, *Chac1*, *Ggh*), involved in glutathione redox status, were also induced by the treatment (Supplementary Fig. 2Sb). Cell signaling molecules such as the Polo

like kinases (*Plk2*, *Plk3*) reported to exert antioxidant functions, as well as *Mapk11*, *Lif* and *Pmepa1* were also upregulated by CAP application (Fig. 2Sb). Of note, the major cellular enzymatic ROS scavengers (superoxide dismutases, glutathione peroxidases, peroxiredoxins and catalase) were detected at high levels in control organoids but their expression did not substantially differ upon CAP-treatment (Table 1). *Pparg*, a master regulator of lipid metabolism and immune response (20), was also found upregulated in CAP-treated organoid cells (Fig. 5a, d). Inflammatory response genes were significantly modulated in CAP-treated organoids: interferon induced *Ifitm2/Ifitm3* and chemokine *Ccl9* were downregulated whereas expression of *Ifnlr1*, *Ilr1*, *Ddx60* and *Pdlim7* were upregulated (Fig. 2Sb). Moreover, consistent with extensive reshaping of epithelial cells, CAP application was associated with upregulation of cytoskeleton organization, cell motility and biological adhesion processes (Fig. 2e, Fig. 2Sb).

Apc deficient-derived organoids exhibit increased resistance to CAP treatment as compared to ISCs-derived organoids

Since ISCs were sensitive to moderate and high doses of CAP, we sought to compare resistance of normal or tumor organoids to this treatment. For this purpose, adult VilCreERT2-Apc$^{flox/flox}$ or VilCreERT2-Apc wild-type (wt) mice were injected with tamoxifen to induce specific deletion of Apc exon 15 in VilCreERT2-Apc$^{flox/flox}$ mice, leading to loss-of-function of this tumor suppressor (designated as Apc Δ). Apc wt and Apc Δ intestinal crypts were isolated and cultured to generate normal and tumor organoid lines, respectively (Fig. 6 a). Efficient recombination in Apc Δ tumor-derived organoids was controlled at initial seeding (Supplementary Fig. 3Sa). Then, upon organoid replating, CAP was directly applied at various doses for 60 s on both kinds of organoids (Fig. 6b). As expected, at day 5, Apc wt organoid survival was substantially reduced at a dose of 50 W and 80 W as compared to untreated organoids (Fig. 6 b,c). Conversely, Apc Δ organoids demonstrated higher survival rates, regardless of the CAP dose (Fig. 6c). Dosage of reactive species in culture supernatants did not demonstrate substantial differences between organoid types at a given CAP-dose, which might have explained the observed higher resistance of Apc Δ vs Apc wt organoids (Supplementary Fig. 3Sb). To further explore the underlying molecular mechanisms, qPCR experiments were performed on samples collected at day

5. With the exception of *Olfm4*, expression of markers for active (Lgr5) and quiescent (Hopx) stem cell populations was maintained in tumor organoids, even at the highest CAP dose (80 W) (Fig. 6d). Regarding cell differentiation, mild CAP dose (30 W) in Apc wt organoids had a tendency to decrease the Paneth lineage vs the other cell types whereas Apc Δ-organoids exhibited limited cell differentiation in any tested condition (Fig. 6d). Interestingly, expression of regeneration marker genes was upregulated in Apc wt organoids upon CAP treatment (30 W), and was detected at much higher levels in tumor organoids even under normal conditions (Fig. 7b). Moreover, tumor organoids maintained proliferation capacity and low cell death behavior following CAP treatment (Fig. 7b). Furthermore, Apc Δ organoids demonstrated increased levels of genes (e. g. *Atf3, Nupr1*) involved in early response to reactive species as compared to Apc wt organoids (Fig. 7b). In addition, cellular transporters (*Slc7a11*) and detoxifying enzymes (*Hmox1*), induced in Apc wt organoids by mild CAP treatment, were expressed at significantly higher levels in basal conditions in tumor organoids (Fig. 7b). Differential expression of the membrane-associated aquaporins has also been proposed to contribute to CAP selectivity by facilitating influx of water and hydrogen peroxide into cancer cells(21). In ISCs and healthy intestinal organoids, RNAseq data showed that *Aqp1, Aqp4 and Aqp11* were the most significantly expressed (Supplementary Fig S3c). CAP treatment particularly reduced *Aqp1* and *Aqp4* levels in Apc wt organoids (Supplementary Fig S3c). Interestingly, irrespective of CAP treatment, tumor organoids were expressing 2-fold less *Aqp1*, *Aqp4* and 10-fold less *Aqp3* levels than normal organoids, whereas Aqp5 expression was increased (Supplementary Fig S3d). Taken together, these experiments indicate that tumor-like organoids deficient for the tumor suppressor Apc demonstrate a higher potential to resist CAP-induced injury as compared to ISC-derived organoids. Such behavior could be, in part, explained by the expression of an oxidative stress resistance program, already active under basal conditions, and reduced cell surface expression of aquaporins.

DISCUSSION

In the present study, we addressed the relevance of a 3D organoid culture to investigate the biological effects of CAP on normal epithelial stem cells and tumor cells isolated from the mouse small intestine. First of all, we studied the parameters that determine CAP effects on cells and found that helium, used as the carrier gas, did not by itself alter organoid growth. We observed toxic effect of direct CAP application to ISC cultures, showing dose-dependency as reported on various cancer lines (21). To determine whether CAP treatment can induce a "bystander effect" as described in radiobiology, in which irradiated cells communicate stress via extracellular signaling to neighboring cells, we also analyzed indirect application of CAP on organoids (Indirect CAP and PAM). In our experimental setting, organoid growth was similarly affected by the three conditions, indicating that the main effect of CAP was mediated by reactive species delivered in the culture medium, with minor contribution of cellular components potentially released from the CAP-treated organoids. Our data also suggest that CAP-mediated cytotoxicity depends in part on long-lived reactive species (typically nitrites, hydrogen peroxide, ozone) since increased levels of nitrites were still detected 24 hours after CAP treatment as compared to controls (Supplementary Fig S3b). On the other hand, it is known that the nature of CAP-generated RONS is conditioned by the composition of the cell culture medium(22). Organoid growth requires a complex medium, including several antioxidant supplements such as N-acetyl cysteine, glutathione, sodium pyruvate and ascorbic acid (23) (24)(25) (26). We hypothesize that the presence of such antioxidants in the medium might have increased the threshold level needed to detect variations in the long-lived ROS species with the DCFH-DA probe (Supplementary Fig S3b).

Moderate (50/60 W) to high (80 W) doses of CAP severely impacted ISC self-renewal and differentiation. Although ISCs express important levels of ROS scavenger enzymes (Supplementary Fig. S3e), previous studies have also reported that, under steady-state conditions, ISCs exhibit two-fold increased levels of ROS as compared to the rest of the epithelium(27). Together, these data are in line with the hypothesis that the application of moderate-to-high CAP doses to ISCs reaches a redox status threshold above which toxic accumulation of RONS occurs, similar to what has been previously described for cancer cell lines(7)(8); this ultimately induces DNA damage and cell death by apoptosis.

Interestingly, moderate CAP dose also elicited an epithelial response with hallmarks of tissue regeneration, characterized by re-expression of a fetal signature, reported to be induced by a variety of insults in the gastrointestinal tract(18)(28)(29)(30). As part of this fetal reprogramming, upregulation of genes coding for factors mainly released by the surrounding stromal compartment (Areg, Ptgs2, etc..), were upregulated in epithelial cells *ex vivo*. This suggests that, upon injury, the epithelium has the intrinsic potential to contribute to the repair process. In the same line, CAP treatment on murine cementoblasts has been reported to induce a regeneration process similar to that elicited by enamel matrix derivatives *in vivo*(31). Moreover, CAP treatment induced a global response to oxidative stress in organoids that involved upregulation of RONS-associated transcription factors and effectors known to regulate intracellular ROS balance and reported to be activated upon CAP treatment(32)(33)(34)(35).

A major observation of our study relates to CAP application effects on tumoral APC-deficient organoids. The potential of CAP treatment in oncology relies on a proposed selective targeting of cancer cells over healthy cells due to higher intracellular levels of ROS in malignant cells (36). However, compared sensitivity of CAP needs to be performed on the same cell type and genetic background, with cells growing under the same culture conditions. This was addressed in the present study by comparing the impact of CAP application on normal “healthy” organoids and tumoral Apc-deficient organoids, the latter being used as a colorectal cancer (CRC) model. Contrary to our initial expectations, tumor organoids exhibited higher resistance to CAP treatment than healthy organoids. Such results could be explained, at least in part, by the fact that Apc-deficient organoids exhibited a much higher antioxidant response at baseline than ISC-derived organoids. The potential contribution of differential expression of aquaporins to CAP selectivity could be interesting to address in future *ex vivo* studies.

In summary, the present study reveals the potential of organoid technology to further investigate the biological effects of CAP on normal and tumoral tissues. Indeed, organoid cultures faithfully reflect cell heterogeneity in epithelial tissues, they are as amenable to “Omics” studies as the cancer cell lines and, from a translational point of view, they can be used to compare various CAP application settings. Our study highlights the importance of considering CAP toxicity on metabolically active resident stem cells in tissues, like the intestine, undergoing permanent self-renewal, in order to adjust the dose of treatment.

Furthermore, CRC development is known to be a multistep process. Following the initial hit mutation in the Apc gene that leads to Wnt signaling overactivation, mutations deregulating other pathways (such as KRAS/TGFb and p53) sequentially accumulate in cancer cells, and correlate with cancer progression(37)(38). Future studies will be needed to investigate the sensitivity of CAP treatment on tumor organoids bearing the aforementioned additional mutations in order to definitely elucidate the potential of CAP for personalized anti-cancer therapy.

MATERIALS AND METHODS

Experimental animals

Adult mice were from the outbred CD1 strain (Charles River Laboratories). To obtain tumor-derived organoids, we crossed Tg(Vil1-cre/ERT2)$^{23Syr/J}$ (39) and Apc$^{tm1Tyj/J}$ designated Apc^{flox} (40). Adult Vil-cre/ERT2/Apc$^{wt/wt}$ and Vil-cre/ERT2/Apc$^{flox/flox}$ were injected intraperitoneally for 3 consecutive days with tamoxifen (2 mg per 30 g of body weight) to induce recombination in the Apc locus and the small intestine was harvested 2-3 days after the last injection. Tamoxifen was dissolved in a sunflower oil/ethanol mixture (9:1) at 10 mg/ml (both products from Sigma-Aldrich).

Ex vivo culture

To generate intestinal organoids, mouse adult small intestine was dissociated with 5 mM EDTA-in DPBS (Gilbco) according to the protocol reported in(41). Briefly, the culture medium consisted of Advanced-DMEM/F12 medium supplemented with 2 mM L-glutamine, N2 and B27 w/o vit.A, gentamycin, penicillin-streptomycin cocktail, 10 mM HEPES (all from Invitrogen), 1 mM N acetyl cysteine (Sigma-Aldrich), 50 ng/ml EGF and 100 ng/ml Noggin (both from Peprotech), and 100 ng/ml CHO-derived mouse R-spondin 1 (R&D System). Culture medium was changed every other day and after 5-6 days in culture, organoids were harvested, mechanically dissociated and replated in fresh Matrigel matrix (catalog 356235 from BD Biosciences). Culture media were supplemented with 10 µM Y-27632 (Sigma Aldrich) in all initial seeding and replating experiments for the first two days. Pictures were acquired with a Moticam Pro camera connected to Motic AE31 microscope.

Cold atmospheric plasma treatment

The cold plasma source was an endoscopic plasma jet allowing for the generation and transport of CAP over long distances as described in our previous work(42). It consists of a tubular DBD chamber made of quartz supplied with helium gas and surrounded by a high-voltage electrode. The power-control source was an AFS (G10S-V) generator, delivering an 18 kHz sinusoidal signal. The discharge chamber was plugged into a polytetrafluoroethylene (PTFE) tube (outer diameter 3 mm, wall thickness 0.75 mm) transporting the plasma post-discharge over > 2 meters. An electrically floating copper wire (diameter 0.2 mm) was inserted partially into the dielectric chamber and extended almost until the end of the PTFE

tube (5 mm before its end) to allow the maintenance of active plasma for several meters and to sustain a plasma plume at the outlet for potential endoscopic treatment. Treatment was performed under a laminar flow hood using a 1.6 lpm helium flow; thus RONS were created by the mixing of CAP with ambient air (42). The power values (0, 30, 50, 60 or 80 W) were set on the AFS-generator. The catheter was placed vertically in a designated test bench. The tip of the catheter was placed at 3 cm from the top of the 12-well plate containing the media to be treated, i.e. the length of the plasma plume. This allowed plasma-generated RONS to reach the medium without the plasma plume touching it, avoiding any electrical connection that would have increased current and RONS creation in a less controlled manner. Fully-grown organoid cultures were dissociated by mechanical pipetting and replated on Matrigel in 12-well plates (VWR, Belgium). Twenty-four hours later, CAP was applied vertically on organoid cultures at room temperature. Each well was placed successively under the plasma plume for 30 s or 60 s. During treatment, the other wells were protected by a designated cover plate to avoid unwanted RONS diffusion to neighboring wells. Following exposure to CAP, treated samples were placed back at 37 °C in a 5% CO_2 incubator (Binder C150) and the medium was changed as indicated in the results section and different endpoints were applied.

Tissue processing and immunohistochemical analysis

Organoid culture samples were fixed with 10% formalin solution, neutral buffered (Sigma-Aldrich) for 20 minutes at room temperature then sedimented through 30% sucrose solution before OCT embedding. Histological protocols as well as immuno-fluorescence/histochemistry experiments on 6 µm sections were carried out as previously described (43). Table 2 lists primary antibodies, TUNEL assay kit and DAPI used. Stained samples were visualized with a DMI600B epifluorescence microscope equipped with a DFC365FX camera (Leica). The number of independent organoid cultures obtained from individual adult mice used for each experiment is reported in Figures and in Figure legends.

Gene expression analysis

qRT-PCR was performed on total RNA extracted from organoid cultures as reported(44). Expression levels of target genes were normalized to that of reference genes (Rpl13, Ywhaz). Table 2 lists the primers used for qPCR studies. *In situ* hybridization experiments were performed according to

manufacturer instructions with the RNAscope kit (ACD-Biotechne) (probes listed in Table 2). Stained samples were visualized with a Nanozoomer digital scanner (Hamamatsu).

RNA seq and Gene Set Enrichment Analysis (GSEA)

RNA quality was checked using a Bioanalyzer 2100 (Agilent technologies). Indexed cDNA libraries were obtained using the Ovation Solo (NuGen) or the NEBNext RNA-Seq Systems following manufacturer recommendations. The multiplexed libraries were loaded onto a NovaSeq 6000 (Illumina) using an S2 flow cell and sequences were produced using a 200 Cycle Kit. Paired-end reads were mapped against the mouse reference genome GRCm38 using STAR software to generate read alignments for each sample. Annotations Mus_musculus.GRCm38.90.gtf were obtained from ftp.Ensembl.org. After transcripts assembling, gene level counts were obtained using HTSeq. Differentially expressed genes were identified with EdgeR method and further analyzed using GSEA MolSig (Broad Institute)(45). Heatmaps were generated using Heatmapper(46) and common signature genes were identified using Venny 2.0 (47).

Detection of reactive species

Detection of reactive species was performed in organoid culture supernatants 24 hours after CAP treatment, as described in (22). Nitrite concentration was measured using a colorimetric assay with the Griess reagent. Absorbance was determined at 570 nm using the iMark Microplate reader (BioRad). Global ROS were detected using the reporter 2',7'-dichlorodihydrofluorescein diacetate (DCFH-DA, D6883 Sigma-Aldrich). The emitted fluorescence of oxidized DFC was detected at 528 nm using the Microwin software on Mithras LB940 reader (Berthold technologies).

Statistical analysis

Statistical analyses were performed with Graph Pad Prism 5. All experimental data are expressed as mean ± s.e.m unless indicated in Figure legends. The significance of differences between groups was determined by appropriate parametric or non-parametric tests as described in the text or Figure legends.

Data availability statement

343 The datasets generated and analyzed during the current study are available in the GEODATASET
344 repository [GEO Accession GSE 178148]. Some datasets analyzed during this study were included in a
345 published article(48) and are available in the GEODATASET repository [GSE 135362].
346

REFERENCES

1. Yan D, Sherman JH, Keidar M. Cold atmospheric plasma, a novel promising anti-cancer treatment modality. Vol. 8, Oncotarget. Impact Journals LLC; 2017. p. 15977–95.
2. Laroussi M. Cold Plasma in Medicine and Healthcare: The New Frontier in Low Temperature Plasma Applications. Front Phys [Internet]. 2020 Mar 20 [cited 2021 Oct 8];8:74. Available from: https://www.frontiersin.org/article/10.3389/fphy.2020.00074/full
3. Dubuc A, Monsarrat P, Virard F, Merbahi N, Sarrette JP, Laurencin-Dalicieux S, et al. Use of cold-atmospheric plasma in oncology: a concise systematic review. Vol. 10, Therapeutic Advances in Medical Oncology. SAGE Publications Inc.; 2018.
4. Nakamura K, Peng Y, Utsumi F, Tanaka H, Mizuno M, Toyokuni S, et al. Novel Intraperitoneal Treatment With Non-Thermal Plasma-Activated Medium Inhibits Metastatic Potential of Ovarian Cancer Cells. Sci Rep. 2017 Dec 1;7(1).
5. Vandamme M, Robert E, Lerondel S, Sarron V, Ries D, Dozias S, et al. ROS implication in a new antitumor strategy based on non-thermal plasma. Int J Cancer. 2012 May 1;130(9):2185–94.
6. Sun Y, Lu Y, Saredy J, Wang X, Drummer IV C, Shao Y, et al. ROS systems are a new integrated network for sensing homeostasis and alarming stresses in organelle metabolic processes. Vol. 37, Redox Biology. Elsevier B.V.; 2020.
7. Bekeschus S, Liebelt G, Menz J, Berner J, Sagwal SK, Wende K, et al. Tumor cell metabolism correlates with resistance to gas plasma treatment: The evaluation of three dogmas. Free Radic Biol Med. 2021 May 1;167:12–28.
8. Perillo B, Di Donato M, Pezone A, Di Zazzo E, Giovannelli P, Galasso G, et al. ROS in cancer therapy: the bright side of the moon. Vol. 52, Experimental and Molecular Medicine. Springer Nature; 2020. p. 192–203.
9. Barker N, Van Es JH, Kuipers J, Kujala P, Van Den Born M, Cozijnsen M, et al. Identification of stem cells in small intestine and colon by marker gene Lgr5. Nature. 2007 Oct 25;449(7165):1003–7.
10. Sprangers J, Zaalberg IC, Maurice MM. Organoid-based modeling of intestinal development,

regeneration, and repair. Vol. 28, Cell Death and Differentiation. Springer Nature; 2021. p. 95–107.

11. Sato T, Vries RG, Snippert HJ, Van De Wetering M, Barker N, Stange DE, et al. Single Lgr5 stem cells build crypt-villus structures in vitro without a mesenchymal niche. Nature. 2009 May 14;459(7244):262–5.

12. Van De Wetering M, Francies HE, Francis JM, Bounova G, Iorio F, Pronk A, et al. Prospective derivation of a living organoid biobank of colorectal cancer patients. Cell. 2015 May 7;161(4):933–45.

13. Roerink SF, Sasaki N, Lee-Six H, Young MD, Alexandrov LB, Behjati S, et al. Intra-tumour diversification in colorectal cancer at the single-cell level. Nature. 2018 Apr 26;556(7702):437–62.

14. Yao Y, Xu X, Yang L, Zhu J, Wan J, Shen L, et al. Patient-Derived Organoids Predict Chemoradiation Responses of Locally Advanced Rectal Cancer. Cell Stem Cell. 2020 Jan 2;26(1):17-26.e6.

15. Tuveson D, Clevers H. Cancer modeling meets human organoid technology. Vol. 364, Science. American Association for the Advancement of Science; 2019. p. 952–5.

16. Driehuis E, Kretzschmar K, Clevers H. Establishment of patient-derived cancer organoids for drug-screening applications. Nat Protoc. 2020 Oct 1;15(10):3380–409.

17. Muñoz J, Stange DE, Schepers AG, Van De Wetering M, Koo BK, Itzkovitz S, et al. The Lgr5 intestinal stem cell signature: Robust expression of proposed quiescent ′+4′ cell markers. EMBO J. 2012 Jul 18;31(14):3079–91.

18. Fernandez Vallone V, Leprovots M, Strollo S, Vasile G, Lefort A, Libert F, et al. Trop2 marks transient gastric fetal epithelium and adult regenerating cells after epithelial damage. Development [Internet]. 2016 May 1 [cited 2019 Sep 10];143(9):1452–63. Available from: http://dev.biologists.org/lookup/doi/10.1242/dev.131490

19. Ghafouri-Fard S, Shoorei H, Taheri M. Non-coding RNAs are involved in the response to oxidative stress. Vol. 127, Biomedicine and Pharmacotherapy. Elsevier Masson SAS; 2020.

20. Korbecki J, Bobiński R, Dutka M. Self-regulation of the inflammatory response by peroxisome

proliferator-activated receptors. Vol. 68, Inflammation Research. Birkhauser Verlag AG; 2019.

21. Yan D, Talbot A, Nourmohammadi N, Cheng X, Canady J, Sherman J, et al. Principles of using Cold Atmospheric Plasma Stimulated Media for Cancer Treatment. Sci Rep. 2015 Dec 17;5.

22. Tornin J, Labay C, Tampieri F, Ginebra MP, Canal C. Evaluation of the effects of cold atmospheric plasma and plasma-treated liquids in cancer cell cultures. Vol. 16, Nature Protocols. Nature Research; 2021. p. 2826–50.

23. Guarino VA, Oldham WM, Loscalzo J, Zhang YY. Reaction rate of pyruvate and hydrogen peroxide: assessing antioxidant capacity of pyruvate under biological conditions. Sci Rep. 2019 Dec 1;9(1).

24. Yang X, Chen G, Yu KN, Yang M, Peng S, Ma J, et al. Cold atmospheric plasma induces GSDME-dependent pyroptotic signaling pathway via ROS generation in tumor cells. Cell Death Dis. 2020 Apr 1;11(4).

25. Nishi K, Iwaihara Y, Tsunoda T, Doi K, Sakata T, Shirasawa S, et al. ROS-induced cleavage of NHLRC2 by caspase-8 leads to apoptotic cell death in the HCT116 human colon cancer cell line article. Cell Death Dis. 2017 Dec 1;8(12).

26. Beyer RE. The role of ascorbate in antioxidant protection of biomembranes: Interaction with vitamin E and coenzyme Q. J Bioenerg Biomembr. 1994 Aug;26(4):349–58.

27. Yui S, Azzolin L, Maimets M, Pedersen MT, Fordham RP, Hansen SL, et al. YAP/TAZ-Dependent Reprogramming of Colonic Epithelium Links ECM Remodeling to Tissue Regeneration. Cell Stem Cell. 2018 Jan 4;22(1):35-49.e7.

28. Ayyaz A, Kumar S, Sangiorgi B, Ghoshal B, Gosio J, Ouladan S, et al. Single-cell transcriptomes of the regenerating intestine reveal a revival stem cell. Nature [Internet]. 2019; Available from: http://dx.doi.org/10.1038/s41586-019-1154-y

29. Nusse YM, Savage AK, Marangoni P, Rosendahl-Huber AKM, Landman TA, De Sauvage FJ, et al. Parasitic helminths induce fetal-like reversion in the intestinal stem cell niche. Nature. 2018 Jul 5;559(7712):109–13.

30. Wang Y, Chiang IL, Ohara TE, Fujii S, Cheng J, Muegge BD, et al. Long-Term Culture

Captures Injury-Repair Cycles of Colonic Stem Cells. Cell [Internet]. 2019;179(5):1144-1159.e15. Available from: https://doi.org/10.1016/j.cell.2019.10.015

31. Eggers B, Marciniak J, Deschner J, Stope MB, Mustea A, Kramer FJ, et al. Cold atmospheric plasma promotes regeneration-associated cell functions of murine cementoblasts in vitro. Int J Mol Sci. 2021 May 2;22(10).

32. Kwong M, Kan YW, Chan JY. The CNC basic leucine zipper factor, Nrf1, is essential for cell survival in response to oxidative stress-inducing agents. Role for Nrf1 in γ-gcs(L) and gss expression in mouse fibroblasts. J Biol Chem. 1999 Dec 24;274(52):37491–8.

33. Tanigawa S, Lee CH, Lin CS, Ku CC, Hasegawa H, Qin S, et al. Jun dimerization protein 2 is a critical component of the Nrf2/MafK complex regulating the response to ROS homeostasis. Cell Death Dis. 2013;4(11).

34. Tabuchi Y, Uchiyama H, Zhao QL, Yunoki T, Andocs G, Nojima N, et al. Effects of nitrogen on the apoptosis of and changes in gene expression in human lymphoma U937 cells exposed to argon-based cold atmospheric pressure plasma. Int J Mol Med. 2016 Jun 1;37(6):1706–14.

35. Kou L, Jiang X, Huang H, Lin X, Zhang Y, Yao Q, et al. The role of transporters in cancer redox homeostasis and cross-talk with nanomedicines. Vol. 15, Asian Journal of Pharmaceutical Sciences. Shenyang Pharmaceutical University; 2020. p. 145–57.

36. Semmler ML, Bekeschus S, Schäfer M, Bernhardt T, Fischer T, Witzke K, et al. Molecular mechanisms of the efficacy of cold atmospheric pressure plasma (CAP) in cancer treatment [Internet]. Vol. 12, Cancers. MDPI AG; 2020 [cited 2020 Feb 21]. Available from: http://www.ncbi.nlm.nih.gov/pubmed/31979114

37. Fodde R. The APC gene in colorectal cancer. Eur J Cancer. 2002;38(7):867–71.

38. Malki A, Elruz RA, Gupta I, Allouch A, Vranic S, Al Moustafa AE. Molecular mechanisms of colon cancer progression and metastasis: Recent insights and advancements. Vol. 22, International Journal of Molecular Sciences. MDPI AG; 2021. p. 1–24.

39. El Marjou F, Janssen KP, Chang BHJ, Li M, Hindie V, Chan L, et al. Tissue-specific and inducible Cre-mediated recombination in the gut epithelium. Genesis. 2004 Jul;39(3):186–93.

40. Robanus-Maandag EC, Koelink PJ, Breukel C, Salvatori DCF, Jagmohan-Changur SC, Bosch

CAJ, et al. A new conditional Apc-mutant mouse model for colorectal cancer. Carcinogenesis. 2010 Feb 22;31(5):946–52.

41. Vallone V, Leprovots M, Vassart G, Garcia M-I. Ex vivo Culture of Fetal Mouse Gastric Epithelial Progenitors. BIO-PROTOCOL. 2017;7(1).

42. Bastin O, Thulliez M, Servais J, Nonclercq A, Delchambre A, Hadefi A, et al. Optical and electrical characteristics of an endoscopic DBD plasma jet. Plasma Med. 2020;10(2):71–90.

43. Garcia MI, Ghiani M, Lefort A, Libert F, Strollo S, Vassart G. LGR5 deficiency deregulates Wnt signaling and leads to precocious Paneth cell differentiation in the fetal intestine. Dev Biol. 2009 Jul 1;331(1):58–67.

44. Mustata RC, Van Loy T, Lefort A, Libert F, Strollo S, Vassart G, et al. Lgr4 is required for Paneth cell differentiation and maintenance of intestinal stem cells ex vivo. EMBO Rep. 2011;12(6):558–64.

45. Subramanian A, Tamayo P, Mootha VK, Mukherjee S, Ebert BL, Gillette MA, et al. Gene set enrichment analysis: A knowledge-based approach for interpreting genome-wide expression profiles. Proc Natl Acad Sci U S A. 2005 Oct 25;102(43):15545–50.

46. Babicki S, Arndt D, Marcu A, Liang Y, Grant JR, Maciejewski A, et al. Heatmapper: web-enabled heat mapping for all. Nucleic Acids Res. 2016 Jul 8;44(W1):W147–53.

47. Oliveros JC (2007-2015). Venny 2.1.0 [Internet]. An interactive tool for comparing lists with Venn's diagrams. [cited 2021 Sep 25]. Available from: https://bioinfogp.cnb.csic.es/tools/venny/index.html

48. Fernandez Vallone V, Leprovots M, Ribatallada-Soriano D, Gerbier R, Lefort A, Libert F, et al. LGR 5 controls extracellular matrix production by stem cells in the developing intestine . EMBO Rep. 2020 Jul 3;21(7).

ACKNOWLEDGMENTS

We are grateful to Sylvie Robine for providing the Vil1-cre/ERT2$^{23Syr/J}$ mouse strain. We acknowledge the contribution of a medical writer, Sandy Field, PhD, for English language editing of this manuscript.

CONFLICT OF INTEREST STATEMENT

The authors have nothing to disclose.

AUTHOR CONTRIBUTION STATEMENT

AH, ML, OB, MT: study concept and design, acquisition of data, analysis and interpretation of data, statistical analysis, drafting of the ms

JD, AN, AD, FR: study concept and design, study supervision, critical revision of the ms, obtained funding

MIG: study concept and design, acquisition of data, analysis and interpretation of data, drafting of the ms, study supervision, obtained funding.

ETHIC STATEMENTS

Animal procedures complied with the guidelines of the European Union and were approved by the local ethics committee CEBEA from Erasme-Faculty of Medicine under the accepted protocol 713N.

FUNDING STATEMENTS

This work was supported by the "Actions de recherche concertées" (ARC, Collective Research Initiatives), the non-for-profit Association Recherche Biomédicale et Diagnostic (ARBD), and the Fondation Michel Cremer.

FIGURE LEGENDS

Figure 1. CAP treatment affects normal growth of intestinal stem cell-derived organoid cultures. **a**. The CAP system allows for generation of a helium CAP that can be transported over long distances for applications in endoscopy. **b**. Direct CAP treatment on organoid cultures generated from small intestine isolated crypts. **c**. Representative pictures of a given field showing growth of CAP-treated or untreated organoids at day 1 (before CAP application) and day 5 (endpoint). Survival rate (%) at day 5 vs day 1, indicated below the images, is expressed as the mean ± SEM (n=4 organoid lines generated from different mice). Curved and straight arrows show fully protruded organoid and spheroid, respectively. Arrowheads indicate declining organoids. Scale bars: 500 µm. **d**. Quantification of organoid complexity at day 5. Representative element categories (Spheroids and Organoids) are defined morphologically on the right. An average number of 195 elements was analyzed per condition per organoid line (n= 3 organoid lines). Data are represented as means ± sem. Two-way ANOVA: interaction **** P< 0.0001 followed by Tukey's multiple comparisons test: a: compared to Untreated conditions, b: compared to 60 s/ 0 W conditions **P< 0.01; ***P< 0.001; ****P< 0.0001.

Figure 2. Impact of the CAP application method on organoid morphology and global gene expression. a. CAP treatment (50 W/60 s) was applied directly to organoid cultures at day 1 (post-replating) for 30 minutes, 3 hours or 24 hours. Then fresh medium was provided until day 3 (endpoint). Alternatively, naïve organoids were cultured at day 1 for 24 hours with freshly-generated CAP-conditioned media (Indirect CAP) or plasma-activated media (PAM). At day 2 (post-replating), fresh culture medium was provided for a further 24 hours until day 3 (endpoint). **b**. Representative pictures of a given field showing organoid growth at day 1 (before CAP application) and day 3. Arrowheads and triangles show individual elements evolving as protruded organoids and spheroids, respectively. Asterisks indicate dying elements. Scale bars: 500 µm. **c**. Quantification of organoid complexity at day 3. An average number of 100 elements was analyzed per condition per organoid line (n= 4 organoid lines). Data are represented as means ± sem. Two-way ANOVA: interaction **** P< 0.0001 followed by Tukey's multiple comparisons test: a, d: ****P< 0.0001, b: ***P< 0.001, c: *P< 0.05. (all compared to untreated). Time of exposure to CAP treatment is indicated (30', 3 h, 1 day) ID: Indirect CAP. **d**.

Heatmap of differentially regulated genes in CAP-treated vs Untreated (Controls) organoids. Samples were treated with CAP directly (Direct), for 30 min (30') or 24 hours between day 1 and day 2 (1 d); indirectly (Indirect) or with PAM for 24 hours between day 1 and day 2 (1 d) or between day 2 and day 3 (2 d). Some of the most-modulated genes are indicated on the right side. **e**. GSEA-Biological processes for upregulated and downregulated gene lists in CAP-treated vs untreated Controls.

Figure 3. CAP treatment decreases the intestinal stem cell pool. a. Venn diagram showing that part of the downregulated gene list in CAP-treated samples vs controls (135 out of 1195 genes) corresponds to the ISC (Intestinal Stem Cell)-associated signature. **b**. Expression levels of some genes of the ISC-associated signature commonly downregulated in CAP-treated organoids vs Untreated controls. CP20M: counts per kilobase of transcript per 20 million mapped reads. Data are represented as means ± sd. n = 4 and 3 samples in Controls and CAP-treated conditions, respectively. **c**. Expression of *Lgr5*, *Axin2*, and *Pycard* genes detected in organoids by RNAscope at day 3. **d**. Immunofluorescence showing Olfm4-expressing cells in organoids at day 3 (red arrows). Cell membranes shown with β-catenin and nuclei counterstained with DAPI. Right panel: Expression levels of *Olfm4* in the various conditions reported in CP20M. Scale bars: 50 µm (panels c and d).

Figure 4. CAP treatment of organoids is associated with Apoptosis. a. Expression levels of DNA repair and apoptosis-related genes in the various conditions reported in CP20M. Data are represented as means ± sd. n = 4 and 3 samples in Controls and CAP-treated conditions, respectively. **b**. Organoid sections were stained with TUNEL for apoptotic cells (visualized by pink asterisks). Cell membranes are shown with β-catenin and nuclei were counterstained with DAPI. Scale bars: 50 µm**.**

Figure 5. CAP treatment induces a global response to reactive species in intestinal stem cell-derived organoids. a. Expression levels of Pro-survival, regeneration and oxidative stress-associated genes in the various conditions reported in CP20M. Data are represented as means ± sd. n = 4 and 3 samples in Controls and CAP-treated conditions, respectively. **b**. Venn diagram showing that part of the upregulated gene list in CAP-treated vs control organoids (50 out of 1267 genes) corresponds to the Trop-2-associated regeneration signature. **c**. Immunofluorescence showing Trop2-expressing cells (visualized by green asterisks) in organoids at day 3. Cell membranes shown with β-catenin and nuclei

559 counterstained with DAPI. **d**. Expression of *Areg*, *Pparg*, and *Hmox1* genes detected in organoids by
560 RNAscope at day 3. Scale bars: 50 µm (panels c and d).

561 **Figure 6. Apc deficient-derived organoids exhibit increased resistance to CAP treatment as**
562 **compared to normal ISC-derived organoids. a.** CAP treatment was applied directly to Apc wt or Apc
563 Δ (Apc-deficient) organoid cultures at day 1 post-replating for 24 hours. Fresh medium was added at
564 days 2 and 4. **b**. Representative pictures of a given organoid type (Apc wt or Apc Δ) at day 5 following
565 CAP treatment at the indicated doses. Scale bars: 500 µm. **c**. Left panel: organoid survival rate (in %).
566 An average number of 120 elements was studied over time per condition per organoid line (n= 6 Apc
567 wt and 5 Apc Δ organoid lines, respectively). Data are represented as means ± sem. Two-way ANOVA:
568 CAP dose ***/Genotype **** P< 0.0001 followed by Sidak's multiple comparisons test: a, ***P<
569 0.001; b, ***P< 0.01; c, *P< 0.05; ns: not significant (all compared to Apc wt-0 W), Right panel:
570 quantification of total RNA extracted/sample at day 5. Each symbol corresponds to a given organoid
571 line. Two-way ANOVA: CAP dose * P< 0.05/Genotype **** P< 0.0001 followed by Sidak's multiple
572 comparisons test: a, ****P< 0.0001; b, *P< 0.05; c, **P< 0.01. (all compared to Apc wt-0 W). **d**. Gene
573 expression analysis by qRT-PCR of the indicated stem cell and differentiation markers. Each symbol
574 corresponds to a given organoid line. Values are normalized to Untreated Apc wt levels. Data are
575 represented as means ± sem. One-way Anova test. **** P< 0.0001; **** P< 0.001; **P< 0.01; *P<
576 0.05; ns: not significant.

577 **Figure 7. Apc deficient-derived organoids exhibit increased resistance to CAP treatment as**
578 **compared to normal intestinal stem cell-derived organoids. a.** Design of the experiment. See Figure
579 Legend Fig. 6a. **b**. Gene expression analysis by qRT-PCR of the indicated markers involved in
580 regeneration, cell growth/apoptosis and response to stress. Each symbol corresponds to a given organoid
581 line. Values are normalized to Untreated Apc wt levels. Data are represented as means ± sem. One-way
582 Anova test. **** P< 0.0001; **** P< 0.001; **P< 0.01; P< 0.05; ns: not significant.

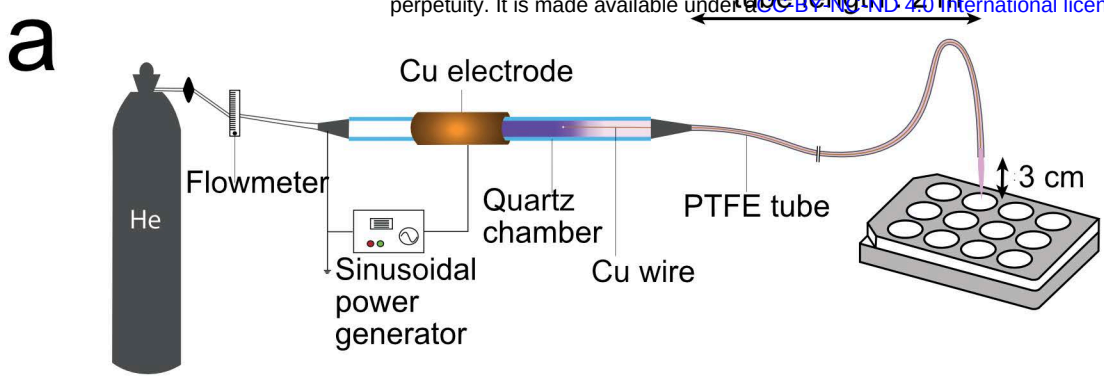

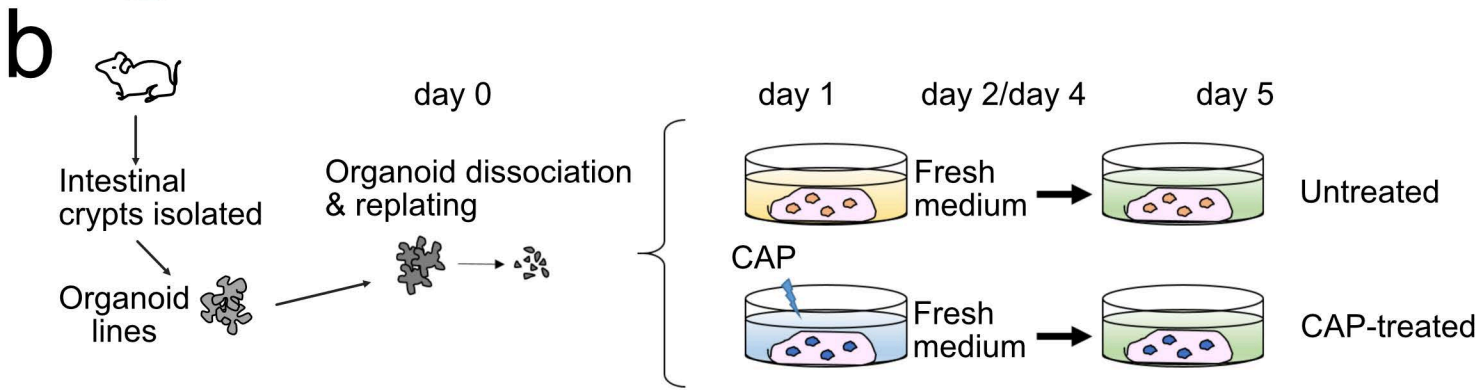

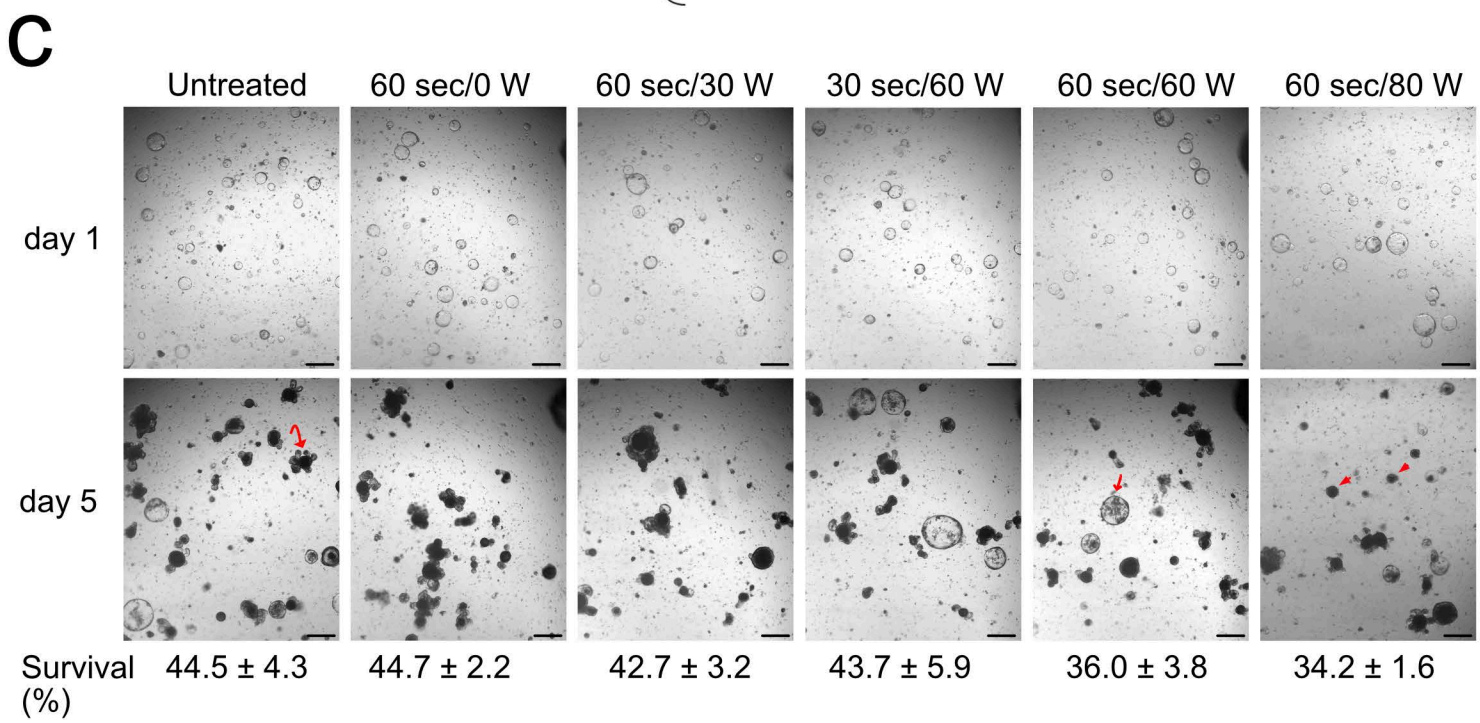

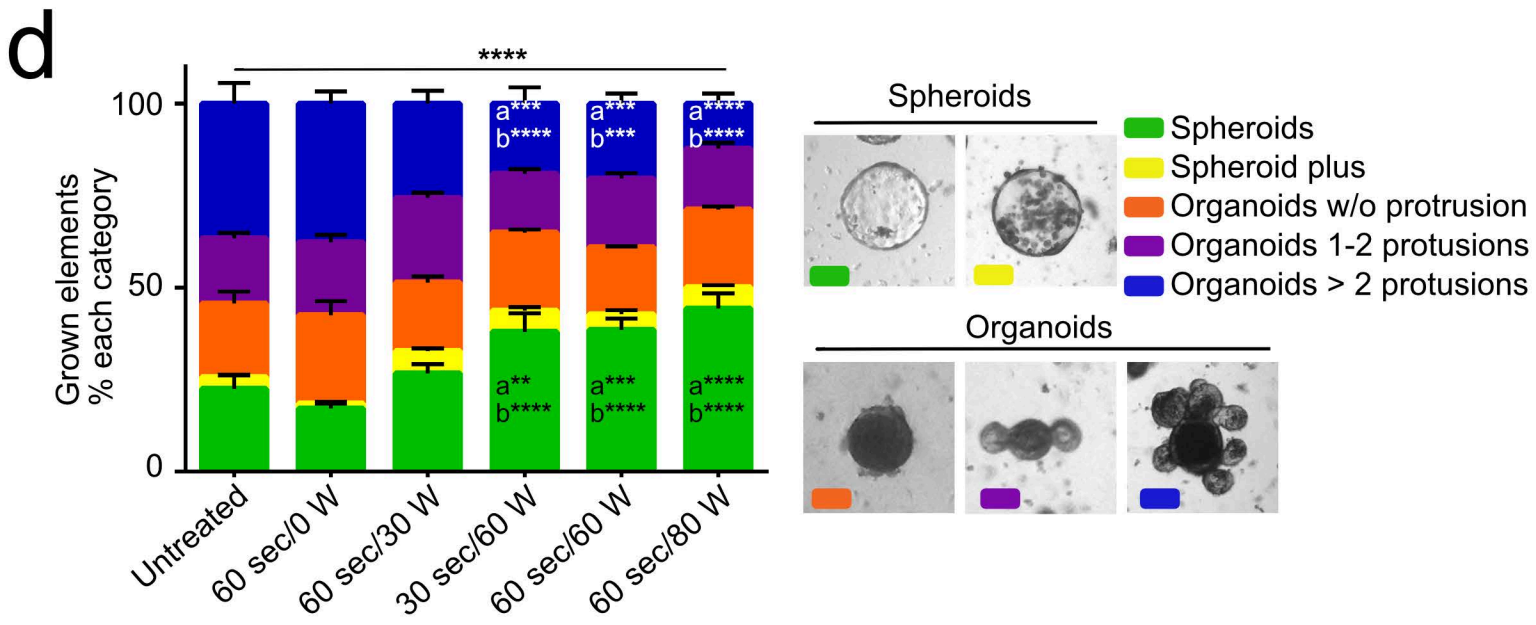

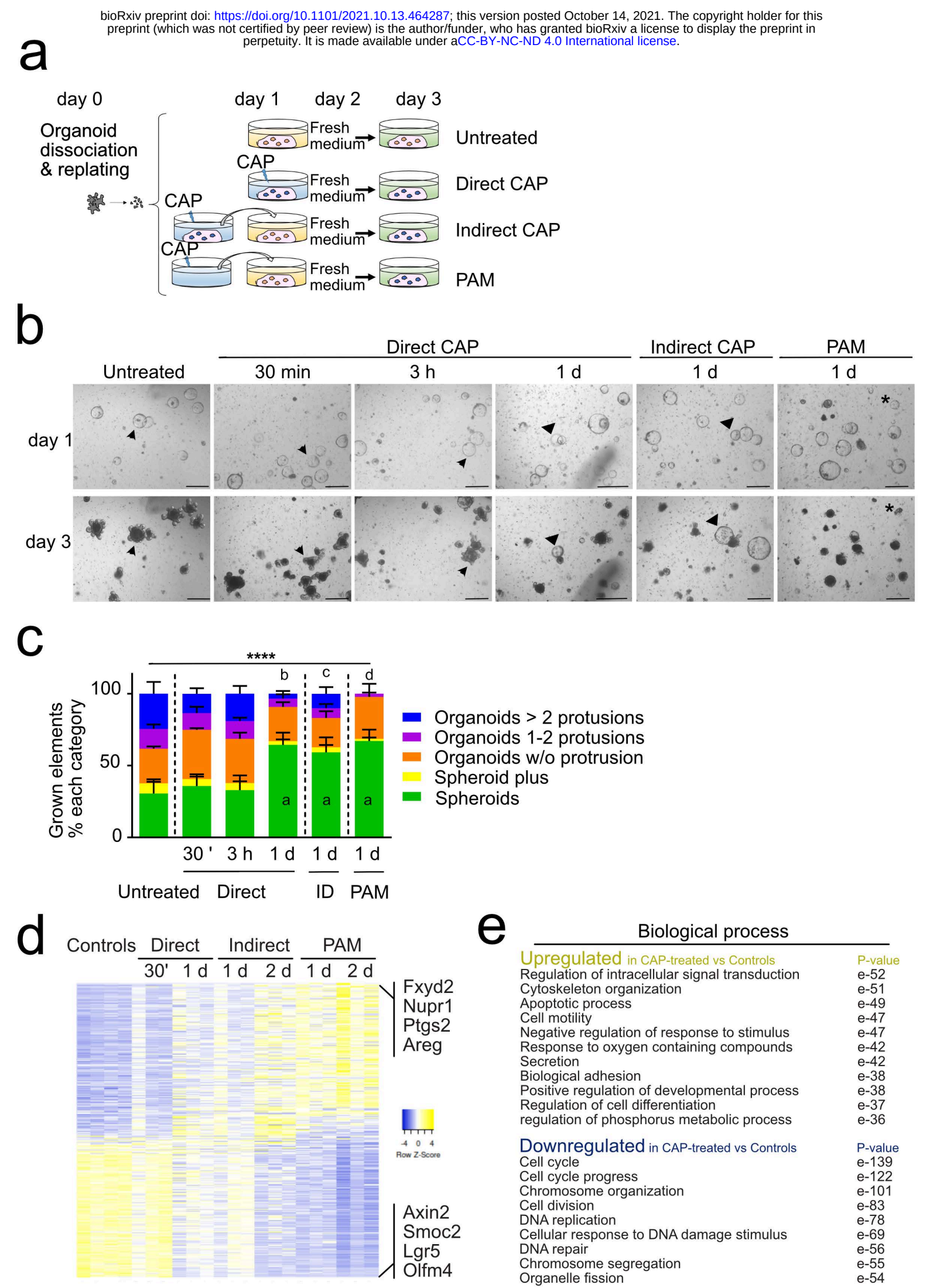

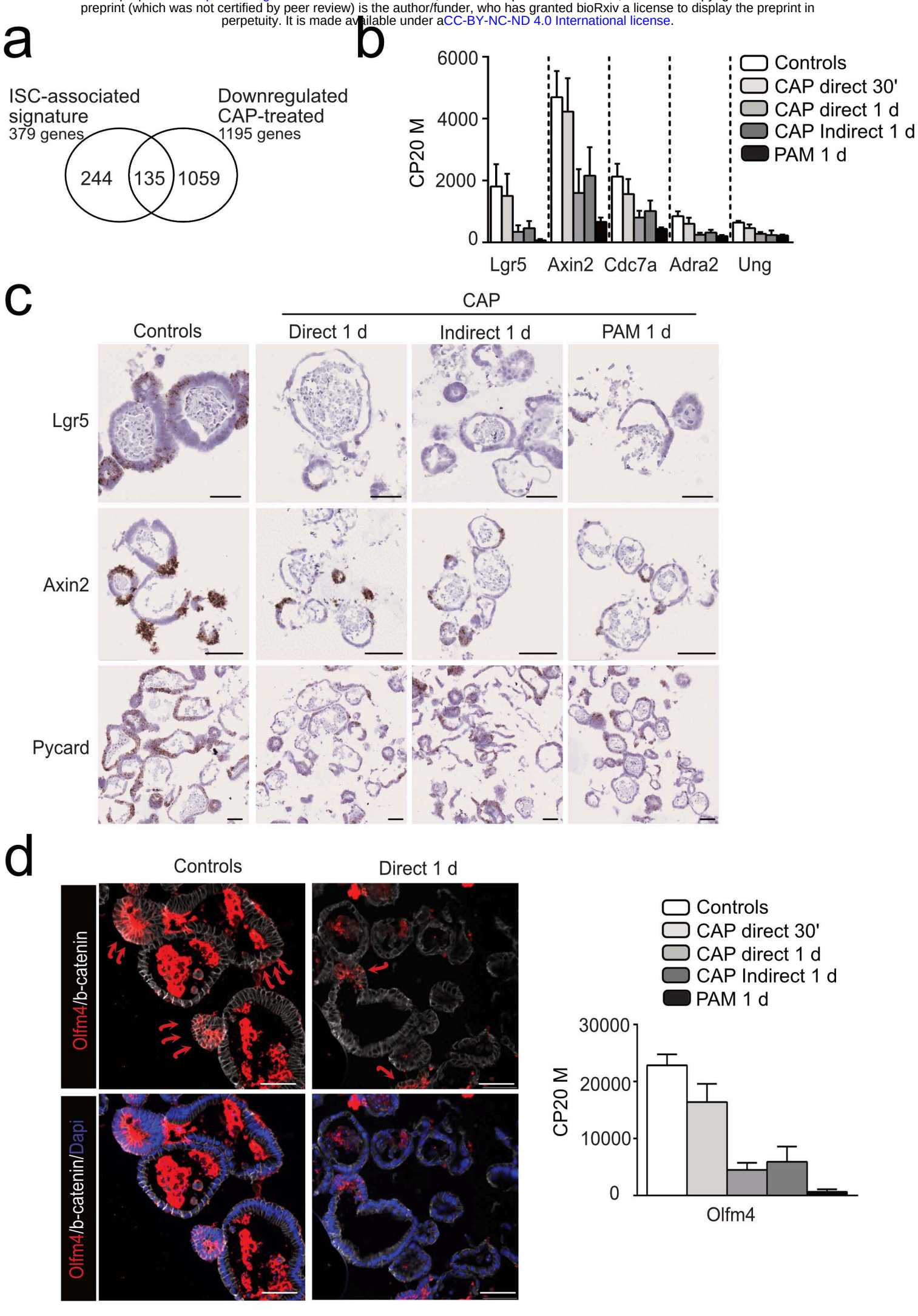

a

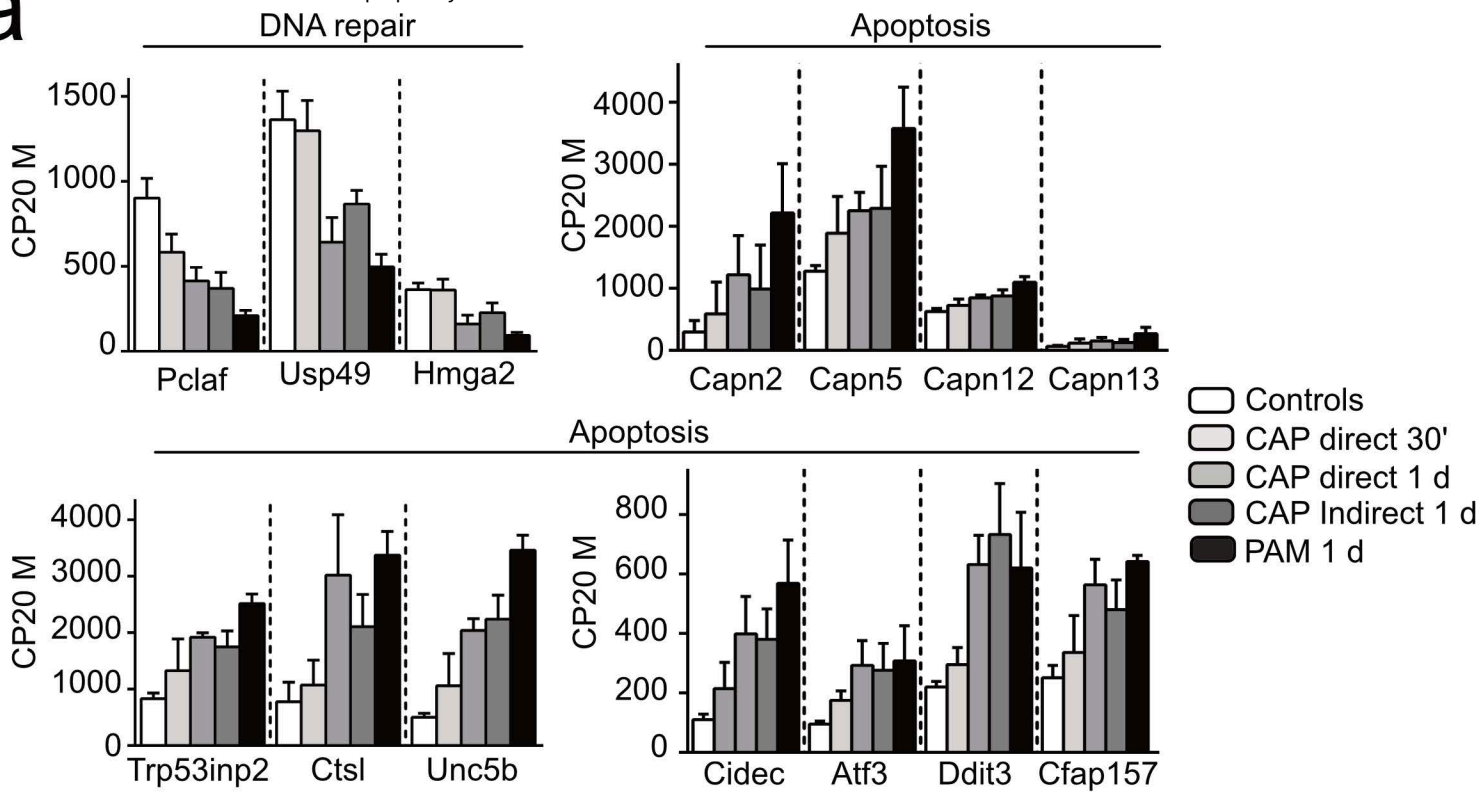

b

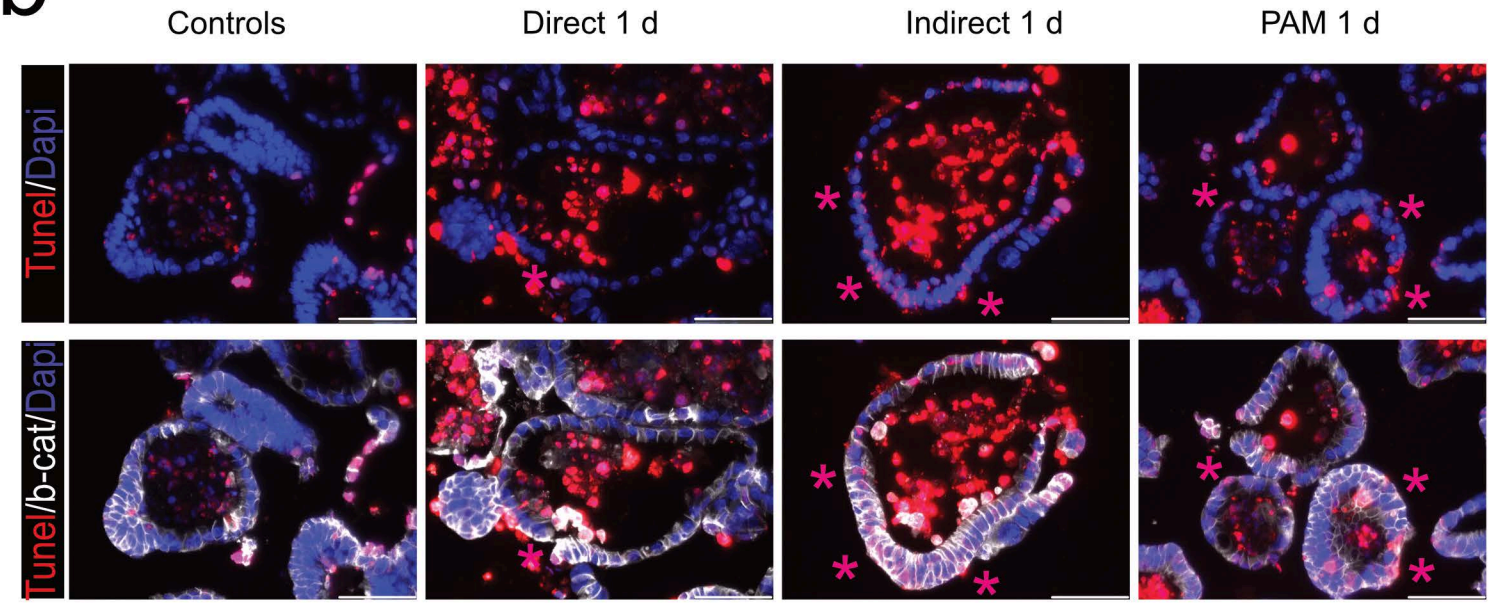

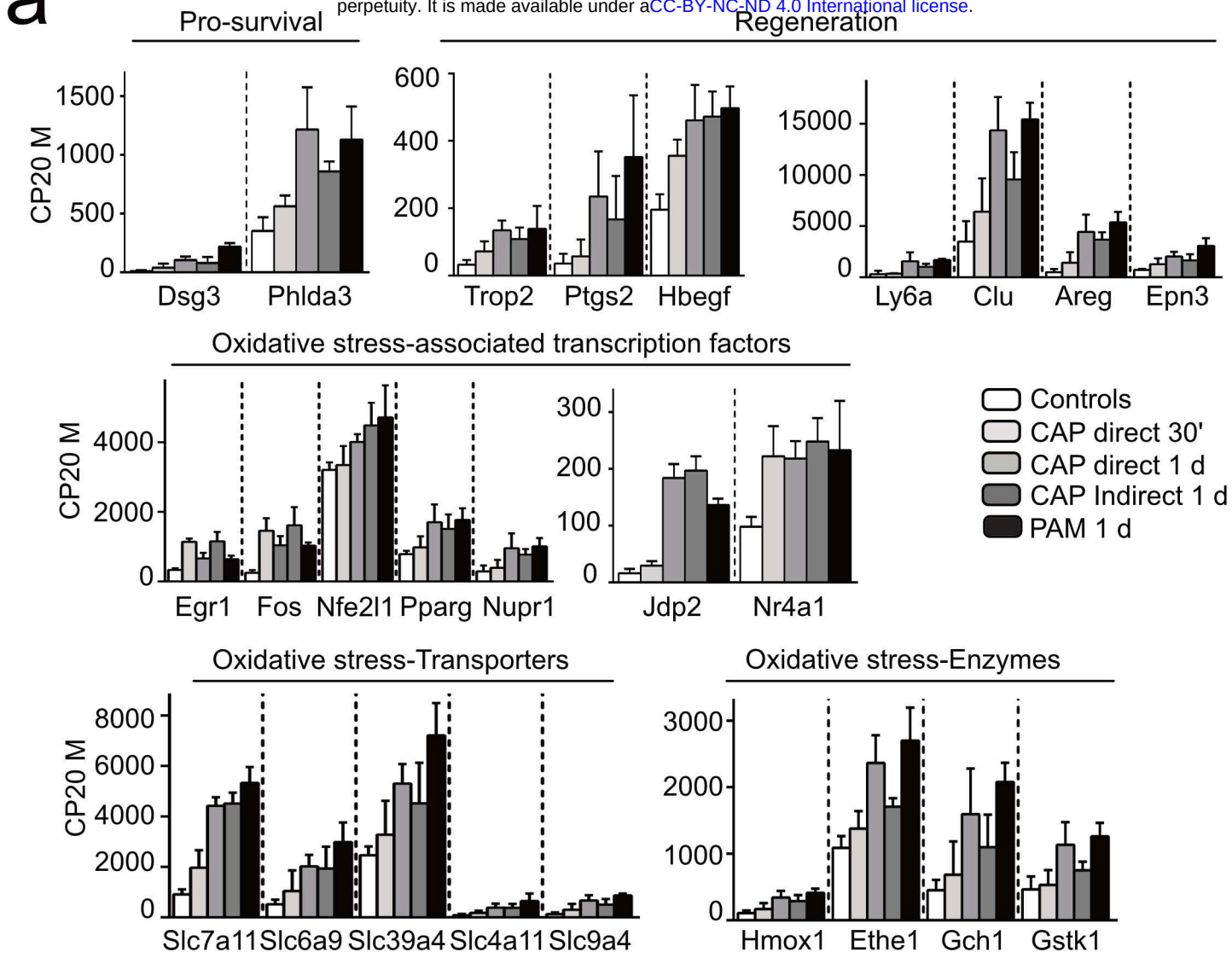

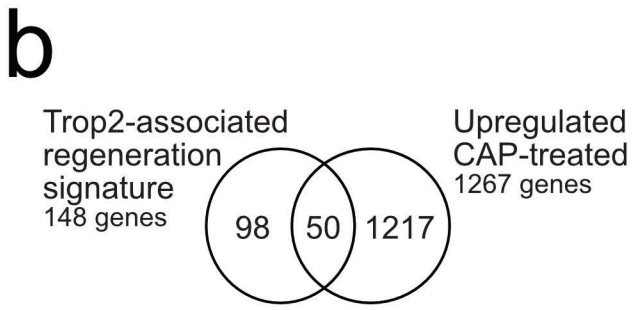

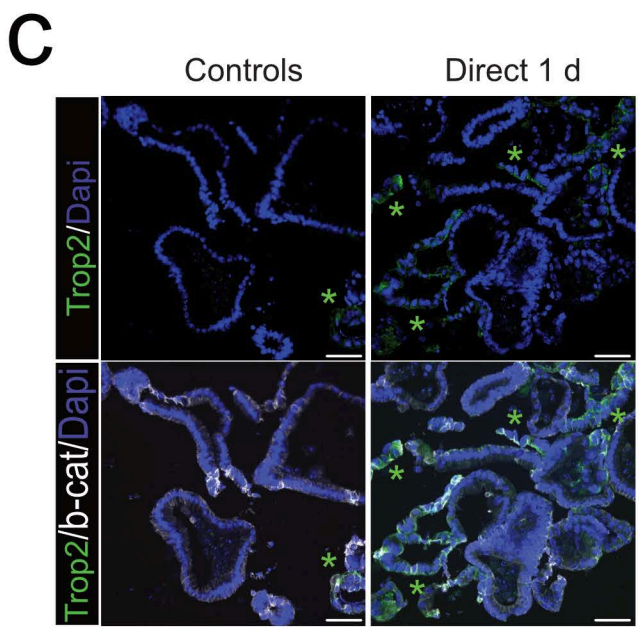

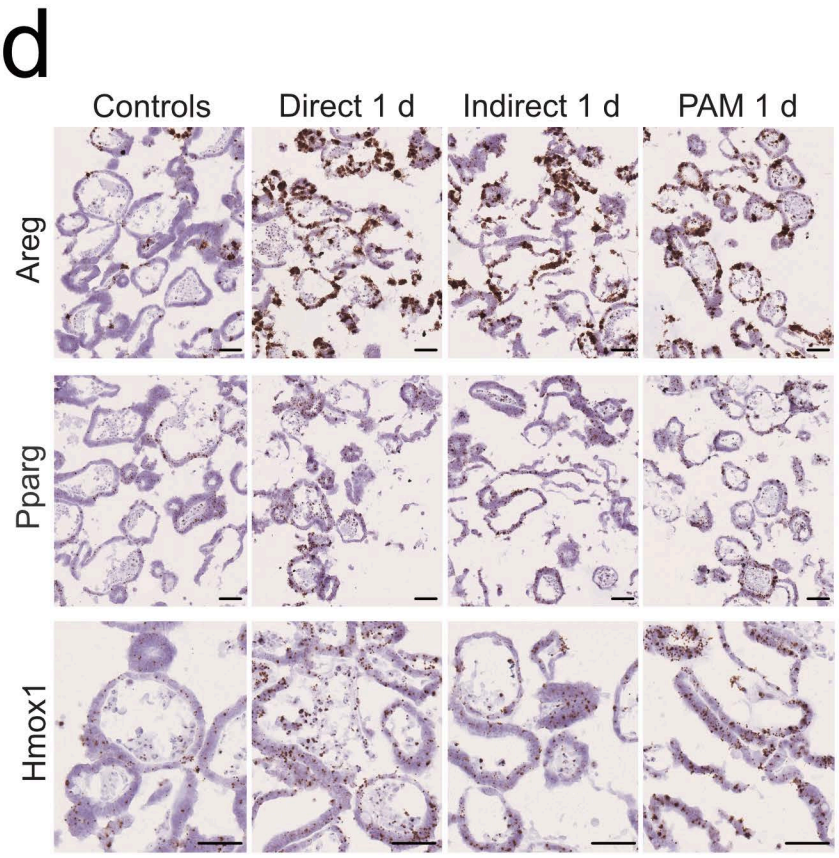

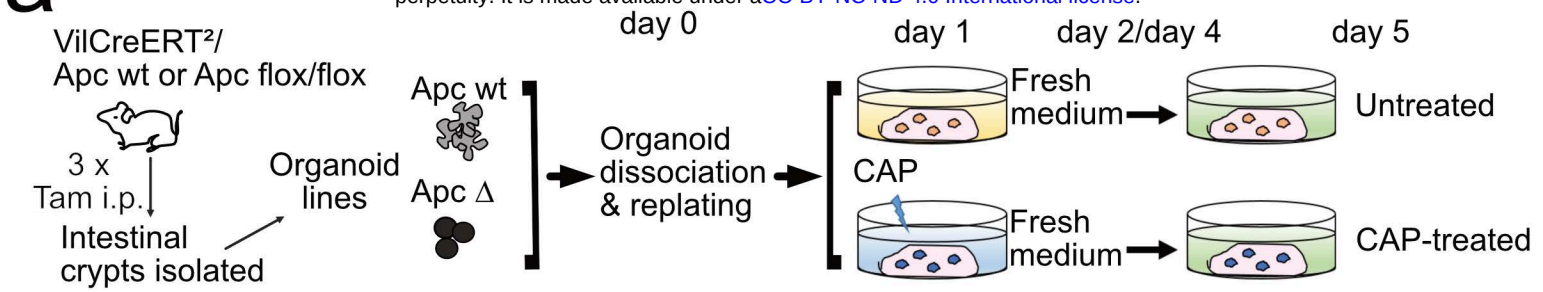

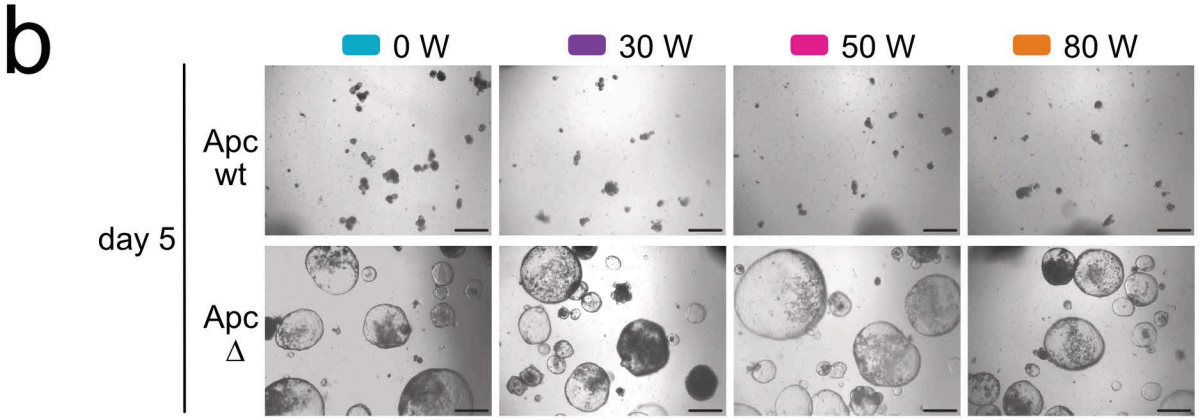

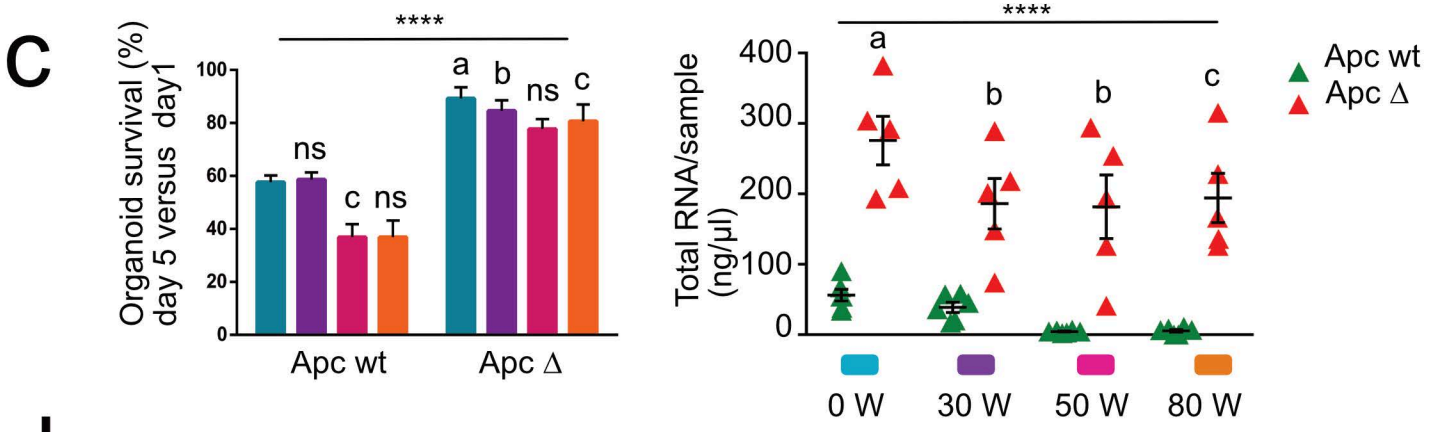

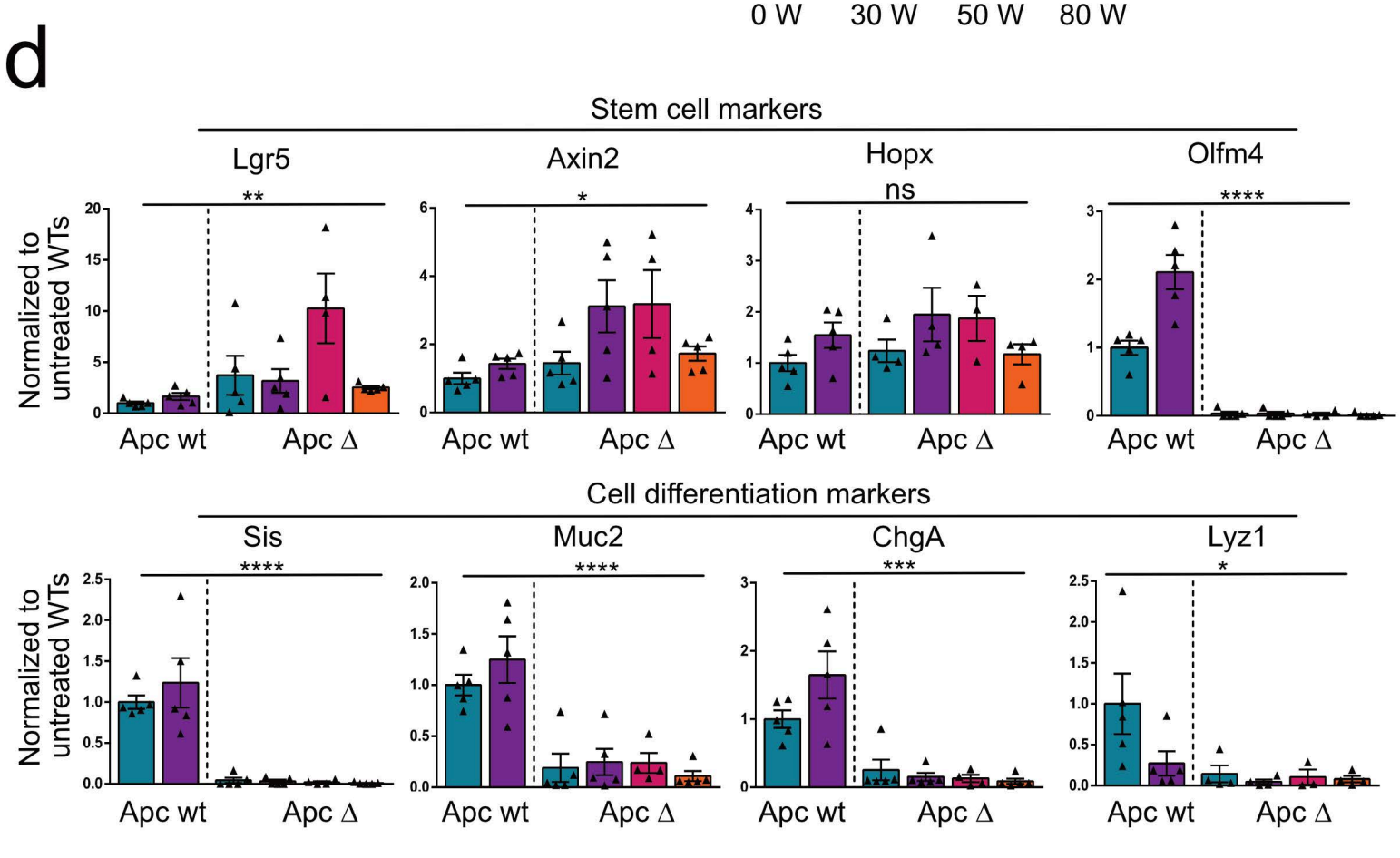

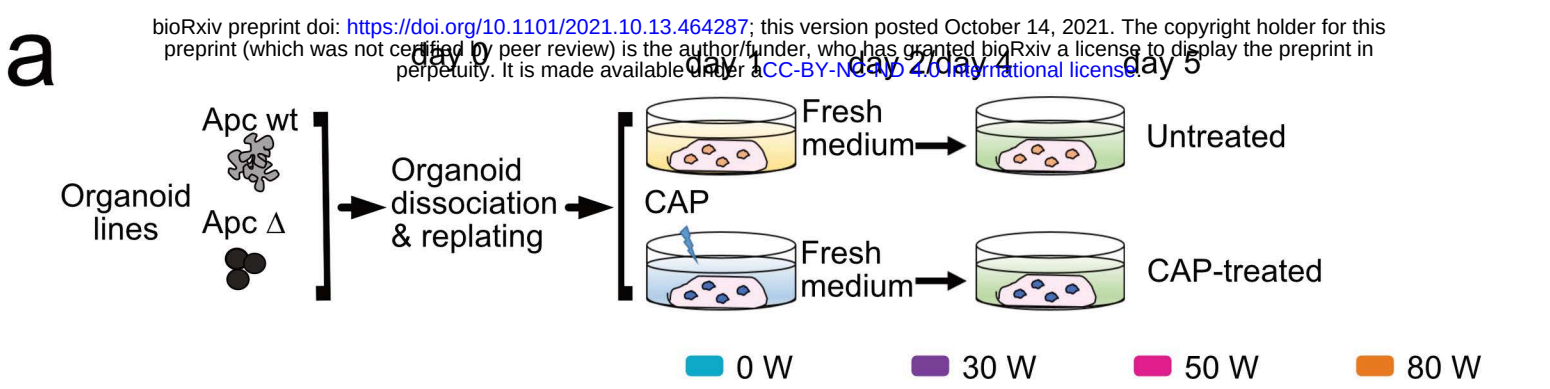

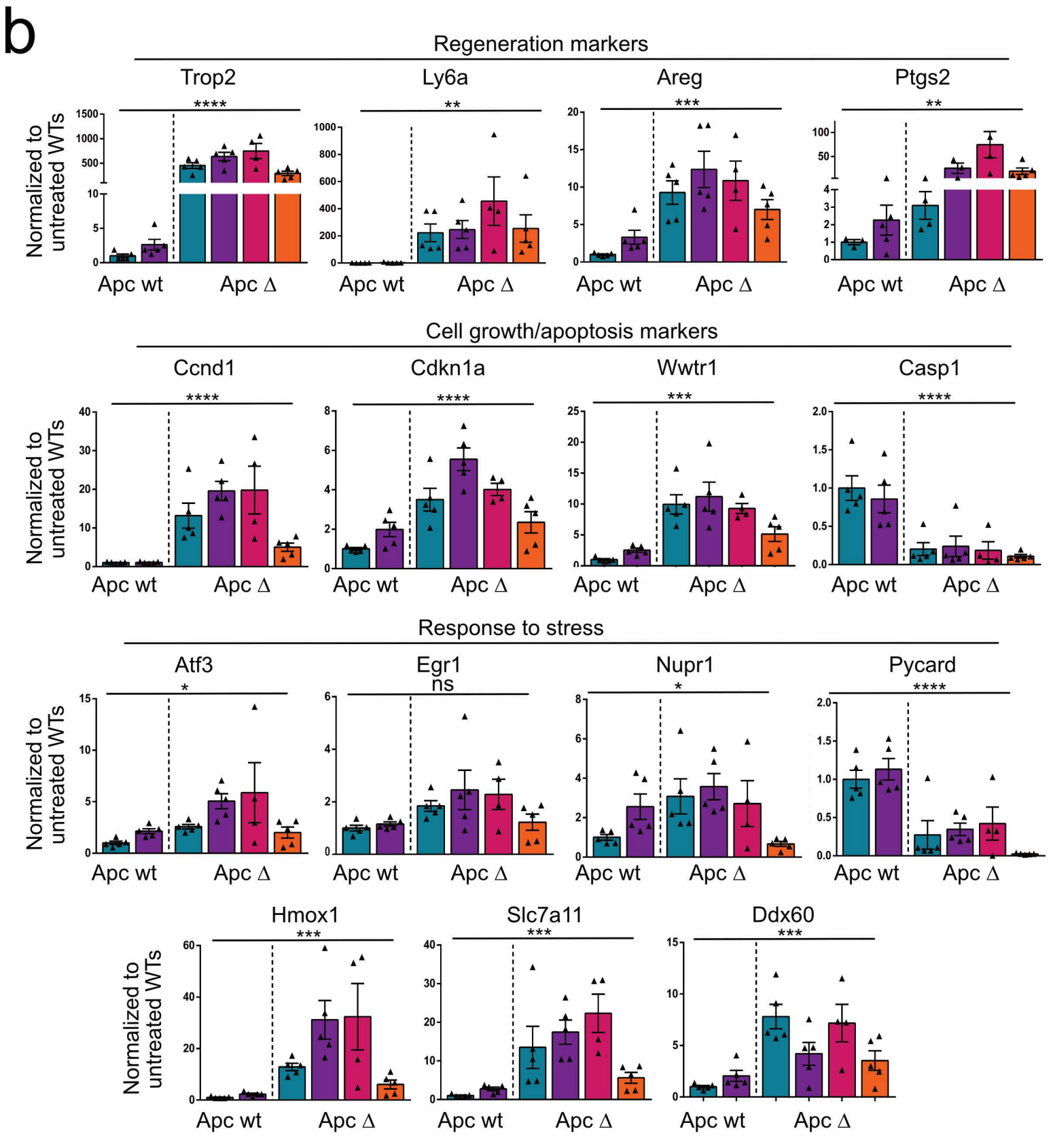

Table 1: List of genes involved in redox control

ROS scavengers

Gene-ID	Gene-Name	Gene-Description	C-CD1 S73 1	C-WT2 S74	C-1-20 S75 3	C-2-20 S76 4	D-2-30 S77	D-CD1-30 S	D-WT2-30 S	D-2-24 S80	D-CD1-24 S	D-WT2-24 S	I-2-30 S83 1	I-CD1-30 S8	I-WT2-30 S8	I-2-24 S86 1	I-CD1-24 S8	I-WT2-24 S8	PAM-2-30 S	PAM-CD1-30	PAM-WT2-30	PAM-2-24 S	PAM-CD1-24	24 S94 22	Gene-Name	Mean Ctrl	Mean Direct 30'	Mean Direct 1 d	Mean Indirect 1 d	Mean Indirect 2d	Mean PAM 1 d	Mean PAM 2d
ENSMUSG00000022982	Sod1	superoxide dismutase 1 soluble [Source:MGI Symbol;Acc:MGI:98351]	6276	7641	5946	6115	4366	5911	5635	6395	6128	6028	4568	5585	5746	5043	5806	5615	5178	4994	5871	5275	5974	6144	Sod1	6494.5	5304.0	6183.7	5299.7	5488.0	5347.7	5624.5
ENSMUSG00000006818	Sod2	superoxide dismutase 2 mitochondrial [Source:MGI Symbol;Acc:MGI:98352]	2482	2678	2400	2384	1924	2267	2191	2462	2254	2073	2000	2190	2061	1729	1971	1591	1844	1923	1848	1180	1777	1297	Sod2	2486.0	2127.3	2263.0	2083.7	1763.7	1871.7	1478.5
ENSMUSG00000072941	Sod3	superoxide dismutase 3 extracellular [Source:MGI Symbol;Acc:MGI:103181]	2	3	5	5	5	4	3	6	6	7	4	3	3	3	4	2	6	6	5	4	1	1	Sod3	3.8	4.0	6.3	3.3	3.0	5.7	2.5
ENSMUSG00000063856	Gpx1	glutathione peroxidase 1 [Source:MGI Symbol;Acc:MGI:104887]	5127	7840	7676	6220	5749	6902	5985	9353	9298	7113	6111	6392	6357	5950	6305	5392	7141	7183	7968	5351	6250	6307	Gpx1	6715.8	6212.0	8588.0	6286.7	5882.3	7430.7	5800.5
ENSMUSG00000042808	Gpx2	glutathione peroxidase 2 [Source:MGI Symbol;Acc:MGI:106609]	6975	7061	7988	7549	7160	7675	8265	10882	9842	7611	6936	7970	6920	8259	9411	6323	7320	8194	7537	11073	7790	4533	Gpx2	7393.3	7700.0	9445.0	7275.3	7997.7	7683.7	9431.5
ENSMUSG00000089987	Gpx2-ps1	glutathione peroxidase 2 pseudogene 1 [Source:MGI Symbol;Acc:MGI:106627]	18	11	13	4	7	9	17	6	14	13	1	18	11	5	25	8	6	14	15	4	14	7	Gpx2-ps1	11.5	11.0	11.0	10.0	12.7	11.7	9.0
ENSMUSG00000018339	Gpx3	glutathione peroxidase 3 [Source:MGI Symbol;Acc:MGI:105102]	19	22	48	47	49	26	34	58	35	46	64	35	50	72	38	53	73	47	50	95	48	67	Gpx3	34.0	36.3	46.3	49.7	54.3	56.7	71.5
ENSMUSG00000075706	Gpx4	glutathione peroxidase 4 [Source:MGI Symbol;Acc:MGI:104767]	3400	4981	4883	3932	3539	3880	4009	6686	5608	4648	3796	3965	4671	4974	4370	4582	4806	4031	5392	4859	5268	6287	Gpx4	4299.0	3809.3	5647.3	4144.0	4642.0	4743.0	5063.5
ENSMUSG00000004344	Gpx5	glutathione peroxidase 5 [Source:MGI Symbol;Acc:MGI:104886]	0	0	0	0	0	0	0	0	0	0	0	2	0	0	0	0	0	0	0	0	0	0	Gpx5	0.0	0.0	0.0	0.7	0.0	0.0	0.0
ENSMUSG00000004341	Gpx6	glutathione peroxidase 6 [Source:MGI Symbol;Acc:MGI:1922762]	0	0	0	0	0	0	0	1	0	0	0	0	0	0	0	0	0	0	0	0	0	0	Gpx6	0.0	0.0	0.3	0.0	0.0	0.0	0.0
ENSMUSG00000028597	Gpx7	glutathione peroxidase 7 [Source:MGI Symbol;Acc:MGI:1914555]	9	3	4	5	6	4	5	3	0	6	3	3	4	6	3	5	4	5	7	20	1	19	Gpx7	5.3	5.0	3.0	3.3	4.7	5.3	10.5
ENSMUSG00000021760	Gpx8	glutathione peroxidase 8 (putative) [Source:MGI Symbol;Acc:MGI:1916840]	2	0	3	0	0	3	0	3	1	0	2	4	2	1	0	0	3	2	0	1	0	0	Gpx8	1.3	1.0	1.3	2.7	0.3	1.7	0.5
ENSMUSG00000028691	Prdx1	peroxiredoxin 1 [Source:MGI Symbol;Acc:MGI:99523]	8941	10608	10647	9960	8201	9105	8982	12952	10278	9033	8614	8835	8850	7098	7555	7308	8746	9024	9396	5486	8157	8058	Prdx1	10039.0	8762.7	10754.3	8766.3	7320.3	9055.3	6821.5
ENSMUSG00000005161	Prdx2	peroxiredoxin 2 [Source:MGI Symbol;Acc:MGI:109486]	3979	4147	4102	4122	2956	3510	3717	4172	3773	3178	2875	3246	3212	2808	2542	2533	3027	2798	2917	1920	2536	2289	Prdx2	4087.5	3394.3	3707.7	3111.0	2627.7	2914.0	2228.0
ENSMUSG00000083998	Prdx2-rs3	peroxiredoxin 2 related sequence 3 [Source:MGI Symbol;Acc:MGI:1859808]	0	0	0	0	0	0	1	0	0	1	0	2	0	0	1	0	0	0	0	0	0	0	Prdx2-rs3	0.0	0.3	0.3	0.7	0.3	0.0	0.0
ENSMUSG00000024997	Prdx3	peroxiredoxin 3 [Source:MGI Symbol;Acc:MGI:88034]	1773	1819	1871	1783	1316	1738	1678	2148	1787	1598	1544	1733	1620	1268	1239	1227	1337	1455	1231	720	1264	978	Prdx3	1811.5	1577.3	1844.3	1632.3	1244.7	1341.0	992.0
ENSMUSG00000025289	Prdx4	peroxiredoxin 4 [Source:MGI Symbol;Acc:MGI:1859815]	469	411	526	605	283	322	361	401	326	231	236	254	236	199	96	114	193	155	153	115	101	70	Prdx4	502.8	322.0	319.3	242.0	136.3	167.0	108.0
ENSMUSG00000024953	Prdx5	peroxiredoxin 5 [Source:MGI Symbol;Acc:MGI:1859821]	2364	2736	2328	2561	2271	2266	2195	3519	2733	2832	2346	2260	2606	2094	2125	2316	3146	2681	3344	2079	2577	2749	Prdx5	2497.3	2244.0	3028.0	2404.0	2178.3	3057.0	2328.0
ENSMUSG00000026701	Prdx6	peroxiredoxin 6 [Source:MGI Symbol;Acc:MGI:894320]	6338	6753	7470	7000	6951	6801	6893	9029	8121	8168	8102	6993	7506	5203	5485	6111	7724	6959	7856	2790	5771	5309	Prdx6	6890.3	6881.7	8439.3	7533.7	5599.7	7513.0	4280.5
ENSMUSG00000050114	Prdx6b	peroxiredoxin 6B [Source:MGI Symbol;Acc:MGI:1336888]	0	0	0	1	7	2	7	0	1	7	1	5	8	8	6	25	0	2	3	5	2	7	Prdx6b	0.3	5.3	2.7	4.7	13.0	1.7	3.5
ENSMUSG00000083737	Prdx6-ps2	peroxiredoxin 6 pseudogene 2 [Source:MGI Symbol;Acc:MGI:1203519]	0	0	0	0	0	0	0	0	0	0	0	0	0	0	0	0	0	0	0	0	0	0	Prdx6-ps2	0.0	0.0	0.0	0.0	0.0	0.0	0.0
ENSMUSG00000027187	Cat	catalase [Source:MGI Symbol;Acc:MGI:88271]	8875	9412	7286	6820	5530	8551	7757	3729	4839	7361	4290	5969	7329	3004	5314	6427	3925	2984	6076	2278	5714	6370	Cat	8098.3	7279.3	5309.7	5862.7	4915.0	4328.3	3996.0

ROS generating systems

Gene-ID	Gene-Name	Gene-Description	C-CD1 S73 1	C-WT2 S74	C-1-20 S75 3	C-2-20 S76 4	D-2-30 S77	D-CD1-30 S	D-WT2-30 S	D-2-24 S80	D-CD1-24 S	D-WT2-24 S	I-2-30 S83 1	I-CD1-30 S8	I-WT2-30 S8	I-2-24 S86 1	I-CD1-24 S8	I-WT2-24 S8	PAM-2-30 S	PAM-CD1-30	PAM-WT2-30	PAM-2-24 S	PAM-CD1-24	24 S94 22	Gene-Name	Mean Ctrl	Mean Direct 30'	Mean Direct 1 d	Mean Indirect 1 d	Mean Indirect 2d	Mean PAM 1 d	Mean PAM 2d
ENSMUSG00000024066	Xdh	xanthine dehydrogenase [Source:MGI Symbol;Acc:MGI:98973]	4179	3804	1971	3788	7127	5029	4980	4364	3869	6723	5608	4548	6258	4551	3725	5964	5531	2852	6156	3536	4449	6238	Xdh	3435.5	5712.0	4985.3	5471.3	4746.7	4846.3	3992.5
ENSMUSG00000064341	mt-Nd1	mitochondrially encoded NADH dehydrogenase 1 [Source:MGI Symbol;Acc:MGI:101787]	22769	24356	20043	18952	18097	25623	25322	21911	23590	20312	19424	28240	22881	10948	14176	11049	14241	15896	17869	9032	14661	10550	mt-Nd1	21530.0	23014.0	21937.7	23515.0	12057.7	16002.0	11846.5
ENSMUSG00000064345	mt-Nd2	mitochondrially encoded NADH dehydrogenase 2 [Source:MGI Symbol;Acc:MGI:102500]	10376	10980	9394	8065	8216	11216	11110	7405	9668	8183	7555	11475	9341	3314	4559	3258	4948	6224	7381	2568	4767	3141	mt-Nd2	9703.8	10180.7	8418.7	9457.0	3710.3	6184.3	3667.5
ENSMUSG00000064360	mt-Nd3	mitochondrially encoded NADH dehydrogenase 3 [Source:MGI Symbol;Acc:MGI:102499]	13	14	4	3	3	16	13	1	5	2	1	10	5	0	7	0	1	9	6	0	10	2	mt-Nd3	8.5	10.7	2.7	5.3	2.3	5.3	5.0
ENSMUSG00000064363	mt-Nd4	mitochondrially encoded NADH dehydrogenase 4 [Source:MGI Symbol;Acc:MGI:102498]	6416	6574	5730	4921	5556	7319	6014	3966	5458	4544	4245	6847	5232	1833	2283	1626	2601	3688	3789	1408	2551	1474	mt-Nd4	5910.3	6296.3	4656.0	5441.3	1914.0	3359.3	1979.5
ENSMUSG00000065947	mt-Nd4l	mitochondrially encoded NADH dehydrogenase 4L [Source:MGI Symbol;Acc:MGI:102497]	8	8	4	1	3	13	13	2	4	2	0	8	4	0	4	0	0	8	5	0	7	2	mt-Nd4l	5.3	9.7	2.7	4.0	1.3	4.3	3.5
ENSMUSG00000064367	mt-Nd5	mitochondrially encoded NADH dehydrogenase 5 [Source:MGI Symbol;Acc:MGI:102496]	25874	26260	23266	22970	22279	27991	22902	13689	20768	17600	16820	25523	20772	7108	8488	6474	9427	12776	13850	5629	9357	6087	mt-Nd5	24592.5	24390.7	17352.3	21038.3	7356.7	12017.7	7493.0
ENSMUSG00000064368	mt-Nd6	mitochondrially encoded NADH dehydrogenase 6 [Source:MGI Symbol;Acc:MGI:102495]	4093	4418	3896	3935	3335	4079	3764	1732	3243	2768	2657	4193	3228	944	1310	835	1155	1374	1975	855	1252	913	mt-Nd6	4085.5	3726.0	2581.0	3359.3	1029.7	1501.3	1053.5
ENSMUSG00000016427	Ndufa1	NADH dehydrogenase (ubiquinone) 1 alpha subcomplex 1 [Source:MGI Symbol;Acc:MGI:1929511]	551	694	678	632	415	511	550	685	591	492	380	495	541	387	424	343	407	337	497	225	477	366	Ndufa1	638.8	492.0	589.3	472.0	384.7	413.7	351.0
ENSMUSG00000026260	Ndufa10	NADH dehydrogenase (ubiquinone) 1 alpha subcomplex 10 [Source:MGI Symbol;Acc:MGI:1914523]	3877	3622	3467	3436	2773	3303	3386	3078	3121	3305	2864	3166	3192	2911	2729	2866	2598	2526	2827	2486	2620	2759	Ndufa10	3600.5	3154.0	3168.0	3074.0	2835.3	2650.3	2553.0
ENSMUSG00000002379	Ndufa11	NADH dehydrogenase (ubiquinone) 1 alpha subcomplex 11 [Source:MGI Symbol;Acc:MGI:1917125]	929	1083	1133	1087	752	923	936	1339	1249	1069	855	881	963	800	804	777	973	922	1148	712	929	883	Ndufa11	1058.0	870.3	1219.0	899.7	793.7	1014.3	820.5
ENSMUSG00000020022	Ndufa12	NADH dehydrogenase (ubiquinone) 1 alpha subcomplex 12 [Source:MGI Symbol;Acc:MGI:1913664]	1129	1151	1192	1039	768	1021	1063	1292	1148	1091	806	1015	1020	1045	941	1072	849	844	1063	1020	1095	1260	Ndufa12	1127.8	950.7	1177.0	947.0	1019.3	918.7	1057.5
ENSMUSG00000036199	Ndufa13	NADH dehydrogenase (ubiquinone) 1 alpha subcomplex 13 [Source:MGI Symbol;Acc:MGI:1914434]	1167	1390	1489	1331	1038	1115	1180	1717	1567	1282	1117	1207	1178	1231	1253	1134	1202	1041	1317	1280	1251	1348	Ndufa13	1344.3	1111.0	1522.0	1167.3	1206.0	1186.7	1265.5
ENSMUSG00000014294	Ndufa2	NADH dehydrogenase (ubiquinone) 1 alpha subcomplex 2 [Source:MGI Symbol;Acc:MGI:1343103]	1252	1596	1640	1876	962	1156	1236	1934	1569	1235	1091	1115	1249	1404	1220	1233	1176	972	1290	1560	1262	1589	Ndufa2	1591.0	1118.0	1579.3	1151.7	1285.7	1146.0	1411.0
ENSMUSG00000035674	Ndufa3	NADH dehydrogenase (ubiquinone) 1 alpha subcomplex 3 [Source:MGI Symbol;Acc:MGI:1913341]	1004	1138	1156	1061	758	1024	910	1388	1246	985	771	906	1000	836	861	844	914	886	1052	871	980	955	Ndufa3	1089.8	897.3	1206.3	892.3	847.0	950.7	925.5
ENSMUSG00000029632	Ndufa4	NADH dehydrogenase (ubiquinone) 1 alpha subcomplex 4 [Source:MGI Symbol;Acc:MGI:107686]	2785	3348	3244	2881	1793	2450	2515	3571	3275	2613	1968	2272	2485	1918	1795	1848	2095	2021	2853	1057	1919	1911	Ndufa4	3064.5	2252.7	3153.0	2241.7	1853.7	2323.0	1488.0
ENSMUSG00000040280	Ndufa4l2	NADH dehydrogenase (ubiquinone) 1 alpha subcomplex 4-like 2 [Source:MGI Symbol;Acc:MGI:3039567]	2	3	6	4	3	7	6	2	5	5	7	12	13	7	10	6	6	4	4	7	4	6	Ndufa4l2	3.8	5.3	4.0	10.7	7.7	4.7	5.5
ENSMUSG00000023089	Ndufa5	NADH dehydrogenase (ubiquinone) 1 alpha subcomplex 5 [Source:MGI Symbol;Acc:MGI:1915452]	479	540	603	537	297	366	459	633	574	499	315	415	507	384	358	386	382	373	526	359	410	455	Ndufa5	539.8	374.0	568.7	412.3	376.0	427.0	384.5
ENSMUSG00000022450	Ndufa6	NADH dehydrogenase (ubiquinone) 1 alpha subcomplex 6 (B14) [Source:MGI Symbol;Acc:MGI:1914380]	1862	1742	1641	1511	961	1274	1539	2012	1586	1744	1148	1270	1852	1529	1374	1934	1333	975	1893	1429	1497	2360	Ndufa6	1689.0	1258.0	1780.7	1423.3	1612.3	1400.3	1463.0
ENSMUSG00000041881	Ndufa7	NADH dehydrogenase (ubiquinone) 1 alpha subcomplex 7 (B14.5a) [Source:MGI Symbol;Acc:MGI:1913666]	1274	1426	1369	1360	982	1004	1222	2042	1594	1364	1182	1125	1470	1337	1106	1292	1406	1060	1580	1211	1294	1460	Ndufa7	1357.3	1069.3	1666.7	1259.0	1245.0	1348.7	1252.5
ENSMUSG00000026895	Ndufa8	NADH dehydrogenase (ubiquinone) 1 alpha subcomplex 8 [Source:MGI Symbol;Acc:MGI:1915625]	1763	1950	2022	2110	1294	1620	1699	1915	1829	1628	1411	1588	1676	1290	1375	1263	1521	1569	1688	758	1323	1147	Ndufa8	1961.3	1537.7	1790.7	1558.3	1309.3	1592.7	1040.5
ENSMUSG00000000399	Ndufa9	NADH dehydrogenase (ubiquinone) 1 alpha subcomplex 9 [Source:MGI Symbol;Acc:MGI:1913358]	2604	2846	2764	2675	2204	2512	2389	2822	2664	2531	2196	2337	2331	2386	2062	2049	2125	2213	2247	2114	2159	2122	Ndufa9	2722.3	2368.3	2672.3	2288.0	2165.7	2195.0	2136.5
ENSMUSG00000030869	Ndufab1	NADH dehydrogenase (ubiquinone) 1 alpha/beta subcomplex 1 [Source:MGI Symbol;Acc:MGI:1917566]	1596	1700	1683	1664	1140	1407	1514	1658	1585	1435	1234	1571	1468	1642	1482	1607	1297	1286	1318	1712	1593	1859	Ndufab1	1660.8	1353.7	1559.3	1424.3	1577.0	1300.3	1652.5
ENSMUSG00000091989	Ndufab1-ps	NADH dehydrogenase (ubiquinone) 1 alpha/beta subcomplex 1 pseudogene [Source:MGI Symbol;Acc:MGI:4936891]	0	3	4	2	1	0	3	1	2	3	2	4	2	2	3	0	3	3	2	2	1	2	Ndufab1-ps	2.3	1.3	2.0	2.7	1.7	2.7	1.5
ENSMUSG00000027305	Ndufaf1	NADH dehydrogenase (ubiquinone) 1 alpha subcomplex assembly factor 1 [Source:MGI Symbol;Acc:MGI:1916952]	332	309	329	258	204	290	261	200	260	265	215	291	276	239	281	283	199	284	284	199	293	283	Ndufaf1	307.0	251.7	241.7	260.7	267.7	255.7	246.0
ENSMUSG00000068184	Ndufaf2	NADH dehydrogenase (ubiquinone) 1 alpha subcomplex assembly factor 2 [Source:MGI Symbol;Acc:MGI:1922847]	130	122	283	170	105	80	109	126	95	71	100	87	81	110	66	64	75	54	66	65	59	61	Ndufaf2	176.3	98.0	97.3	89.3	80.0	65.0	62.0
ENSMUSG00000070283	Ndufaf3	NADH dehydrogenase (ubiquinone) 1 alpha subcomplex assembly factor 3 [Source:MGI Symbol;Acc:MGI:1913956]	392	380	372	400	259	299	372	423	315	313	257	317	298	347	307	297	276	286	306	319	313	293	Ndufaf3	386.0	310.0	350.3	290.7	317.0	289.3	316.0
ENSMUSG00000028261	Ndufaf4	NADH dehydrogenase (ubiquinone) 1 alpha subcomplex assembly factor 4 [Source:MGI Symbol;Acc:MGI:1915743]	709	835	840	752	549	663	655	713	646	608	515	706	657	691	628	586	411	520	526	421	730	647	Ndufaf4	784.0	622.3	655.7	626.0	635.0	485.7	575.5
ENSMUSG00000027384	Ndufaf5	NADH dehydrogenase (ubiquinone) complex I assembly factor 5 [Source:MGI Symbol;Acc:MGI:1916737]	231	273	305	248	174	211	244	358	354	226	249	284	226	263	271	219	220	206	229	231	287	274	Ndufaf5	264.3	209.7	312.7	253.0	251.0	218.3	259.0
ENSMUSG00000050323	Ndufaf6	NADH dehydrogenase (ubiquinone) complex I assembly factor 6 [Source:MGI Symbol;Acc:MGI:1924197]	226	208	256	229	125	160	199	209	164	177	149	184	191	184	167	182	128	120	123	129	141	158	Ndufaf6	229.8	161.3	183.3	174.7	177.7	123.7	135.0
ENSMUSG00000024082	Ndufaf7	NADH dehydrogenase (ubiquinone) 1 alpha subcomplex assembly factor 7 [Source:MGI Symbol;Acc:MGI:1920944]	352	317	392	394	268	307	314	438	317	275	303	309	326	335	277	308	289	250	266	260	304	246	Ndufaf7	363.8	296.3	343.3	312.7	306.7	268.3	282.0
ENSMUSG00000078572	Ndufaf8	NADH dehydrogenase (ubiquinone) 1 alpha subcomplex assembly factor 8 [Source:MGI Symbol;Acc:MGI:1913676]	429	489	500	448	347	409	417	496	451	438	302	374	423	305	324	373	307	271	467	245	343	467	Ndufaf8	466.5	391.0	461.7	366.3	334.0	348.3	294.0
ENSMUSG00000040048	Ndufb10	NADH dehydrogenase (ubiquinone) 1 beta subcomplex 10 [Source:MGI Symbol;Acc:MGI:1915592]	1201	1374	1364	1303	793	1109	955	1281	1282	1161	840	1027	1153	808	860	834	943	947	1130	455	888	753	Ndufb10	1310.5	952.3	1241.3	1006.7	834.0	1006.7	671.5
ENSMUSG00000031059	Ndufb11	NADH dehydrogenase (ubiquinone) 1 beta subcomplex 11 [Source:MGI Symbol;Acc:MGI:1349919]	1749	1846	1833	1788	1002	1529	1408	1783	1588	1253	968	1359	1316	1229	1262	1213	1112	901	1116	1007	1279	1294	Ndufb11	1804.0	1313.0	1541.3	1214.3	1234.7	1043.0	1143.0
ENSMUSG00000002416	Ndufb2	NADH dehydrogenase (ubiquinone) 1 beta subcomplex 2 [Source:MGI Symbol;Acc:MGI:1915448]	731	881	963	835	565	710	740	1098	996	713	590	699	724	597	564	474	670	607	706	347	554	592	Ndufb2	852.5	671.7	935.7	671.0	545.0	661.0	450.5
ENSMUSG00000026032	Ndufb3	NADH dehydrogenase (ubiquinone) 1 beta subcomplex 3 [Source:MGI Symbol;Acc:MGI:1913745]	542	581	643	590	408	480	506	684	625	525	384	463	546	331	361	342	433	432	572	228	347	377	Ndufb3	589.0	464.7	611.3	464.3	344.7	479.0	287.5
ENSMUSG00000022820	Ndufb4	NADH dehydrogenase (ubiquinone) 1 beta subcomplex 4 [Source:MGI Symbol;Acc:MGI:1915444]	317	361	361	289	192	263	284	418	355	284	214	271	280	285	251	258	281	225	307	179	275	335	Ndufb4	332.0	246.3	352.3	255.0	264.7	271.0	227.0
ENSMUSG00000027673	Ndufb5	NADH dehydrogenase (ubiquinone) 1 beta subcomplex 5 [Source:MGI Symbol;Acc:MGI:1913296]	1897	2439	2202	2180	1401	1874	1880	2311	2067	1775	1330	1732	1782	1602	1628	1574	1426	1267	1628	1316	1622	1715	Ndufb5	2179.5	1718.3	2051.0	1614.7	1601.3	1440.3	1469.0
ENSMUSG00000071014	Ndufb6	NADH dehydrogenase (ubiquinone) 1 beta subcomplex 6 [Source:MGI Symbol;Acc:MGI:2684983]	1125	1412	1458	1337	853	1068	1020	1853	1585	1191	1033	1052	1176	1174	1017	1024	1156	1047	1342	1000	1080	1224	Ndufb6	1333.0	980.3	1543.0	1087.0	1071.7	1181.7	1040.0
ENSMUSG00000033938	Ndufb7	NADH dehydrogenase (ubiquinone) 1 beta subcomplex 7 [Source:MGI Symbol;Acc:MGI:1914166]	1183	1384	1448	1386	1023	1126	1166	1603	1506	1230	1012	1091	1222	981	967	873	1088	1011	1359	779	1018	1035	Ndufb7	1350.3	1105.0	1446.3	1108.3	940.3	1152.7	898.5
ENSMUSG00000025204	Ndufb8	NADH dehydrogenase (ubiquinone) 1 beta subcomplex 8 [Source:MGI Symbol;Acc:MGI:1914514]	1907	2360	2293	2169	1484	1854	1727	2864	2570	1853	1657	1753	1877	1956	1631	1621	1895	1844	2136	1880	1832	1905	Ndufb8	2182.3	1688.3	2429.0	1762.3	1736.0	1958.3	1856.0
ENSMUSG00000022354	Ndufb9	NADH dehydrogenase (ubiquinone) 1 beta subcomplex 9 [Source:MGI Symbol;Acc:MGI:1913468]	3191	3011	2875	2691	1754	2274	2973	3462	3207	3405	1958	2252	3423	2430	2246	2930	2322	2010	3531	1892	2509	3682	Ndufb9	2942.0	2333.7	3358.0	2544.3	2535.3	2621.0	2200.5
ENSMUSG00000037152	Ndufc1	NADH dehydrogenase (ubiquinone) 1 subcomplex unknown 1 [Source:MGI Symbol;Acc:MGI:1913627]	783	922	1003	1036	667	826	793	1216	1033	822	715	850	857	879	840	802	767	621	902	806	900	953	Ndufc1	936.0	762.0	1023.7	807.3	840.3	763.3	853.0
ENSMUSG00000030647	Ndufc2	NADH dehydrogenase (ubiquinone) 1 subcomplex unknown 2 [Source:MGI Symbol;Acc:MGI:1344370]	1099	1303	1331	1357	786	927	1071	1582	1370	1047	831	950	1051	750	772	695	875	831	1009	384	670	697	Ndufc2	1272.5	928.0	1333.0	944.0	739.0	905.0	527.0
ENSMUSG00000025968	Ndufs1	NADH dehydrogenase (ubiquinone) Fe-S protein 1 [Source:MGI Symbol;Acc:MGI:2443241]	3659	3226	3360	3664	3249	3501	3567	3580	3108	3334	3301	3402	3461	2771	2879	2576	2847	3003	2777	2146	2717	2420	Ndufs1	3477.3	3439.0	3340.7	3388.0	2742.0	2875.7	2431.5
ENSMUSG00000013593	Ndufs2	NADH dehydrogenase (ubiquinone) Fe-S protein 2 [Source:MGI Symbol;Acc:MGI:2385112]	5352	6119	5724	5659	4362	5116	4954	5490	5340	4910	4405	4792	4691	4808	4520	4284	4147	3968	4476	4515	4777	4646	Ndufs2	5713.5	4810.7	5246.7	4629.3	4537.3	4197.0	4646.0
ENSMUSG00000005510	Ndufs3	NADH dehydrogenase (ubiquinone) Fe-S protein 3 [Source:MGI Symbol;Acc:MGI:1915599]	1378	1472	1485	1414	1094	1303	1440	1490	1401	1408	1036	1213	1366	1056	1153	1155	1085	1190	1381	958	1128	1205	Ndufs3	1437.3	1279.0	1433.0	1205.0	1121.3	1218.7	1043.0
ENSMUSG00000021764	Ndufs4	NADH dehydrogenase (ubiquinone) Fe-S protein 4 [Source:MGI Symbol;Acc:MGI:1343135]	756	919	1029	1096	856	736	776	1863	1058	808	987	798	791	1310	798	700	1182	791	890	1329	753	783	Ndufs4	950.0	789.3	1243.0	858.7	936.0	954.3	1041.0
ENSMUSG00000028648	Ndufs5	NADH dehydrogenase (ubiquinone) Fe-S protein 5 [Source:MGI Symbol;Acc:MGI:1890889]	453	442	502	447	325	388	395	686	547	499	382	428	431	385	325	301	444	407	493	207	312	332	Ndufs5	461.0	369.3	577.3	413.7	337.0	448.0	259.5
ENSMUSG00000021606	Ndufs6	NADH dehydrogenase (ubiquinone) Fe-S protein 6 [Source:MGI Symbol;Acc:MGI:107932]	1191	1448	1492	1460	903	1132	1066	1729	1283	1093	1017	1011	1093	1257	1098	1063	1134	945	1162	1185	1094	1185	Ndufs6	1397.8	1033.7	1368.3	1040.3	1139.3	1080.3	1139.5
ENSMUSG00000020153	Ndufs7	NADH dehydrogenase (ubiquinone) Fe-S protein 7 [Source:MGI Symbol;Acc:MGI:1922656]	2015	2012	2015	2187	1600	1828	2007	2343	2073	2082	1624	1782	2016	1797	1659	1900	1716	1583	1968	1846	1603	1965	Ndufs7	2057.3	1811.7	2166.0	1807.3	1785.3	1755.7	1724.5
ENSMUSG00000059734	Ndufs8	NADH dehydrogenase (ubiquinone) Fe-S protein 8 [Source:MGI Symbol;Acc:MGI:2385079]	1435	1768	1685	1661	1062	1359	1299	1881	1683	1228	1154	1327	1230	1249	1122	1025	1105	1042	1156	1079	1221	1181	Ndufs8	1637.3	1240.0	1597.3	1237.0	1132.0	1101.0	1150.0
ENSMUSG00000037916	Ndufv1	NADH dehydrogenase (ubiquinone) flavoprotein 1 [Source:MGI Symbol;Acc:MGI:107851]	3911	4131	3885	4243	3241	3801	3758	3978	3851	3849	3450	3737	3830	3253	3179	3051	3009	3198	3327	2673	3247	2838	Ndufv1	4042.5	3600.0	3892.7	3672.3	3161.0	3178.0	2960.0
ENSMUSG00000024099	Ndufv2	NADH dehydrogenase (ubiquinone) flavoprotein 2 [Source:MGI Symbol;Acc:MGI:1920150]	2507	2982	3034	2684	1799	2200	2322	3305	2832	2344	2049	2241	2387	2060	1853	1914	2037	1955	2368	1551	1943	2033	Ndufv2	2801.8	2107.0	2827.0	2225.7	1942.3	2120.0	1747.0
ENSMUSG00000024038	Ndufv3	NADH dehydrogenase (ubiquinone) flavoprotein 3 [Source:MGI Symbol;Acc:MGI:1890894]	1442	1599	1497	1493	1121	1359	1201	1332	1277	1283	1070	1158	1256	928	1012	1040	1201	933	1278	671	1020	1026	Ndufv3	1507.8	1227.0	1297.3	1161.3	993.3	1137.3	845.5
ENSMUSG00000021577	Sdha	succinate dehydrogenase complex subunit A flavoprotein (Fp) [Source:MGI Symbol;Acc:MGI:1914195]	9061	9302	9044	9155	8200	8986	8664	8642	8325	8728	8225	8768	8613	7672	7816	7064	7648	7349	7752	7213	7935	6977	Sdha	9140.5	8616.7	8565.0	8535.3	7517.3	7583.0	7574.0
ENSMUSG00000074211	Sdhaf1	succinate dehydrogenase complex assembly factor 1 [Source:MGI Symbol;Acc:MGI:1915582]	516	505	512	474	286	329	487	456	448	467	345	390	473	382	448	495	364	344	444	302	357	379	Sdhaf1	501.8	367.3	457.0	402.7	441.7	384.0	329.5
ENSMUSG00000024668	Sdhaf2	succinate dehydrogenase complex assembly factor 2 [Source:MGI Symbol;Acc:MGI:1913322]	593	767	742	694	622	633	645	842	849	632	634	674	620	760	760	736	686	798	801	784	802	707	Sdhaf2	699.0	633.3	774.3	642.7	752.0	761.7	793.0
ENSMUSG00000042505	Sdhaf3	succinate dehydrogenase complex assembly factor 3 [Source:MGI Symbol;Acc:MGI:1913288]	111	176	196	166	133	132	153	146	135	111	117	123	126	118	146	124	106	66	110	62	132	113	Sdhaf3	162.3	139.3	130.7	122.0	129.3	94.0	97.0
ENSMUSG00000026154	Sdhaf4	succinate dehydrogenase complex assembly factor 4 [Source:MGI Symbol;Acc:MGI:1915252]	119	169	180	165	103	130	138	241	211	134	127	137	157	131	136	103	158	132	154	87	125	89	Sdhaf4	158.3	123.7	195.3	140.3	123.3	148.0	106.0
ENSMUSG00000009863	Sdhb	succinate dehydrogenase complex subunit B iron sulfur (Ip) [Source:MGI Symbol;Acc:MGI:1914930]	3687	4005	3914	4123	2974	3449	3567	4593	4388	3968	3167	3390	4082	3840	3141	3409	3517	2907	4093	3189	3487	4051	Sdhb	3932.3	3330.0	4316.3	3546.3	3463.3	3505.7	3338.0
ENSMUSG00000058076	Sdhc	succinate dehydrogenase complex subunit C integral membrane protein [Source:MGI Symbol;Acc:MGI:1913302]	3616	3990	3931	4298	3274	3406	3606	4036	3527	3654	3359	3316	3511	2821	2689	2832	3356	2905	3457	2288	2905	2857	Sdhc	3958.8	3428.7	3739.0	3395.3	2780.7	3239.3	2596.5
ENSMUSG00000000171	Sdhd	succinate dehydrogenase complex subunit D integral membrane protein [Source:MGI Symbol;Acc:MGI:1914175]	4593	5381	5213	4626	3634	4346	4518	5007	4495	4202	3490	3758	4131	2867	2986	3173	3434	3307	4275	2128	3101	3222	Sdhd	4953.3	4166.0	4568.0	3793.0	3008.7	3672.0	2614.5
ENSMUSG00000022110	Sucla2	succinate-Coenzyme A ligase ADP-forming beta subunit [Source:MGI Symbol;Acc:MGI:1306775]	2251	2343	2409	2393	1891	2198	2253	2426	1949	2159	1787	1840	2145	1741	1751	2187	1728	1597	2106	1915	1959	2632	Sucla2	2349.0	2114.0	2178.0	1924.0	1893.0	1810.3	1937.0
ENSMUSG00000052738	Suclg1	succinate-CoA ligase GDP-forming alpha subunit [Source:MGI Symbol;Acc:MGI:1927234]	3290	3512	3423	3499	2823	3070	3135	3404	3065	3179	2927	2934	3130	2947	2711	2742	2973	2726	3039	2301	2683	2679	Suclg1	3431.0	3009.3	3216.0	2997.0	2800.0	2912.7	2492.0
ENSMUSG00000061838	Suclg2	succinate-Coenzyme A ligase GDP-forming beta subunit [Source:MGI Symbol;Acc:MGI:1306824]	3053	3097	2716	3006	2714	2844	2895	3213	2959	2934	3009	2859	2806	2373	2352	1893	2844	2763	2548	1722	2114	1559	Suclg2	2968.0	2817.7	3035.3	2891.3	2206.0	2718.3	1918.0
ENSMUSG00000005882	Uqcc1	ubiquinol-cytochrome c reductase complex assembly factor 1 [Source:MGI Symbol;Acc:MGI:1929472]	934	844	827	866	637	787	860	813	765	745	740	754	865	806	737	848	653	715	660	611	706	775	Uqcc1	867.8	761.3	774.3	786.3	797.0	676.0	658.5
ENSMUSG00000024208	Uqcc2	ubiquinol-cytochrome c reductase complex assembly factor 2 [Source:MGI Symbol;Acc:MGI:1914517]	614	731	791	703	544	512	534	1217	908	564	612	595	592	1023	937	631	780	745	769	1186	890	814	Uqcc2	709.8	530.0	896.3	599.7	863.7	764.7	1038.0
ENSMUSG00000071654	Uqcc3	ubiquinol-cytochrome c reductase complex assembly factor 3 [Source:MGI Symbol;Acc:MGI:2147553]	287	358	328	355	170	225	212	248	276	220	152	210	204	148	174	180	153	174	208	140	200	169	Uqcc3	332.0	202.3	248.0	188.7	167.3	178.3	170.0
ENSMUSG00000059534	Uqcr10	ubiquinol-cytochrome c reductase complex III subunit X [Source:MGI Symbol;Acc:MGI:1913402]	2394	2603	2643	2759	1704	2150	2282	3198	2637	2209	1816	1980	2245	1718	1673	1643	2117	1654	2342	1338	1797	1903	Uqcr10	2599.8	2045.3	2681.3	2013.7	1678.0	2037.7	1567.5
ENSMUSG00000020163	Uqcr11	ubiquinol-cytochrome c reductase complex III subunit XI [Source:MGI Symbol;Acc:MGI:1913844]	1847	2168	2195	1921	1329	1693	1776	2311	2185	1749	1430	1678	1673	951	1047	866	1467	1334	1768	444	1051	910	Uqcr11	2032.8	1599.3	2081.7	1593.7	954.7	1523.0	747.5
ENSMUSG00000021520	Uqcrb	ubiquinol-cytochrome c reductase binding protein [Source:MGI Symbol;Acc:MGI:1914780]	1273	1322	1471	1319	849	1037	1032	1912	1401	1149	1035	1116	1140	1202	1088	1083	1134	1066	1240	1312	1213	1432	Uqcrb	1346.3	972.7	1487.3	1097.0	1124.3	1146.7	1262.5
ENSMUSG00000025651	Uqcrc1	ubiquinol-cytochrome c reductase core protein 1 [Source:MGI Symbol;Acc:MGI:107876]	9545	10758	10431	10661	10003	10685	10270	11695	11892	11143	10087	10658	10551	10494	9508	9506	10242	10015	10380	10616	10521	9961	Uqcrc1	10348.8	10319.3	11576.7	10432.0	9836.0	10212.3	10568.5
ENSMUSG00000030884	Uqcrc2	ubiquinol cytochrome c reductase core protein 2 [Source:MGI Symbol;Acc:MGI:1914253]	6682	7161	7046	6260	5588	6576	6537	7828	6733	6390	5854	6231	6133	6068	5553	5478	5736	5266	5942	5884	5819	5793	Uqcrc2	6787.3	6233.7	6983.7	6072.7	5699.7	5648.0	5851.5
ENSMUSG00000038462	Uqcrfs1	ubiquinol-cytochrome c reductase Rieske iron-sulfur polypeptide 1 [Source:MGI Symbol;Acc:MGI:1913944]	3891	4551	4224	4545	3178	3614	3636	4336	3935	3673	3019	3353	3517	2848	2825	3005	3044	2725	3537	2442	3136	3333	Uqcrfs1	4302.8	3476.0	3981.3	3296.3	2892.7	3102.0	2789.0
ENSMUSG00000063882	Uqcrh	ubiquinol-cytochrome c reductase hinge protein [Source:MGI Symbol;Acc:MGI:1913826]	2549	3117	2880	2758	1693	2316	2275	2907	2808	2246	1643	1966	2274	1153	1422	1405	1825	1622	2461	678	1475	1533	Uqcrh	2826.0	2094.7	2653.7	1961.0	1326.7	1969.3	1076.5
ENSMUSG00000037438	Uqcrh-ps1	ubiquinol-cytochrome c reductase hinge protein pseudogene 1 [Source:MGI Symbol;Acc:MGI:3641869]	0	0	2	0	0	0	0	0	0	0	0	0	2	1	1	0	1	1	0	0	0	0	Uqcrh-ps1	0.5	0.0	0.0	0.7	0.7	0.7	0.0
ENSMUSG00000081413	Uqcrh-ps2	ubiquinol-cytochrome c reductase hinge protein pseudogene 2 [Source:MGI Symbol;Acc:MGI:3650492]	0	0	0	0	0	0	0	1	0	0	0	0	0	0	0	1	1	0	0	0	0	0	Uqcrh-ps2	0.0	0.0	0.3	0.0	0.3	0.3	0.0
ENSMUSG00000044894	Uqcrq	ubiquinol-cytochrome c reductase complex III subunit VII [Source:MGI Symbol;Acc:MGI:107807]	3813	4215	4054	3932	2712	3378	3588	4959	4487	3820	3014	3502	3811	3526	3566	3432	3364	2923	3872	2539	3675	3789	Uqcrq	4003.5	3226.0	4422.0	3442.3	3508.0	3386.3	3107.0
ENSMUSG00000029361	Nos1	nitric oxide synthase 1 neuronal [Source:MGI Symbol;Acc:MGI:97360]	0	0	1	0	1	1	0	3	0	0	1	0	0	0	0	0	1	1	0	1	2	1	Nos1	0.3	0.7	1.0	0.3	0.0	0.7	1.5
ENSMUSG00000038473	Nos1ap	nitric oxide synthase 1 (neuronal) adaptor protein [Source:MGI Symbol;Acc:MGI:1917979]	101	57	83	59	97	84	106	47	73	100	142	94	131	119	94	126	135	76	107	101	76	169	Nos1ap	75.0	95.7	73.3	122.3	113.0	106.0	88.5
ENSMUSG00000020826	Nos2	nitric oxide synthase 2 inducible [Source:MGI Symbol;Acc:MGI:97361]	156	56	137	393	1131	112	205	915	103	318	1711	93	208	4045	559	767	1718	117	367	6805	567	1392	Nos2	185.5	482.7	445.3	670.7	1790.3	734.0	3686.0
ENSMUSG00000028978	Nos3	nitric oxide synthase 3 endothelial cell [Source:MGI Symbol;Acc:MGI:97362]	54	36	34	31	93	57	82	71	136	70	79	106	113	71	74	83	71	126	89	45	58	81	Nos3	38.8	77.3	92.3	99.3	76.0	95.3	51.5
ENSMUSG00000003421	Nosip	nitric oxide synthase interacting protein [Source:MGI Symbol;Acc:MGI:1913644]	638	650	679	764	690	663	689	674	629	645	643	597	648	599	613	556	629	649	569	574	539	517	Nosip	682.8	680.7	649.3	629.3	589.3	615.7	556.5
ENSMUSG00000034738	Nostrin	nitric oxide synthase trafficker [Source:MGI Symbol;Acc:MGI:3606242]	653	714	663	643	655	578	590	835	638	711	691	623	690	811	716	1043	780	736	957	859	794	1385	Nostrin	668.3	607.7	728.0	668.0	856.7	824.3	826.5
ENSMUSG00000036285	Noa1	nitric oxide associated 1 [Source:MGI Symbol;Acc:MGI:1914306]	1225	1154	1125	1484	800	1086	1006	813	846	813	821	991	900	802	789	739	659	747	623	441	651	504	Noa1	1247.0	964.0	824.0	904.0	776.7	676.3	546.0
ENSMUSG00000032323	Cyp11a1	cytochrome P450 family 11 subfamily a polypeptide 1 [Source:MGI Symbol;Acc:MGI:88582]	2	1	2	5	5	4	4	1	4	3	3	4	5	2	0	2	5	5	5	4	1	1	Cyp11a1	2.5	4.3	2.7	4.0	1.3	5.0	2.5
ENSMUSG00000075604	Cyp11b1	cytochrome P450 family 11 subfamily b polypeptide 1 [Source:MGI Symbol;Acc:MGI:88583]	0	0	0	0	5	2	0	4	1	4	12	4	4	11	3	3	10	20	13	21	5	14	Cyp11b1	0.0	2.3	3.0	6.7	5.7	14.3	13.0
ENSMUSG00000022589	Cyp11b2	cytochrome P450 family 11 subfamily b polypeptide 2 [Source:MGI Symbol;Acc:MGI:88584]	0	0	0	0	3	0	0	0	0	1	3	2	1	6	0	1	3	7	3	7	2	2	Cyp11b2	0.0	1.0	0.3	2.0	2.3	4.3	4.5
ENSMUSG00000003555	Cyp17a1	cytochrome P450 family 17 subfamily a polypeptide 1 [Source:MGI Symbol;Acc:MGI:88586]	3	1	0	0	2	2	1	0	2	0	2	4	0	4	3	0	2	0	0	5	2	4	Cyp17a1	1.0	1.7	0.7	2.0	2.3	0.7	3.5
ENSMUSG00000032274	Cyp19a1	cytochrome P450 family 19 subfamily a polypeptide 1 [Source:MGI Symbol;Acc:MGI:88587]	0	0	0	0	1	0	0	0	1	0	1	0	0	1	1	2	1	3	1	2	0	0	Cyp19a1	0.0	0.3	0.3	0.3	1.3	1.7	1.0
ENSMUSG00000032315	Cyp1a1	cytochrome P450 family 1 subfamily a polypeptide 1 [Source:MGI Symbol;Acc:MGI:88588]	14	15	73	10	112	116	55	203	255	218	70	74	77	36	102	27	111	704	159	162	124	35	Cyp1a1	28.0	94.3	225.3	73.7	55.0	324.7	143.0
ENSMUSG00000032310	Cyp1a2	cytochrome P450 family 1 subfamily a polypeptide 2 [Source:MGI Symbol;Acc:MGI:88589]	1	0	3	0	1	2	1	2	3	0	1	0	0	0	1	0	1	2	2	1	1	0	Cyp1a2	1.0	1.3	1.7	0.3	0.3	1.7	1.0
ENSMUSG00000024087	Cyp1b1	cytochrome P450 family 1 subfamily b polypeptide 1 [Source:MGI Symbol;Acc:MGI:88590]	3	1	20	2	9	13	18	37	25	57	21	9	15	2	0	1	41	112	48	3	0	2	Cyp1b1	6.5	13.3	39.7	15.0	1.0	67.0	1.5
ENSMUSG00000049439	Cyp20a1	cytochrome P450 family 20 subfamily a polypeptide 1 [Source:MGI Symbol;Acc:MGI:1925201]	381	343	461	469	373	320	310	634	479	305	519	356	354	558	329	303	492	463	370	430	307	305	Cyp20a1	413.5	334.3	472.7	409.7	396.7	441.7	368.5
ENSMUSG00000024365	Cyp21a1	cytochrome P450 family 21 subfamily a polypeptide 1 [Source:MGI Symbol;Acc:MGI:88591]	0	0	0	0	1	0	0	0	1	0	0	0	1	1	0	0	2	0	0	4	0	1	Cyp21a1	0.0	0.3	0.3	0.3	0.3	0.7	2.0
ENSMUSG00000092471	Cyp21a2-ps	cytochrome P450 family 21 subfamily a polypeptide 2 pseudogene [Source:MGI Symbol;Acc:MGI:3645529]	1	0	0	1	0	0	0	0	0	0	0	0	0	0	0	0	2	0	0	2	0	0	Cyp21a2-ps	0.5	0.0	0.0	0.0	0.0	0.7	1.0
ENSMUSG00000038567	Cyp24a1	cytochrome P450 family 24 subfamily a polypeptide 1 [Source:MGI Symbol;Acc:MGI:88593]	0	0	0	0	0	0	0	0	0	0	0	0	0	0	0	0	0	0	0	1	0	0	Cyp24a1	0.0	0.0	0.0	0.0	0.0	0.0	0.5
ENSMUSG00000024987	Cyp26a1	cytochrome P450 family 26 subfamily a polypeptide 1 [Source:MGI Symbol;Acc:MGI:1096359]	2	1	1	0	0	2	0	0	2	1	0	3	0	5	0	8	0	0	1	9	1	6	Cyp26a1	1.0	0.7	1.0	1.0	4.3	0.3	5.0
ENSMUSG00000063415	Cyp26b1	cytochrome P450 family 26 subfamily b polypeptide 1 [Source:MGI Symbol;Acc:MGI:2176159]	2	0	1	0	4	1	3	0	2	2	5	6	3	5	17	7	5	3	2	11	8	6	Cyp26b1	0.8	2.7	1.3	4.7	9.7	3.3	9.5
ENSMUSG00000062432	Cyp26c1	cytochrome P450 family 26 subfamily c polypeptide 1 [Source:MGI Symbol;Acc:MGI:2679699]	4	1	5	1	6	8	3	2	7	3	4	4	3	7	9	9	0	2	4	6	9	15	Cyp26c1	2.8	5.7	4.0	3.7	8.3	2.0	7.5
ENSMUSG00000026170	Cyp27a1	cytochrome P450 family 27 subfamily a polypeptide 1 [Source:MGI Symbol;Acc:MGI:88594]	74	15	55	36	178	68	139	323	285	378	290	188	293	122	108	218	413	396	471	83	139	151	Cyp27a1	45.0	128.3	328.7	257.0	149.3	426.7	111.0
ENSMUSG00000006724	Cyp27b1	cytochrome P450 family 27 subfamily b polypeptide 1 [Source:MGI Symbol;Acc:MGI:1098274]	7	2	4	2	4	8	4	3	6	2	9	7	2	9	10	8	5	2	3	11	7	10	Cyp27b1	3.8	5.3	3.7	6.0	9.0	3.3	9.0
ENSMUSG00000060407	Cyp2a12	cytochrome P450 family 2 subfamily a polypeptide 12 [Source:MGI Symbol;Acc:MGI:105055]	0	0	1	0	0	0	0	0	0	0	0	0	0	0	0	0	1	0	0	0	0	0	Cyp2a12	0.3	0.0	0.0	0.0	0.0	0.3	0.0
ENSMUSG00000108487	Cyp2a21-ps	cytochrome P450 family 2 subfamily a polypeptide 21 pseudogene [Source:MGI Symbol;Acc:MGI:3647278]	0	0	0	0	0	0	0	0	0	1	0	0	0	0	0	0	0	0	1	0	0	0	Cyp2a21-ps	0.0	0.0	0.3	0.0	0.0	0.3	0.0
ENSMUSG00000091867	Cyp2a22	cytochrome P450 family 2 subfamily a polypeptide 22 [Source:MGI Symbol;Acc:MGI:3648316]	0	0	0	0	0	0	0	0	0	0	0	0	0	0	0	0	0	0	0	0	0	0	Cyp2a22	0.0	0.0	0.0	0.0	0.0	0.0	0.0
ENSMUSG00000074254	Cyp2a4	cytochrome P450 family 2 subfamily a polypeptide 4 [Source:MGI Symbol;Acc:MGI:88596]	1	1	0	1	0	0	1	0	1	0	0	0	0	0	0	0	1	3	0	1	0	0	Cyp2a4	0.8	0.3	0.3	0.0	0.0	1.3	0.5
ENSMUSG00000005547	Cyp2a5	cytochrome P450 family 2 subfamily a polypeptide 5 [Source:MGI Symbol;Acc:MGI:88597]	0	0	0	1	5	1	2	1	2	1	1	0	2	0	0	12	2	4	34	7	6	13	Cyp2a5	0.3	2.7	1.3	1.0	4.0	13.3	6.5
ENSMUSG00000022818	Cyp2ab1	cytochrome P450 family 2 subfamily ab polypeptide 1 [Source:MGI Symbol;Acc:MGI:3644957]	0	0	1	0	0	0	0	0	1	0	1	3	0	3	4	2	2	1	0	2	4	0	Cyp2ab1	0.3	0.0	0.3	1.3	3.0	1.0	3.0
ENSMUSG00000030483	Cyp2b10	cytochrome P450 family 2 subfamily b polypeptide 10 [Source:MGI Symbol;Acc:MGI:88598]	3734	5216	8410	3316	4836	7702	5516	3855	6142	6308	3235	5171	4581	1575	3654	3727	2809	3649	5085	1266	4587	3875	Cyp2b10	5169.0	6018.0	5435.0	4329.0	2985.3	3847.7	2926.5
ENSMUSG00000040583	Cyp2b13	cytochrome P450 family 2 subfamily b polypeptide 13 [Source:MGI Symbol;Acc:MGI:88599]	11	16	26	13	24	22	12	24	32	34	18	14	26	6	9	13	33	35	48	4	13	17	Cyp2b13	16.5	19.3	30.0	19.3	9.3	38.7	8.5
ENSMUSG00000066704	Cyp2b19	cytochrome P450 family 2 subfamily b polypeptide 19 [Source:MGI Symbol;Acc:MGI:107303]	0	0	1	1	0	0	0	0	1	0	0	0	2	0	3	0	2	0	5	0	0	1	Cyp2b19	0.5	0.0	0.3	0.7	1.0	2.3	0.0
ENSMUSG00000040650	Cyp2b23	cytochrome P450 family 2 subfamily b polypeptide 23 [Source:MGI Symbol;Acc:MGI:3646735]	0	0	0	0	0	0	0	0	0	0	0	0	0	0	0	0	1	0	2	0	0	0	Cyp2b23	0.0	0.0	0.0	0.0	0.0	1.0	0.0
ENSMUSG00000108544	Cyp2b26-ps	cytochrome P450 family 2 subfamily b polypeptide 26 pseudogene [Source:MGI Symbol;Acc:MGI:3648075]	0	0	0	0	1	0	1	0	0	0	0	2	0	0	0	0	0	0	0	0	0	0	Cyp2b26-ps	0.0	0.7	0.0	0.7	0.0	0.0	0.0
ENSMUSG00000108606	Cyp2b27-ps	cytochrome P450 family 2 subfamily b polypeptide 27 pseudogene [Source:MGI Symbol;Acc:MGI:3643081]	0	1	0	2	3	1	2	3	3	3	5	3	0	2	1	1	5	7	4	2	3	2	Cyp2b27-ps	0.8	2.0	3.0	2.7	1.0	5.3	2.5
ENSMUSG00000040660	Cyp2b9	cytochrome P450 family 2 subfamily b polypeptide 9 [Source:MGI Symbol;Acc:MGI:88600]	3	0	3	3	6	2	4	5	7	8	9	6	4	3	1	3	4	10	19	1	4	2	Cyp2b9	2.3	4.0	6.7	6.3	2.3	11.0	2.5
ENSMUSG00000003053	Cyp2c29	cytochrome P450 family 2 subfamily c polypeptide 29 [Source:MGI Symbol;Acc:MGI:103238]	2695	3619	5282	958	1849	4689	4226	3407	8264	7736	1896	4857	3980	1224	6005	3744	2932	10935	10695	1587	6790	4211	Cyp2c29	3138.5	3588.0	6469.0	3577.7	3657.7	8187.3	4188.5
ENSMUSG00000042248	Cyp2c37	cytochrome P450 family 2. subfamily c polypeptide 37 [Source:MGI Symbol;Acc:MGI:1306806]	148	184	160	52	37	137	74	27	87	128	15	59	82	35	216	106	21	50	100	59	217	140	Cyp2c37	136.0	82.7	80.7	52.0	119.0	57.0	138.0
ENSMUSG00000032808	Cyp2c38	cytochrome P450 family 2 subfamily c polypeptide 38 [Source:MGI Symbol;Acc:MGI:1306819]	754	1487	1432	634	314	1027	534	100	358	363	117	371	256	135	629	233	102	238	371	246	735	361	Cyp2c38	1076.8	625.0	273.7	248.0	332.3	237.0	490.5
ENSMUSG00000025003	Cyp2c39	cytochrome P450 family 2 subfamily c polypeptide 39 [Source:MGI Symbol;Acc:MGI:1306818]	28	62	71	34	24	40	27	16	57	34	9	24	24	7	44	18	11	58	43	11	61	25	Cyp2c39	48.8	30.3	35.7	19.0	23.0	37.3	36.0
ENSMUSG00000025004	Cyp2c40	cytochrome P450 family 2 subfamily c polypeptide 40 [Source:MGI Symbol;Acc:MGI:1306815]	20	25	17	27	9	24	12	9	14	17	10	14	17	10	20	6	4	9	12	7	15	16	Cyp2c40	22.3	15.0	13.3	13.7	12.0	8.3	11.0
ENSMUSG00000025197	Cyp2c44	cytochrome P450 family 2 subfamily c polypeptide 44 [Source:MGI Symbol;Acc:MGI:1888897]	51	40	50	53	89	53	40	75	30	31	67	34	37	32	8	7	82	26	41	29	19	10	Cyp2c44	48.5	60.7	45.3	46.0	15.7	49.7	24.0
ENSMUSG00000054827	Cyp2c50	cytochrome P450 family 2 subfamily c polypeptide 50 [Source:MGI Symbol;Acc:MGI:2147497]	44	63	44	16	10	39	26	5	23	37	9	16	21	6	54	25	7	14	28	14	66	45	Cyp2c50	41.8	25.0	21.7	15.3	28.3	16.3	40.0
ENSMUSG00000093610	Cyp2c53-ps	cytochrome P450 family 2 subfamily c polypeptide 53-ps [Source:MGI Symbol;Acc:MGI:3646306]	8	20	27	6	7	20	24	13	21	25	10	20	27	10	22	24	12	33	34	12	34	33	Cyp2c53-ps	15.3	17.0	19.7	19.0	18.7	26.3	23.0
ENSMUSG00000067225	Cyp2c54	cytochrome P450 family 2 subfamily c polypeptide 54 [Source:MGI Symbol;Acc:MGI:3642960]	22	20	19	7	9	18	23	17	30	57	14	19	41	6	23	13	10	36	81	3	28	27	Cyp2c54	17.0	16.7	34.7	24.7	14.0	42.3	15.5
ENSMUSG00000025002	Cyp2c55	cytochrome P450 family 2 subfamily c polypeptide 55 [Source:MGI Symbol;Acc:MGI:1919332]	343	253	336	130	194	316	414	232	594	644	185	320	444	182	469	552	145	466	518	79	310	382	Cyp2c55	265.5	308.0	490.0	316.3	401.0	376.3	194.5
ENSMUSG00000067231	Cyp2c65	cytochrome P450 family 2 subfamily c polypeptide 65 [Source:MGI Symbol;Acc:MGI:1919553]	5556	7307	6246	5317	6975	6692	6166	9162	7685	7958	6710	6400	7154	5001	5308	6450	7884	8141	8946	3485	6411	6758	Cyp2c65	6106.5	6611.0	8268.3	6754.7	5586.3	8323.7	4948.0
ENSMUSG00000067229	Cyp2c66	cytochrome P450 family 2 subfamily c polypeptide 66 [Source:MGI Symbol;Acc:MGI:1917138]	4102	6108	6219	3644	3311	5589	4098	4606	5985	5192	3074	4879	4436	3700	6292	5707	3208	5299	5111	3078	6795	6177	Cyp2c66	5018.3	4332.7	5261.0	4129.7	5233.0	4539.3	4936.5
ENSMUSG00000062624	Cyp2c67	cytochrome P450 family 2 subfamily c polypeptide 67 [Source:MGI Symbol;Acc:MGI:3612288]	149	239	199	158	118	179	142	100	133	102	101	141	134	74	146	84	96	88	124	56	144	89	Cyp2c67	186.3	146.3	111.7	125.3	101.3	102.7	100.0
ENSMUSG00000074882	Cyp2c68	cytochrome P450 family 2 subfamily c polypeptide 68 [Source:MGI Symbol;Acc:MGI:3612287]	1135	1534	1257	1079	667	1199	993	587	647	874	443	754	816	390	707	647	467	375	800	276	780	862	Cyp2c68	1251.3	953.0	702.7	671.0	581.3	547.3	528.0
ENSMUSG00000092008	Cyp2c69	cytochrome P450 family 2 subfamily c polypeptide 69 [Source:MGI Symbol;Acc:MGI:3721049]	3	8	7	3	3	2	2	1	7	1	2	4	1	3	28	0	4	1	3	4	6	3	Cyp2c69	5.3	2.3	3.0	2.3	10.3	2.7	5.0
ENSMUSG00000060613	Cyp2c70	cytochrome P450 family 2 subfamily c polypeptide 70 [Source:MGI Symbol;Acc:MGI:2385878]	292	303	392	284	169	228	202	103	133	142	105	134	133	38	24	27	88	94	161	69	70	90	Cyp2c70	317.8	199.7	126.0	124.0	29.7	114.3	69.5
ENSMUSG00000094806	Cyp2d10	cytochrome P450 family 2 subfamily d polypeptide 10 [Source:MGI Symbol;Acc:MGI:88602]	140	41	57	61	155	78	332	122	134	322	127	61	347	54	168	72	155	131	362	156	89	86	Cyp2d10	74.8	188.3	192.7	178.3	98.0	216.0	122.5
ENSMUSG00000068085	Cyp2d11	cytochrome P450 family 2 subfamily d polypeptide 11 [Source:MGI Symbol;Acc:MGI:88603]	4	3	2	1	3	2	10	1	1	10	2	4	4	2	5	1	4	1	5	3	5	4	Cyp2d11	2.5	5.0	4.0	3.3	2.7	3.3	4.0
ENSMUSG00000096852	Cyp2d12	cytochrome P450 family 2 subfamily d polypeptide 12 [Source:MGI Symbol;Acc:MGI:88604]	1	0	0	2	0	1	2	0	1	3	0	0	3	1	1	0	0	2	2	0	0	1	Cyp2d12	0.8	1.0	1.3	1.0	0.7	1.3	0.0
ENSMUSG00000061740	Cyp2d22	cytochrome P450 family 2 subfamily d polypeptide 22 [Source:MGI Symbol;Acc:MGI:1929474]	25	21	24	34	40	26	39	17	22	40	20	28	49	54	180	36	36	15	49	147	78	64	Cyp2d22	26.0	35.0	26.3	32.3	90.0	33.3	112.5
ENSMUSG00000022445	Cyp2d26	cytochrome P450 family 2 subfamily d polypeptide 26 [Source:MGI Symbol;Acc:MGI:1923529]	9249	7834	5463	5671	5786	6894	9469	3747	5257	10575	4150	5426	10265	4311	4836	10310	5286	3263	10636	4267	8222	15735	Cyp2d26	7054.3	7383.0	6526.3	6613.7	6485.7	6395.0	6244.5
ENSMUSG00000094559	Cyp2d34	cytochrome P450 family 2 subfamily d polypeptide 34 [Source:MGI Symbol;Acc:MGI:2385022]	807	345	363	441	516	417	1020	190	259	556	246	233	720	129	94	161	214	158	417	109	149	350	Cyp2d34	489.0	651.0	335.0	399.7	128.0	263.0	129.0
ENSMUSG00000075517	Cyp2d37-ps	cytochrome P450 family 2 subfamily d polypeptide 37 pseudogene [Source:MGI Symbol;Acc:MGI:3721937]	2	0	0	2	3	3	4	0	3	5	2	2	7	1	2	2	1	3	4	2	3	0	Cyp2d37-ps	1.0	3.3	2.7	3.7	1.7	2.7	2.5
ENSMUSG00000068083	Cyp2d40	cytochrome P450 family 2 subfamily d polypeptide 40 [Source:MGI Symbol;Acc:MGI:1919004]	7	2	5	10	7	7	6	7	4	15	2	11	7	8	5	11	7	3	8	6	18	16	Cyp2d40	6.0	6.7	8.7	6.7	8.0	6.0	12.0
ENSMUSG00000058613	Cyp2d41-ps	cytochrome P450 family 2 subfamily d member 41 pseudogene [Source:MGI Symbol;Acc:MGI:3645691]	0	0	4	1	3	4	2	0	2	6	4	4	3	0	1	6	3	4	5	4	4	7	Cyp2d41-ps	1.3	3.0	2.7	3.7	2.3	4.0	4.0
ENSMUSG00000068086	Cyp2d9	cytochrome P450 family 2 subfamily d polypeptide 9 [Source:MGI Symbol;Acc:MGI:88606]	89	37	64	63	133	68	292	49	79	259	45	37	233	22	21	26	69	63	320	47	30	68	Cyp2d9	63.3	164.3	129.0	105.0	23.0	150.7	38.5
ENSMUSG00000025479	Cyp2e1	cytochrome P450 family 2 subfamily e polypeptide 1 [Source:MGI Symbol;Acc:MGI:88607]	61	28	17	14	4	27	50	6	20	34	11	37	43	1	9	15	6	4	36	0	29	12	Cyp2e1	30.0	27.0	20.0	30.3	8.3	15.3	14.5
ENSMUSG00000052974	Cyp2f2	cytochrome P450 family 2 subfamily f polypeptide 2 [Source:MGI Symbol;Acc:MGI:88608]	0	0	1	1	1	0	0	1	0	1	0	2	1	0	0	1	5	3	3	5	2	1	Cyp2f2	0.5	0.3	0.7	1.0	0.3	3.7	1.5
ENSMUSG00000049685	Cyp2g1	cytochrome P450 family 2 subfamily g polypeptide 1 [Source:MGI Symbol;Acc:MGI:109612]	0	0	0	0	0	0	0	0	0	1	0	0	0	0	1	0	0	0	0	0	0	0	Cyp2g1	0.0	0.0	0.3	0.0	0.3	0.0	0.0
ENSMUSG00000066097	Cyp2j11	cytochrome P450 family 2 subfamily j polypeptide 11 [Source:MGI Symbol;Acc:MGI:2140224]	4	18	17	10	14	9	16	15	9	9	11	13	5	15	17	14	5	11	14	14	16	29	Cyp2j11	12.3	13.0	11.0	9.7	15.3	10.0	15.0
ENSMUSG00000081225	Cyp2j12	cytochrome P450 family 2 subfamily j polypeptide 12 [Source:MGI Symbol;Acc:MGI:3717097]	0	1	1	1	0	0	1	0	0	1	1	3	1	1	1	0	1	1	3	0	0	0	Cyp2j12	0.8	0.3	0.3	1.7	0.7	1.7	0.0
ENSMUSG00000028571	Cyp2j13	cytochrome P450 family 2 subfamily j polypeptide 13 [Source:MGI Symbol;Acc:MGI:2385197]	13	9	10	10	5	9	6	8	8	14	6	9	10	1	7	5	7	5	8	2	14	10	Cyp2j13	10.5	6.7	10.0	8.3	4.3	6.7	8.0
ENSMUSG00000082119	Cyp2j14-ps	cytochrome P450 family 2 subfamily j member 14 pseudogene [Source:MGI Symbol;Acc:MGI:3651954]	0	0	1	0	0	0	0	1	0	0	0	0	0	0	0	0	1	1	0	0	1	0	Cyp2j14-ps	0.3	0.0	0.3	0.0	0.0	0.7	0.5
ENSMUSG00000084286	Cyp2j15-ps	cytochrome P450 family 2 subfamily j member 15 pseudogene [Source:MGI Symbol;Acc:MGI:3652069]	1	0	0	0	0	0	0	0	0	0	0	0	0	1	0	0	0	0	0	0	0	0	Cyp2j15-ps	0.3	0.0	0.0	0.0	0.3	0.0	0.0
ENSMUSG00000052520	Cyp2j5	cytochrome P450 family 2 subfamily j polypeptide 5 [Source:MGI Symbol;Acc:MGI:1270149]	14	29	27	38	35	31	26	24	32	57	17	53	33	33	79	26	28	39	61	47	59	34	Cyp2j5	27.0	30.7	37.7	34.3	46.0	42.7	53.0
ENSMUSG00000052914	Cyp2j6	cytochrome P450 family 2 subfamily j polypeptide 6 [Source:MGI Symbol;Acc:MGI:1270148]	11212	15338	13179	11016	10146	12442	11626	10672	13036	15922	8894	11853	12696	8173	12740	9863	11354	13147	22515	8414	16782	14612	Cyp2j6	12686.3	11404.7	13210.0	11147.7	10258.7	15672.0	12598.0
ENSMUSG00000081362	Cyp2j7	cytochrome P450 family 2 subfamily j polypeptide 7 [Source:MGI Symbol;Acc:MGI:2449816]	1	5	3	3	3	0	2	3	2	3	2	0	1	3	3	2	3	2	3	1	2	3	Cyp2j7	3.0	1.7	2.7	1.0	2.7	2.7	1.5
ENSMUSG00000082681	Cyp2j7-ps1	cytochrome P450 family 2 subfamily j polypeptide 7 pseudogene 1 [Source:MGI Symbol;Acc:MGI:3651268]	0	0	0	0	0	0	0	0	0	0	0	0	0	0	0	0	0	0	0	0	0	0	Cyp2j7-ps1	0.0	0.0	0.0	0.0	0.0	0.0	0.0
ENSMUSG00000083801	Cyp2j7-ps2	cytochrome P450 family 2 subfamily j polypeptide 7 pseudogene 2 [Source:MGI Symbol;Acc:MGI:3651264]	0	0	0	0	0	0	0	0	0	0	0	0	0	0	0	0	0	0	0	0	0	0	Cyp2j7-ps2	0.0	0.0	0.0	0.0	0.0	0.0	0.0
ENSMUSG00000080884	Cyp2j7-ps3	cytochrome P450 family 2 subfamily j polypeptide 7 pseudogene 3 [Source:MGI Symbol;Acc:MGI:3651269]	0	0	0	0	0	0	0	0	0	0	0	0	0	0	0	0	0	0	0	0	0	0	Cyp2j7-ps3	0.0	0.0	0.0	0.0	0.0	0.0	0.0
ENSMUSG00000082932	Cyp2j8	cytochrome P450 family 2 subfamily j polypeptide 8 [Source:MGI Symbol;Acc:MGI:2449817]	8	9	10	5	8	9	10	4	7	6	11	5	11	2	19	7	5	4	8	2	11	7	Cyp2j8	8.0	9.0	5.7	9.0	9.3	5.7	6.5
ENSMUSG00000015224	Cyp2j9	cytochrome P450 family 2 subfamily j polypeptide 9 [Source:MGI Symbol;Acc:MGI:1921769]	281	270	267	192	179	278	269	222	311	373	187	282	331	146	233	288	165	231	412	106	347	358	Cyp2j9	252.5	242.0	302.0	266.7	222.3	269.3	226.5
ENSMUSG00000030670	Cyp2r1	cytochrome P450 family 2 subfamily r polypeptide 1 [Source:MGI Symbol;Acc:MGI:2449771]	2	1	7	2	4	1	0	9	2	1	5	3	2	1	0	0	7	2	0	0	0	0	Cyp2r1	3.0	1.7	4.0	3.3	0.3	3.0	0.0
ENSMUSG00000040703	Cyp2s1	cytochrome P450 family 2 subfamily s polypeptide 1 [Source:MGI Symbol;Acc:MGI:1921384]	4558	4182	2399	3466	3865	3502	2624	2448	2534	3239	3149	2714	2925	2242	2252	3887	3272	2015	3335	1142	2220	3441	Cyp2s1	3651.3	3330.3	2740.3	2929.3	2793.7	2874.0	1681.0
ENSMUSG00000078787	Cyp2t4	cytochrome P450 family 2 subfamily t polypeptide 4 [Source:MGI Symbol;Acc:MGI:2686296]	37	46	55	39	54	54	41	35	39	44	46	58	41	43	69	46	46	40	36	59	59	60	Cyp2t4	44.3	49.7	39.3	48.3	52.7	40.7	59.0
ENSMUSG00000027983	Cyp2u1	cytochrome P450 family 2 subfamily u polypeptide 1 [Source:MGI Symbol;Acc:MGI:1918769]	879	658	504	694	533	900	972	163	360	796	271	658	1070	130	349	473	192	132	341	31	318	319	Cyp2u1	683.8	801.7	439.7	666.3	317.3	221.7	174.5
ENSMUSG00000029541	Cyp2w1	cytochrome P450 family 2 subfamily w polypeptide 1 [Source:MGI Symbol;Acc:MGI:3616076]	66	47	31	20	17	44	69	8	35	40	22	59	58	25	33	37	9	25	41	4	30	34	Cyp2w1	41.0	43.3	27.7	46.3	31.7	25.0	17.0
ENSMUSG00000023963	Cyp39a1	cytochrome P450 family 39 subfamily a polypeptide 1 [Source:MGI Symbol;Acc:MGI:1927096]	130	126	116	101	70	85	99	83	97	86	102	138	135	92	112	130	83	66	58	36	93	67	Cyp39a1	118.3	84.7	88.7	125.0	111.3	69.0	64.5
ENSMUSG00000056035	Cyp3a11	cytochrome P450 family 3 subfamily a polypeptide 11 [Source:MGI Symbol;Acc:MGI:88609]	8095	13178	11944	6694	5526	9083	7842	4761	6607	9652	3144	5109	7067	1595	4397	7898	4487	6577	14656	2133	8192	12687	Cyp3a11	9977.8	7483.7	7006.7	5106.7	4630.0	8573.3	5162.5
ENSMUSG00000029727	Cyp3a13	cytochrome P450 family 3 subfamily a polypeptide 13 [Source:MGI Symbol;Acc:MGI:88610]	1056	1589	2507	4523	10351	1746	1966	16383	3562	4210	10809	2258	3344	9780	2201	3695	18480	5051	9001	10798	4459	6962	Cyp3a13	2418.8	4687.7	8051.7	5470.3	5225.3	10844.0	7628.5
ENSMUSG00000038656	Cyp3a16	cytochrome P450 family 3 subfamily a polypeptide 16 [Source:MGI Symbol;Acc:MGI:106099]	12	25	16	14	6	11	10	12	16	17	10	6	16	6	4	9	7	9	27	5	9	25	Cyp3a16	16.8	9.0	15.0	10.7	6.3	14.3	7.0
ENSMUSG00000029630	Cyp3a25	cytochrome P450 family 3 subfamily a polypeptide 25 [Source:MGI Symbol;Acc:MGI:1930638]	1848	2876	3189	2457	2656	2448	2355	2164	1403	2696	2000	1584	2643	484	526	1804	1987	575	2830	281	961	2126	Cyp3a25	2592.5	2486.3	2087.7	2075.7	938.0	1797.3	621.0
ENSMUSG00000075551	Cyp3a41a	cytochrome P450 family 3 subfamily a polypeptide 41A [Source:MGI Symbol;Acc:MGI:1858451]	3	7	6	12	7	4	3	7	2	3	3	4	8	1	2	3	6	7	12	2	5	8	Cyp3a41a	7.0	4.7	4.0	5.0	2.0	8.3	3.5
ENSMUSG00000075552	Cyp3a41b	cytochrome P450 family 3 subfamily a polypeptide 41B [Source:MGI Symbol;Acc:MGI:3714859]	0	1	0	1	0	0	0	1	1	0	0	2	1	1	0	0	2	0	0	0	0	0	Cyp3a41b	0.5	0.0	0.7	1.0	0.3	0.7	0.0
ENSMUSG00000054417	Cyp3a44	cytochrome P450 family 3 subfamily a polypeptide 44 [Source:MGI Symbol;Acc:MGI:2449818]	17	21	20	15	8	18	19	13	12	25	8	15	13	5	6	23	7	17	30	5	18	29	Cyp3a44	18.3	15.0	16.7	12.0	11.3	18.0	11.5
ENSMUSG00000070419	Cyp3a57	cytochrome P450 family 3 subfamily a polypeptide 57 [Source:MGI Symbol;Acc:MGI:3646373]	9	7	3	5	15	6	14	22	18	32	20	6	30	8	6	15	16	20	39	10	14	28	Cyp3a57	6.0	11.7	24.0	18.7	9.7	25.0	12.0
ENSMUSG00000061292	Cyp3a59	cytochrome P450 family 3 subfamily a polypeptide 59 [Source:MGI Symbol;Acc:MGI:3769707]	13	15	30	39	31	22	19	35	13	7	28	11	12	4	4	18	32	5	15	4	3	8	Cyp3a59	24.3	24.0	18.3	17.0	8.7	17.3	3.5
ENSMUSG00000106040	Cyp3a63-ps	cytochrome P450 family 3 subfamily a member 63 pseudogene [Source:MGI Symbol;Acc:MGI:3717142]	3	7	10	5	2	3	4	7	9	8	3	8	11	1	4	4	6	5	12	0	6	6	Cyp3a63-ps	6.3	3.0	8.0	7.3	3.0	7.7	3.0
ENSMUSG00000021259	Cyp46a1	cytochrome P450 family 46 subfamily a polypeptide 1 [Source:MGI Symbol;Acc:MGI:1341877]	0	2	1	0	0	0	0	0	0	0	0	2	1	0	0	1	0	0	0	1	1	0	Cyp46a1	0.8	0.0	0.0	1.0	0.3	0.0	1.0
ENSMUSG00000066072	Cyp4a10	cytochrome P450 family 4 subfamily a polypeptide 10 [Source:MGI Symbol;Acc:MGI:88611]	44	19	7	13	18	15	80	14	8	101	14	7	82	4	7	50	7	11	89	0	2	28	Cyp4a10	20.8	37.7	41.0	34.3	20.3	35.7	1.0
ENSMUSG00000066071	Cyp4a12a	cytochrome P450 family 4 subfamily a polypeptide 12a [Source:MGI Symbol;Acc:MGI:88612]	2	8	2	2	5	3	0	7	5	0	5	3	0	5	3	1	1	4	2	5	8	6	Cyp4a12a	3.5	2.7	4.0	2.7	3.0	2.3	6.5
ENSMUSG00000078597	Cyp4a12b	cytochrome P450 family 4 subfamily a polypeptide 12B [Source:MGI Symbol;Acc:MGI:3611747]	0	0	0	0	0	1	0	0	3	0	1	4	0	3	1	1	0	4	1	0	3	1	Cyp4a12b	0.0	0.3	1.0	1.7	1.7	1.7	1.5
ENSMUSG00000028715	Cyp4a14	cytochrome P450 family 4 subfamily a polypeptide 14 [Source:MGI Symbol;Acc:MGI:1096550]	0	0	0	0	0	0	0	0	0	0	0	0	0	0	0	0	0	0	0	0	0	0	Cyp4a14	0.0	0.0	0.0	0.0	0.0	0.0	0.0
ENSMUSG00000081823	Cyp4a28-ps	cytochrome P450 family 4 subfamily a polypeptide 28 pseudogene [Source:MGI Symbol;Acc:MGI:1932405]	0	0	0	0	0	0	0	0	0	0	0	0	0	0	0	0	0	0	0	0	0	0	Cyp4a28-ps	0.0	0.0	0.0	0.0	0.0	0.0	0.0
ENSMUSG00000083138	Cyp4a29	cytochrome P450 family 4 subfamily a polypeptide 29 [Source:MGI Symbol;Acc:MGI:3717143]	0	0	1	1	1	0	0	0	2	3	4	2	1	1	0	1	1	2	5	1	0	2	Cyp4a29	0.5	0.3	1.7	2.3	0.7	2.7	0.5
ENSMUSG00000082889	Cyp4a29-ps1	cytochrome P450 family 4 subfamily a polypeptide 29 pseudogene 1 [Source:MGI Symbol;Acc:MGI:3651920]	0	0	0	0	0	0	0	0	0	0	0	0	0	0	0	0	0	0	0	0	0	0	Cyp4a29-ps1	0.0	0.0	0.0	0.0	0.0	0.0	0.0
ENSMUSG00000084346	Cyp4a30b	cytochrome P450 family 4 subfamily a polypeptide 30b [Source:MGI Symbol;Acc:MGI:3717145]	0	0	0	2	1	1	1	0	2	0	0	2	1	0	1	0	0	1	0	0	0	0	Cyp4a30b	0.5	1.0	0.7	1.0	0.3	0.3	0.0
ENSMUSG00000083190	Cyp4a30-ps	cytochrome P450 family 4 subfamily a member 30 pseudogene [Source:MGI Symbol;Acc:MGI:3649426]	1	0	0	1	0	0	0	0	2	0	0	0	0	1	0	0	1	1	1	0	0	1	Cyp4a30-ps	0.5	0.0	0.7	0.0	0.0	1.0	0.0
ENSMUSG00000028712	Cyp4a31	cytochrome P450 family 4 subfamily a polypeptide 31 [Source:MGI Symbol;Acc:MGI:3028580]	1	1	2	1	4	0	7	2	6	3	1	0	12	1	0	3	2	3	10	0	2	4	Cyp4a31	1.3	3.7	3.7	4.3	1.3	5.0	1.0
ENSMUSG00000063929	Cyp4a32	cytochrome P450 family 4 subfamily a polypeptide 32 [Source:MGI Symbol;Acc:MGI:3717148]	4	6	5	4	7	8	12	5	7	10	8	3	13	5	2	12	7	6	11	12	6	17	Cyp4a32	4.8	9.0	7.3	8.0	6.3	8.0	9.0
ENSMUSG00000028713	Cyp4b1	cytochrome P450 family 4 subfamily b polypeptide 1 [Source:MGI Symbol;Acc:MGI:103225]	886	1446	857	880	876	1094	1217	841	1235	1600	752	1183	1450	625	816	1111	1013	845	2261	527	1515	1704	Cyp4b1	1017.3	1062.3	1225.3	1128.3	850.7	1373.0	1021.0
ENSMUSG00000081006	Cyp4b1-ps1	cytochrome P450 family 4 subfamily b polypeptide 1 pseudogene 1 [Source:MGI Symbol;Acc:MGI:3651921]	3	1	2	1	1	2	1	3	1	2	3	3	1	2	0	0	1	2	2	0	1	5	Cyp4b1-ps1	1.8	1.3	2.0	2.3	0.7	1.7	0.5
ENSMUSG00000083457	Cyp4b1-ps2	cytochrome P450 family 4 subfamily b polypeptide 1 pseudogene 2 [Source:MGI Symbol;Acc:MGI:3649236]	1	1	3	4	1	3	3	4	4	5	2	2	4	0	2	2	1	3	5	0	2	3	Cyp4b1-ps2	2.3	2.3	4.3	2.7	1.3	3.0	1.0
ENSMUSG00000024055	Cyp4f13	cytochrome P450 family 4 subfamily f polypeptide 13 [Source:MGI Symbol;Acc:MGI:2158641]	1109	1131	1193	938	1240	1136	1268	917	1050	1602	1139	1078	1601	847	741	1147	1281	869	1996	692	962	1340	Cyp4f13	1092.8	1214.7	1189.7	1272.7	911.7	1382.0	827.0
ENSMUSG00000024292	Cyp4f14	cytochrome P450 family 4 subfamily f polypeptide 14 [Source:MGI Symbol;Acc:MGI:1927669]	2168	1831	1417	1669	1952	2349	2564	1606	1519	2627	1578	1593	2229	1179	701	1470	1434	484	1853	1223	1116	2966	Cyp4f14	1771.3	2288.3	1917.3	1800.0	1116.7	1257.0	1169.5
ENSMUSG00000073424	Cyp4f15	cytochrome P450 family 4 subfamily f polypeptide 15 [Source:MGI Symbol;Acc:MGI:2146921]	93	26	17	9	13	15	62	4	5	46	1	4	42	0	1	10	1	6	50	0	4	16	Cyp4f15	36.3	30.0	18.3	15.7	3.7	19.0	2.0
ENSMUSG00000048440	Cyp4f16	cytochrome P450 family 4 subfamily f polypeptide 16 [Source:MGI Symbol;Acc:MGI:1917351]	1510	1376	1469	1245	1231	1143	1274	987	1188	1417	988	904	1248	717	626	1084	1201	1029	1921	677	1025	2722	Cyp4f16	1400.0	1216.0	1197.3	1046.7	809.0	1383.7	851.0
ENSMUSG00000091586	Cyp4f17	cytochrome P450 family 4 subfamily f polypeptide 17 [Source:MGI Symbol;Acc:MGI:3646233]	21	26	45	24	70	40	37	56	83	40	85	60	48	46	52	42	77	90	54	77	63	35	Cyp4f17	29.0	49.0	59.7	64.3	46.7	73.7	70.0
ENSMUSG00000003484	Cyp4f18	cytochrome P450 family 4 subfamily f polypeptide 18 [Source:MGI Symbol;Acc:MGI:1919304]	0	0	1	0	2	1	0	0	1	0	0	0	0	0	1	1	2	0	0	2	2	2	Cyp4f18	0.3	1.0	0.3	0.0	0.7	0.7	2.0
ENSMUSG00000062464	Cyp4f37	cytochrome P450 family 4 subfamily f polypeptide 37 [Source:MGI Symbol;Acc:MGI:3780112]	9	15	14	11	11	15	11	17	18	11	10	11	9	8	5	12	7	11	12	5	6	25	Cyp4f37	12.3	12.3	15.3	10.0	8.3	10.0	5.5
ENSMUSG00000061126	Cyp4f39	cytochrome P450 family 4 subfamily f polypeptide 39 [Source:MGI Symbol;Acc:MGI:2445210]	6	3	10	7	3	6	5	8	11	9	4	7	11	4	2	3	5	12	10	2	1	7	Cyp4f39	6.5	4.7	9.3	7.3	3.0	9.0	1.5
ENSMUSG00000090700	Cyp4f40	cytochrome P450 family 4 subfamily f polypeptide 40 [Source:MGI Symbol;Acc:MGI:3645508]	514	390	419	353	385	398	476	258	326	447	334	342	457	233	177	427	255	168	333	109	170	367	Cyp4f40	419.0	419.7	343.7	377.7	279.0	252.0	139.5
ENSMUSG00000024295	Cyp4f41-ps	cytochrome P450 family 4 subfamily f polypeptide 41 pseudogene [Source:MGI Symbol;Acc:MGI:1925125]	5	3	4	5	5	4	3	3	7	4	3	0	5	5	3	7	4	7	4	2	2	3	Cyp4f41-ps	4.3	4.0	4.7	2.7	5.0	5.0	2.0
ENSMUSG00000079057	Cyp4v3	cytochrome P450 family 4 subfamily v polypeptide 3 [Source:MGI Symbol;Acc:MGI:2142763]	2258	2356	2001	1902	1446	1931	2071	925	1023	2092	857	1149	1955	524	786	1075	991	511	2282	474	1019	1486	Cyp4v3	2129.3	1816.0	1346.7	1320.3	795.0	1261.3	746.5
ENSMUSG00000047155	Cyp4x1	cytochrome P450 family 4 subfamily x polypeptide 1 [Source:MGI Symbol;Acc:MGI:1932403]	0	0	0	0	0	1	0	0	1	0	1	0	0	1	0	0	0	2	0	1	1	1	Cyp4x1	0.0	0.3	0.3	0.3	0.3	0.7	1.0
ENSMUSG00000086896	Cyp4x1os	cytochrome P450 family 4 subfamily x polypeptide 1 opposite strand [Source:MGI Symbol;Acc:MGI:3649427]	0	0	0	0	0	0	0	0	0	0	0	0	0	0	0	0	0	0	0	0	0	0	Cyp4x1os	0.0	0.0	0.0	0.0	0.0	0.0	0.0
ENSMUSG00000001467	Cyp51	cytochrome P450 family 51 [Source:MGI Symbol;Acc:MGI:106040]	6736	7457	7451	8386	8182	6193	5682	12092	7376	7118	9696	6793	7085	13866	10046	11809	10785	6924	7957	13701	12030	13996	Cyp51	7507.5	6685.7	8862.0	7858.0	11907.0	8555.3	12865.5
ENSMUSG00000028240	Cyp7a1	cytochrome P450 family 7 subfamily a polypeptide 1 [Source:MGI Symbol;Acc:MGI:106091]	0	0	0	0	0	0	0	0	0	0	0	0	0	0	0	1	0	0	0	0	1	0	Cyp7a1	0.0	0.0	0.0	0.0	0.3	0.0	0.5
ENSMUSG00000039519	Cyp7b1	cytochrome P450 family 7 subfamily b polypeptide 1 [Source:MGI Symbol;Acc:MGI:104978]	0	0	0	0	0	0	0	0	0	0	0	0	0	0	0	0	0	0	0	0	0	0	Cyp7b1	0.0	0.0	0.0	0.0	0.0	0.0	0.0
ENSMUSG00000050445	Cyp8b1	cytochrome P450 family 8 subfamily b polypeptide 1 [Source:MGI Symbol;Acc:MGI:1338044]	0	0	1	2	3	0	1	1	0	0	0	0	0	1	0	0	0	0	0	0	1	1	Cyp8b1	0.8	1.3	0.3	0.0	0.3	0.0	0.5
ENSMUSG00000031257	Nox1	NADPH oxidase 1 [Source:MGI Symbol;Acc:MGI:2450016]	1423	950	1999	1977	1709	768	1234	739	292	488	791	362	531	684	236	332	467	112	209	237	215	184	Nox1	1587.3	1237.0	506.3	561.3	417.3	262.7	226.0
ENSMUSG00000023802	Nox3	NADPH oxidase 3 [Source:MGI Symbol;Acc:MGI:2681162]	0	0	0	0	0	0	0	0	0	0	0	0	0	0	0	0	0	1	0	0	0	0	Nox3	0.0	0.0	0.0	0.0	0.0	0.3	0.0
ENSMUSG00000030562	Nox4	NADPH oxidase 4 [Source:MGI Symbol;Acc:MGI:1354184]	1	0	2	1	1	3	1	2	3	3	4	3	5	1	4	4	1	1	8	2	0	1	Nox4	1.0	1.7	2.7	4.0	3.0	3.3	1.0
ENSMUSG00000036805	Noxa1	NADPH oxidase activator 1 [Source:MGI Symbol;Acc:MGI:2449980]	280	272	532	426	523	278	385	471	255	259	437	268	284	191	102	114	402	234	224	141	98	84	Noxa1	377.5	395.3	328.3	329.7	135.7	286.7	119.5
ENSMUSG00000019320	Noxo1	NADPH oxidase organizer 1 [Source:MGI Symbol;Acc:MGI:1919143]	1247	979	1412	1234	1305	951	1309	1777	1255	1154	1336	952	1163	1131	687	623	1331	833	1145	766	511	483	Noxo1	1218.0	1188.3	1395.3	1150.3	813.7	1103.0	638.5
ENSMUSG00000072919	Noxred1	NADP+ dependent oxidoreductase domain containing 1 [Source:MGI Symbol;Acc:MGI:1918525]	3	9	14	5	10	9	8	6	10	7	9	9	3	11	11	9	5	9	6	14	12	12	Noxred1	7.8	9.0	7.7	7.0	10.3	6.7	13.0
ENSMUSG00000040466	Blvrb	biliverdin reductase B (flavin reductase (NADPH)) [Source:MGI Symbol;Acc:MGI:2385271]	241	250	219	243	125	180	214	185	163	177	168	154	196	112	109	171	148	97	204	71	131	186	Blvrb	238.3	173.0	175.0	172.7	130.7	149.7	101.0
ENSMUSG00000006471	Ndor1	NADPH dependent diflavin oxidoreductase 1 [Source:MGI Symbol;Acc:MGI:1926047]	801	776	793	742	946	853	978	719	980	894	777	900	932	959	1002	1163	708	953	831	941	881	978	Ndor1	778.0	925.7	864.3	869.7	1041.3	830.7	911.0
ENSMUSG00000033268	Duox1	dual oxidase 1 [Source:MGI Symbol;Acc:MGI:2139422]	11	3	12	10	40	11	25	23	10	18	40	7	14	24	12	11	40	17	21	31	8	13	Duox1	9.0	25.3	17.0	20.3	15.7	26.0	19.5
ENSMUSG00000068452	Duox2	dual oxidase 2 [Source:MGI Symbol;Acc:MGI:3036280]	546	161	571	403	2135	201	542	1418	306	552	2180	157	348	1537	139	431	2347	340	819	1553	143	444	Duox2	420.3	959.3	758.7	895.0	702.3	1168.7	848.0
ENSMUSG00000027224	Duoxa1	dual oxidase maturation factor 1 [Source:MGI Symbol;Acc:MGI:2384861]	18	15	27	18	82	9	25	108	30	23	106	14	17	105	9	20	131	31	54	78	11	23	Duoxa1	19.5	38.7	53.7	45.7	44.7	72.0	44.5
ENSMUSG00000027225	Duoxa2	dual oxidase maturation factor 2 [Source:MGI Symbol;Acc:MGI:1914061]	32	24	75	41	226	28	51	287	63	71	291	30	45	232	18	62	353	66	144	208	27	68	Duoxa2	43.0	101.7	140.3	122.0	104.0	187.7	117.5
ENSMUSG00000024529	Lox	lysyl oxidase [Source:MGI Symbol;Acc:MGI:96817]	0	0	0	0	0	0	0	0	0	0	1	2	0	0	0	0	1	0	0	0	0	0	Lox	0.0	0.0	0.0	1.0	0.0	0.3	0.0
ENSMUSG00000032818	Loxhd1	lipoxygenase homology domains 1 [Source:MGI Symbol;Acc:MGI:1914609]	0	0	0	0	0	1	0	0	0	0	0	0	0	0	0	0	0	0	1	0	0	0	Loxhd1	0.0	0.3	0.0	0.0	0.0	0.3	0.0
ENSMUSG00000032334	Loxl1	lysyl oxidase-like 1 [Source:MGI Symbol;Acc:MGI:106096]	0	0	0	0	0	0	0	1	0	0	2	0	0	0	0	0	0	0	0	1	0	0	Loxl1	0.0	0.0	0.3	0.7	0.0	0.0	0.5
ENSMUSG00000034205	Loxl2	lysyl oxidase-like 2 [Source:MGI Symbol;Acc:MGI:2137913]	3	2	6	3	4	1	2	3	3	1	5	4	4	4	1	1	2	3	3	6	1	1	Loxl2	3.5	2.3	2.3	4.3	2.0	2.7	3.5
ENSMUSG00000000693	Loxl3	lysyl oxidase-like 3 [Source:MGI Symbol;Acc:MGI:1337004]	229	239	256	251	178	203	240	215	234	190	171	227	211	222	212	197	143	152	158	129	184	163	Loxl3	243.8	207.0	213.0	203.0	210.3	151.0	156.5
ENSMUSG00000025185	Loxl4	lysyl oxidase-like 4 [Source:MGI Symbol;Acc:MGI:1914823]	10	85	136	240	558	132	33	660	430	103	580	290	51	1057	3410	89	876	950	267	3965	1140	95	Loxl4	117.8	241.0	397.7	307.0	1518.7	697.7	2552.5
ENSMUSG00000009350	Mpo	myeloperoxidase [Source:MGI Symbol;Acc:MGI:97137]	0	0	1	0	0	0	0	0	0	1	0	2	0	1	1	1	0	3	0	2	0	0	Mpo	0.3	0.0	0.3	0.7	1.0	1.0	1.0
ENSMUSG00000025037	Maoa	monoamine oxidase A [Source:MGI Symbol;Acc:MGI:96915]	12315	14990	14906	11677	11797	13418	13806	13656	11274	17650	12098	14916	18418	16803	14399	24656	11625	5218	14856	11292	21105	30391	Maoa	13472.0	13007.0	14193.3	15144.0	18619.3	10566.3	16198.5
ENSMUSG00000040147	Maob	monoamine oxidase B [Source:MGI Symbol;Acc:MGI:96916]	850	1199	1228	1712	1283	1144	750	859	582	750	893	792	602	828	1132	510	783	341	483	908	962	730	Maob	1247.3	1059.0	730.3	762.3	823.3	535.7	935.0
ENSMUSG00000042626	Shc1	src homology 2 domain-containing transforming protein C1 [Source:MGI Symbol;Acc:MGI:98296]	1816	1670	1743	1814	1934	1762	1807	1861	1680	1714	1897	1756	1633	1684	1689	1653	1768	1896	1576	1768	1649	1685	Shc1	1760.8	1834.3	1751.7	1762.0	1675.3	1746.7	1708.5
ENSMUSG00000020312	Shc2	SHC (Src homology 2 domain containing) transforming protein 2 [Source:MGI Symbol;Acc:MGI:106180]	19	15	28	29	35	17	16	18	15	17	20	18	21	24	14	8	30	12	17	15	14	7	Shc2	22.8	22.7	16.7	19.7	15.3	19.7	14.5
ENSMUSG00000021448	Shc3	src homology 2 domain-containing transforming protein C3 [Source:MGI Symbol;Acc:MGI:106179]	0	0	0	1	2	2	0	0	0	1	3	0	0	2	6	0	0	1	1	4	2	1	Shc3	0.3	1.3	0.3	1.0	2.7	0.7	3.0
ENSMUSG00000035109	Shc4	SHC (Src homology 2 domain containing) family member 4 [Source:MGI Symbol;Acc:MGI:2655364]	55	47	58	47	28	48	29	34	36	26	37	32	38	29	39	30	21	36	20	24	30	24	Shc4	51.8	35.0	32.0	35.7	32.7	25.7	27.0
ENSMUSG00000022322	Shcbp1	Shc SH2-domain binding protein 1 [Source:MGI Symbol;Acc:MGI:1338802]	413	384	502	447	294	351	379	330	320	246	236	274	260	113	154	132	161	223	148	57	132	59	Shcbp1	436.5	341.3	298.7	256.7	133.0	177.3	94.5
ENSMUSG00000042708	Shcbp1l	Shc SH2-domain binding protein 1-like [Source:MGI Symbol;Acc:MGI:1919086]	6	5	10	3	17	18	7	5	10	5	12	20	13	18	11	12	7	4	4	12	38	15	Shcbp1l	6.0	14.0	6.7	15.0	13.7	5.0	25.0
ENSMUSG00000039154	Shd	src homology 2 domain-containing transforming protein D [Source:MGI Symbol;Acc:MGI:1099461]	1	2	0	1	3	1	1	1	5	1	5	0	0	3	3	10	0	1	0	3	1	8	Shd	1.0	1.7	2.3	1.7	5.3	0.3	2.0
ENSMUSG00000046280	She	src homology 2 domain-containing transforming protein E [Source:MGI Symbol;Acc:MGI:1099462]	0	0	1	0	0	0	0	0	0	0	0	0	0	0	0	1	0	2	1	0	1	0	She	0.3	0.0	0.0	0.0	0.3	1.0	0.5
ENSMUSG00000033256	Shf	Src homology 2 domain containing F [Source:MGI Symbol;Acc:MGI:3613669]	262	169	223	203	185	173	297	185	181	225	186	203	274	159	211	192	194	176	280	96	138	107	Shf	214.3	218.3	197.0	221.0	187.3	216.7	117.0
ENSMUSG00000027261	Hao1	hydroxyacid oxidase 1 liver [Source:MGI Symbol;Acc:MGI:96011]	1	0	3	0	0	0	0	0	0	0	0	2	0	0	0	0	0	0	0	0	0	0	Hao1	1.0	0.0	0.0	0.7	0.0	0.0	0.0
ENSMUSG00000027870	Hao2	hydroxyacid oxidase 2 [Source:MGI Symbol;Acc:MGI:96012]	0	0	0	0	0	0	0	0	0	0	0	0	0	0	0	0	0	0	0	0	0	0	Hao2	0.0	0.0	0.0	0.0	0.0	0.0	0.0
ENSMUSG00000024903	Lao1	L-amino acid oxidase 1 [Source:MGI Symbol;Acc:MGI:2140628]	0	0	0	0	0	0	0	0	0	0	0	0	0	0	0	0	0	0	0	0	0	0	Lao1	0.0	0.0	0.0	0.0	0.0	0.0	0.0
ENSMUSG00000009356	Lpo	lactoperoxidase [Source:MGI Symbol;Acc:MGI:1923363]	1	1	1	3	5	2	5	3	2	9	10	2	15	16	2	20	9	4	7	3	3	10	Lpo	1.5	4.0	4.7	9.0	12.7	6.7	3.0
ENSMUSG00000064351	mt-Co1	mitochondrially encoded cytochrome c oxidase I [Source:MGI Symbol;Acc:MGI:102504]	53912	61578	46422	43865	45316	54809	53841	44052	47872	43735	42002	55746	48693	26665	29828	24217	30279	35505	37453	23220	31399	22931	mt-Co1	51444.3	51322.0	45219.7	48813.7	26903.3	34412.3	27309.5
ENSMUSG00000064354	mt-Co2	mitochondrially encoded cytochrome c oxidase II [Source:MGI Symbol;Acc:MGI:102503]	13	11	12	16	12	9	7	9	10	8	5	16	4	4	4	2	4	4	10	1	6	3	mt-Co2	13.0	9.3	9.0	8.3	3.3	6.0	3.5
ENSMUSG00000064358	mt-Co3	mitochondrially encoded cytochrome c oxidase III [Source:MGI Symbol;Acc:MGI:102502]	16	18	11	10	10	10	11	18	6	9	8	17	9	1	6	5	4	9	5	2	2	6	mt-Co3	13.8	10.3	11.0	11.3	4.0	6.0	2.0
ENSMUSG00000000959	Oxa1l	oxidase assembly 1-like [Source:MGI Symbol;Acc:MGI:1916339]	1981	1826	1778	1871	1535	1876	1844	1508	1653	1834	1685	1896	1866	1707	1617	1720	1585	1462	1518	1525	1703	1610	Oxa1l	1864.0	1751.7	1665.0	1815.7	1681.3	1521.7	1614.0
ENSMUSG00000025464	Paox	polyamine oxidase (exo-N4-amino) [Source:MGI Symbol;Acc:MGI:1916983]	380	364	459	480	828	378	349	1397	697	464	1119	516	516	1002	501	597	1435	979	716	1049	573	591	Paox	420.8	518.3	852.7	717.0	700.0	1043.3	811.0
ENSMUSG00000029998	Pcyox1	prenylcysteine oxidase 1 [Source:MGI Symbol;Acc:MGI:1914131]	2483	2677	2281	2415	2142	2398	2183	1867	1971	1871	2030	1784	1896	1659	1680	1687	2088	1863	1980	1232	1581	1485	Pcyox1	2464.0	2241.0	1903.0	1903.3	1675.3	1977.0	1406.5
ENSMUSG00000024579	Pcyox1l	prenylcysteine oxidase 1 like [Source:MGI Symbol;Acc:MGI:3606062]	591	435	462	509	420	447	515	392	475	408	438	505	512	304	291	260	364	411	319	98	200	106	Pcyox1l	499.3	460.7	425.0	485.0	285.0	364.7	149.0
ENSMUSG00000017453	Pipox	pipecolic acid oxidase [Source:MGI Symbol;Acc:MGI:1197006]	206	96	326	168	65	98	138	37	33	67	30	29	63	21	13	34	17	17	38	18	24	37	Pipox	199.0	100.3	45.7	40.7	22.7	24.0	21.0

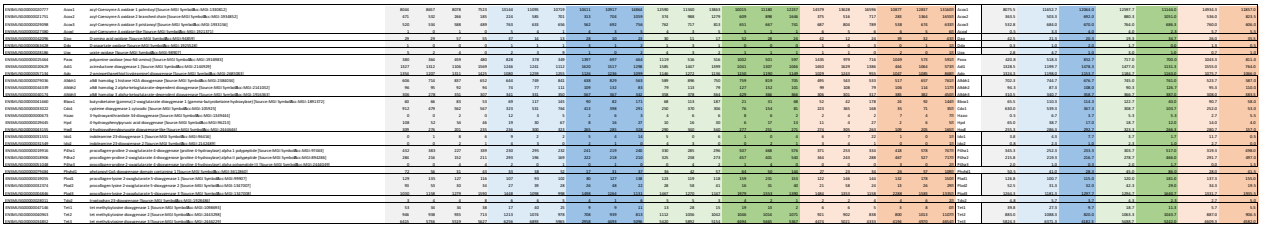

TABLE 2. List of material used for immunostainings, in situ hybridization and qRT-PCR experiments

Immunostainings	**Antibodies**	**Catalogue number**	**Manufacturer**
	Goat anti-Trop2	AF650	R&D systems
	Mouse anti-Beta catenin	610154	BD transduction laboratories
	Rabbit anti-Olfactomedin 4	#14369	cell signaling tech
	TUNEL assay	12156792910	Roche
	DAPI	D9542	Sigma-Aldrich
RNAscope probes	**Gene**	**Catalogue number**	**Manufacturer**
	m Areg	430501	Advanced cell diagnostics
	m Axin 2	400331	Advanced cell diagnostics
	m Hmox1	498811	Advanced cell diagnostics
	m Lgr5	312171	Advanced cell diagnostics
	m Pparg	513371	Advanced cell diagnostics
	m Pycard	439581	Advanced cell diagnostics
qPCR primers	**Gene**	**Forward primer**	**Reverse primer**
	Aqp1	AGCTGGTACTGTGCGTTCTG	GTAGTCAATCGCCAGCAGGT
	Aqp3	TGCCTTGCGCTAGCTACTTT	GAAGCATCTCCCCACAACGA
	Aqp4	TGCCCGTAATCTGACTCCCA	AATGTCCACACTTACCCCACC
	Aqp5	ATTGGCTTGTCGTCGGTCACACT	CCAGAAGACCCAGTGAGAGG
	Areg	GCGAATGCAGATACATCGAGAA	CGCTGTGAGTCTTCATGGATTTT
	Atf3	GTCACCAAGTCTGAGGCGG	GTTTCGACACTTGGCAGCAG
	Axin2	TGACTCTCCTTCCAGATCCCA	TGCCCACACTAGGCTGACA
	Casp1	GACTGGGACCCTCAAGTTTTGCCC	CACCACCCTTCAGGATGGCCT
	Ccnd1	CCTGCTACCGCACAACGCAC	GCCTGGCGCAGGCTTGACTC
	Cdkn1a	ATCCTGCAAGAGGCCTGGAGAGG	CACGAGGTCGGACGCCTATGGA
	Chga	TCCCCACTGCAGCATCCAGTTC	CCTTCAGACGGCAGAGCTTCGG
	Ddx60	AGTGATGAGCCTTTGTTGAGGA	TCGTTCATGATGGCATCTCCC
	Egr1	GAGCACCTGACCACAGAGTC	GCGGCCAGTATAGGTGATGG
	Hmox1	CATAGCCCGGAGCCTGAATC	CAAATCCTGGGGCATGCTGT
	Hopx	GTGCCTGCGATCTTGGTGGCT	GCCTGACCTTACGTCTGTCCCG
	Lgr5	CCTACTCGAAGACTTACCCAGT	GCATTGGGGTGAATGATAGCA
	Ly6A	GAAAGAGCTCAGGGACTGGAGTGTT	TTAGGAGGGCAGATGGGTAAGCAA
	Lyz1	GAGACCGAAGCACCGACTATG	CGGTTTTGACATTGTGTTCGC
	Muc2	ATGCCCACCTCCTCAAAGAC	GTAGTTTCCGTTGGAACAGTGAA
	Nupr1	AATACCAACCGCCCTAGCC	TGTGGTCTGGCCTTATCTCC
	Olfm4	CAGCTGCCTGGTTGCCTCCG	GGCAGGTCCCATGGCTGTCC
	Ptgs2	CTGACCCCCAAGGCTCAAAT	TTTAAGTCCACTCCATGGCCC
	Pycard	GAGCAGCTGCAAACGACTAA	CTGGTCCACAAAGTGTCCTGT
	Rpl13	CCCGTGGCGATTGTGAA	TCATTGTCCTTCTGTGCAGGTT
	Sis	TTCAAGAAATCACAACATTCAATTTACTAG	CTAAAACTTTCTTTGACATTTGAGCAA
	Slc7a11	AGCTAACTGACTGCCCCTGG	ACTCAGAGGTGTGTTTCAGCC
	Trop2	AGAACGCGTCGCAGAAGGGC	CGGCGGCCCATGAACAGTGA
	Wwtr1	CGGTTCCGGGGATGTAAGAG	GAACTGACGAGCTGGAACCC
	Ywhaz	TGCAACGATCTACTGTCTCTTTTG	CGGTAGTAGTCACCCTTCATTTTCA

SUPPLEMENTARY FIGURE LEGENDS

Figure S1. Impact of the CAP application method on organoid morphology. a. CAP-conditioned media and PAM generated by treatment with 50 W for 60 s at day 1 were applied directly to organoid cultures at day 2 post-replating for 24 hours (until day 3). **b**. Representative pictures of a given field showing growth of organoids at day 2 (before CAP application) and day 3 (endpoint of the experiment). Triangles show individual elements evolving as protruded organoids and spheroids in untreated and CAP-treated cultures, respectively. Right panels: insets of the pictures at day 3. Scale bars: 500 µm. **c**. Quantification of organoid complexity at day 3. An average number of 100 elements was analyzed over time per condition per organoid line (n= 4 organoid lines). Data are represented as means ± sem. Two-way ANOVA: interaction ** P< 0.01 followed by Dunnett's multiple comparisons test: *** P< 0.001, ** P< 0.01, * P< 0.05, ns not significant (all compared to untreated).

Figure S2. Impact of the CAP application method on global gene expression of intestinal organoids.

a. Heatmap of the most differentially regulated genes in CAP-treated versus Untreated (Controls) organoids at the early time post-treatment (30 min). **b**. Expression levels of Cys metabolism-, cell signaling-, inflammation- and cytoskeleton organization-associated genes in the various conditions. Data are represented as means ± sd. n = 4 and 3 samples in Controls and CAP-treated conditions, respectively. CP20M: counts per kilobase of transcript per 20 million mapped reads.

Figure S3. Apc deficient-derived organoids exhibit increased resistance to CAP treatment as compared to normal intestinal stem cell-derived organoids.

a. Organoid growth of Apc wt and Apc Δ crypts upon initial seeding in culture media containing ENR (EGF, Noggin, Rspondin1) or EN (EGF, Noggin). Representative pictures of a given field showing organoid morphology at day 1 and day 4. Apc Δ organoid efficiently grow in EN conditions as compared to Apc wt organoids. Scale bars: 500 µm. **b**. Measurement of reactive species in culture supernatants of

Apc wt and Apc Δ organoids 24 hours after direct CAP treatment at the indicated doses. DCFDA dye was used to measure ROS levels. A.U. Arbitrary Units. Each symbol corresponds to a given organoid line. Data are represented as means ± sem. One-way Anova test. **** P< 0.0001. **c**. Expression levels of aquaporin-encoding genes. Left panel: Aqp expression in Lgr5+ve ISC. Data were analyzed from the Gene Expression Omnibus GSE135362 dataset; Right panel: Aqp expression in control and CAP-treated organoids (this work). CP20M: counts per kilobase of transcript per 20 million mapped reads (n =2 samples). **d**. Gene expression analysis by qRT-PCR of Aquaporins in Apc wt and Apc Δ organoids. Each symbol corresponds to a given organoid line. Values are normalized to Untreated Apc wt levels. Data are represented as means ± sem. One-way Anova test. **** P< 0.0001; *** P< 0.001. **e**. Expression levels of ROS scavenger enzymes in Lgr5+ve ISC. Data were analyzed from the Gene Expression Omnibus GSE135362 dataset. CP20M: counts per kilobase of transcript per 20 million mapped reads (n =2 samples).

a

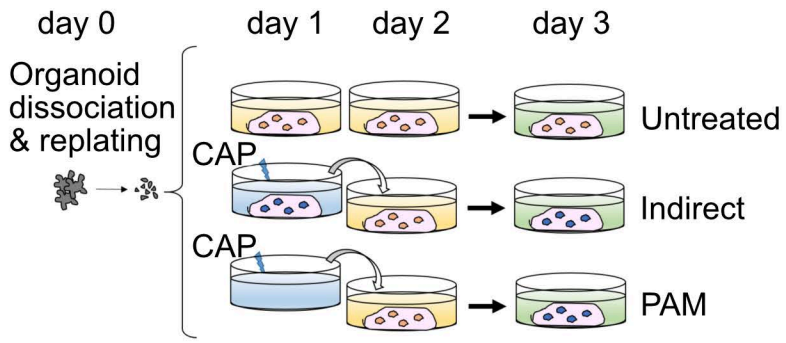

b

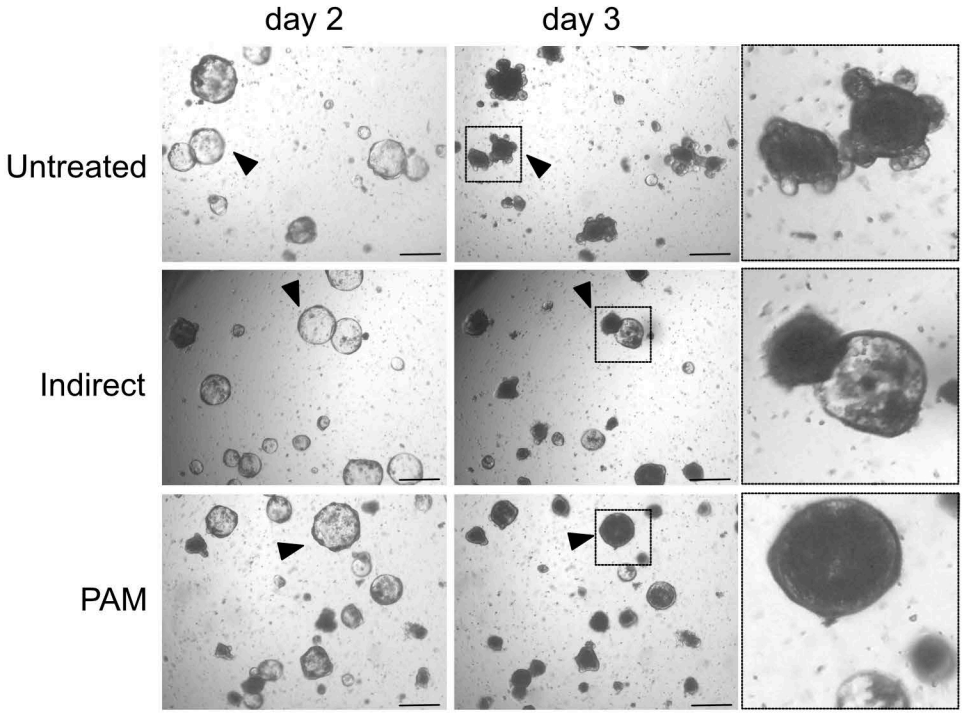

c